ANALYTICAL STUDY ON THE WAVE SCATTERING BY CANONICAL TWO-DIMENSIONAL OBSTACLES

DISSERTATION

Submitted in Partial Fulfillment of the Requirements
for the Degree of Doctor of Engineering
in the Graduate School of Science and Engineering, Chuo University

By

Takashi Nagasaka, B.E., M.E.

Chuo University

March 2017

ANALYTICAL STUDY ON THE WAVE SCATTERING BY CANONICAL TWO-DIMENSIONAL OBSTACLES

DISSERTATION

Submitted in Partial Fulfillment of the Requirements
for the Degree of Doctor of Engineering
in the Graduate School of Science and Engineering, Chuo University

By

Takashi Nagasaka, B.E., M.E.

Chuo University

March 2017

Dissertation Committee:
Prof. I. Shoji, Chuo University
Prof. H. Shirai, Chuo University
Prof. T. Yamasaki, Nihon University

Approved by:

Prof. K. Kobayashi, Advisor
Department of Electrical, Electronic,
and Communication Engineering

ABSTRACT

ANALYTICAL STUDY ON THE WAVE SCATTERING BY CANONICAL TWO-DIMENSIONAL OBSTACLES

Contributed by

TAKASHI NAGASAKA
Electrical, Electronic, and Communication Engineering Course
Graduated School of Science of Engineering
Chuo University
Tokyo, Japan

Supervised by

PROFESSOR KAZUYA KOBAYASHI
Department of Electrical, Electronic, and Communication Engineering
Faculty of Science of Engineering
Chuo University
Tokyo, Japan

The analysis of wave scattering and diffraction problems involving canonical objects is one of the important subjects in electromagnetic theory and radar cross section (RCS) studies. Various analytical and numerical methods have been developed so far and the scattering problems have been investigated for many kinds of two- and three-dimensional structures. Among a number of analysis methods, the Wiener-Hopf technique is known as a rigorous, function-theoretic approach for electromagnetic wave problems related to canonical geometries. In this doctoral dissertation, we shall consider a thin material strip that are important from both the theoretical and engineering viewpoints, and analyze the electromagnetic wave diffraction by means of the Wiener-Hopf technique. It is shown that our final solutions are valid over a broad frequency range. Numerical examples are presented for various physical parameters, and the far field scattering characteristics are

discussed in detail. Some comparisons with other existing methods are also given.

This dissertation is composed of two parts. In the first part, the plane wave diffraction by a thin material strip is analyzed for H polarization using the Wiener-Hopf approach together with approximate boundary conditions. Introducing the Fourier transform of the scattered field and applying approximate boundary conditions in the transform domain, the problem is formulated in terms of the simultaneous Wiener-Hopf equations, which are solved exactly via the factorization and decomposition procedure. However, the solution is formal since branch-cut integrals with unknown integrands are involved. By using a rigorous asymptotic method, we shall derive a high-frequency solution of the Wiener-Hopf equations, which is expressed in terms of an infinite asymptotic series and accounts for all the higher order multiple diffraction effects rigorously. Our solution is valid for the strip width greater than about the incident wavelength and requires numerical inversion of an appropriate matrix equation. The scattered field in the real space is evaluated asymptotically by taking the Fourier inverse of the solution in the transform domain and applying the saddle point method. It is to be noted that our final solution is uniformly valid in incidence and observation angles. Numerical examples of the RCS are presented for various physical parameters and far field scattering characteristics of the strip are discussed in detail.

In the second part of this dissertation, we shall consider the same strip geometry as in first part, and analyzed the E-polarized plane wave diffraction by applying the Wiener-Hopf technique together with approximate boundary conditions. Introducing the Fourier transform of the scattered field and applying the approximate boundary conditions in the transform domain, the problem is formulated in terms of the simultaneous Wiener-Hopf equations satisfied by unknown spectral functions. The Wiener-Hopf equations are then solved via the factorization and decomposition procedure leading to the exact solution. However, the solution is formal in the sense that branch-cut integrals with unknown integrands are involved. Applying a rigorous asymptotic method similar to the first part, we shall derive a high-frequency solution to the Wiener-Hopf equations, which is valid for the strip width greater than about the incident wavelength. The scattered field in the real space is evaluated asymptotically by taking the Fourier inverse of the solution in the transform domain and applying the saddle point method of integration. Numerical examples of the RCS are presented for various physical parameters and far field scattering characteristics of the strip are discussed in detail

VITA

Takashi Nagasaka received the B.E. (Bachelor of Engineering) and the M.E. (Master of Engineering) degrees in Electrical, Electronic, and Communication Engineering from Chuo University, Tokyo, Japan in 2013 and 2015, respectively. He is currently working towards the D.E. (Doctor of Engineering) degree in Electrical, Electronic, and Communication Engineering, Chuo University, Tokyo, Japan.

He received the Honorary Mention: Next to the Best, MMET*2016 and URSI Young Scientist Paper Contest, 16th IEEE International Conference on Mathematical Methods in Electromagnetic Theory (MMET*2016), Lviv, Ukraine, July 2016. He also recieved the 2017 URSI Young Scientists Award and the Third Prize, Fourth International URSI Student Prize Paper Competition, XXXIInd URSI General Assembly and Scientific Symposium (URSI GASS 2017), Montreal, Canada, August 2017.

His research interests are in the area of approximate boundary conditions, canonical problems, developments of rigorous mathematical techniques as applied to electromagnetic wave problems, scattering and diffraction, and radar cross section.

DEDICATION

To my mother

ACKNOWLEDGMENTS

Firstly, I would like to express my deepest and sincere gratitude to my advisor, Professor Kazuya Kobayashi for his continuous guidance and support during the entire course of preparation of this dissertation. I am also very much thankful to the members of the Dissertation Committee, Professor Ichiro Shoji, Professor Hiroshi Shirai, and Professor Tsuneki Yamasaki, for their valuable suggestions, which have led to improvements of the contents of this dissertation.

I would like to sincerely express my gratitude to Dr. Olga V. Shapoval of the Institute of Radio-Physics and Electronics of the National Academy of Sciences of Ukraine (IRE NASU) for her valuable comments on my doctoral research.

I would like to thank to Dr. Toru Eizawa, a graduate of the Kobayashi Laboratory, for his progressive and useful study on my doctoral research.

Lastly I would also like to express my gratitude to my mother and my aunt, Astuko Nagasaka and Shizuyo Hori.

TABLE OF CONTENTS

LIST OF FIGURES

1. INTRODUCTORY REMARKS

1.1. Wiener-Hopf Technique for Scattering Problems

The analysis of wave scattering and diffraction problems involving canonical obstacles is one of the important subjects in area of the electromagnetic theory. Various analytical and numerical methods have been developed so far and have been investigated for many kinds of two- and three-dimensional obstacles [1]-[5]. In, 1986, Sommerfeld [6] obtained the exact solution to the diffraction by a wedge, which was expressed in form of complex integral representation, by introducing the idea of multiple-valued functions that are single-valued, bounded, and continuous on the appropriate Riemann surface. As a special case, he further considered a semi-infinite plate by wedge angle to zero, and showed that the solution could be simplified to yield the Fresnel integral representation. His method of solution for scattering and diffraction problems is known as the *Sommerfeld theory of diffraction*, and is famous as a classical result in the diffraction by wedge-shaped obstacles [7].

The Wiener-Hopf technique is one of the powerful, rigorous approach for analyzing wave scattering and diffraction problems related to canonical obstracts, which is mathematically rigorous in the sense that the edge condition required for the uniqueness of the solution is explicitly incorporated into the analysis. In 1931, Wiener and Hopf [8] showed that a certain singular integral equation could be solved exactly by using the series of Fourier transforms and functions of a complex variable. This integral equation and their method of solution are known as the *Wiener-Hopf equation* and the *Wiener-Hopf technique*, respectively, and had a great impact on the progress in the theory of wave scattering and diffraction. In 1941, Magnus [9] reduced the diffraction problem by a semi-infinite plate to the solution for a singular integral equation. Shortly afterward, Copson [10] and Schwinger [11] independently, for the first time, solve this integral equation by applying the Wiener-Hopf technique, and derived the same solution as Sommerfeld. Since then, the importance of the Wiener-Hopf technique has been highly recognized and various scattering and propagation problems have been solved by this technique [12[-[16]. The Wiener-Hopf technique is very efficient in solving wave scattering and diffraction problems related to canonical obstacles, since it gives solutions valid over a wide frequency range. It is important to note that the range of applicability of the Wiener-Hopf technique is still growing and a number of complicated diffraction problems have been solved by several authors such as Kobayashi *et al.* [17]-[25], Serbest and Büyükaksoy [26], [27] and Lüneburg [28] by following extensions of the method based on the Wiener-Hopf technique.

The Wiener-Hopf technique was developed to solve the following integral equation of the first kind [8]:

$$\int_0^\infty k(z-z')f(z')dz' = g(z), \quad 0 < z < \infty, \tag{1.1}$$

where $k(z-z')$ and $g(z)$ are given, and $f(z')$ is the unknown function to be determined. The term $k(z-z')$ is the kernel of the Wiener-Hopf integral equation and its explicit form is deduced form Green's function associated with the geometry under consideration. The fundamental procedure in the Wiener-Hopf technique is to take the Fourier transform of (1.1) to derive a functional equation in the complex domain (*Wiener-Hopf equation*), which is then solved via the so-called *factorization*. Let $\alpha = \sigma + i\tau (\equiv \mathrm{Re}\,\alpha + \mathrm{Im}\,\alpha)$ be a Fourier transform variable and let $K(\alpha)$ be the Fourier transform of $k(z)$, regular in the strip $\tau_- < \tau < \tau_+$ of the complex α-plane. Here, $K(\alpha)$ is called the *kernel function.* The factorization is to split a function $K(\alpha)$ into the multiplication form, as in

$$K(\alpha) = K_+(\alpha)K_-(\alpha), \tag{1.2}$$

where $K_+(\alpha)$ and $K_-(\alpha)$ are regular and nonzero in the upper half-plane $\tau > \tau_-$ and the lower half-plane $\tau < \tau_+$, respectively, and show an algebraic behavior at infinity.

1.2. Contributions of This Work

We shall describe main results and contributions of this dissertation. The analysis of the scattering and diffraction by canonical obstacles is an important subject in electromagnetic theory and radar cross section (RCS) studies. Various analytical and numerical methods have been developed thus far and the scattering have been investigated for a number of two- and three-dimensional obstacles. However, there are only a few papers treating the diffraction by canonical obstacles with arbitrary permittivity and permeability.

The aims of this dissertation are to analyze the diffraction by two-dimensional obstacles having various physical parameters applying the Wiener-Hopf technique. In particular, we shall consider a material strip with various physical parameters involving the obstacles with arbitrary permittivity and permeability, and analyze the plane wave diffraction by a thin material using the Wiener-Hopf technique and approximate boundary conditions. Our final solution is obtained the case where the thickness and width are small and large compared with the wavelength, respectively, and valid for the strip width greater

than about the incident wavelength via a use of rigorous asymptotic method.

In past related research, Volakis [29] analyzed the H-polarized plane wave diffraction by a thin material strip using the dual integral equation approach [30] and the extended spectral ray method [31] together with approximate boundary conditions [32]. In his paper [29], Volakis first solved rigorously the diffraction problem involving a single material half-plane, and subsequently obtained a high-frequency solution to the original strip problem by superposing the singly diffracted fields from the two independent half-planes and the doubly/triply diffracted fields from the edges of the two half-planes. Therefore his analysis is not rigorous in the sense of boundary value problems, and may not be applicable unless the strip width is relatively large compared with the wavelength. This problem has been solved more recently by Shapoval *et al.* [33], [34] by using the generalized boundary conditions and the singular integral equation.

In Chapter 2, we shall consider the same Volakis's problem [29], and analyze the H-polarized plane wave diffraction by a thin material strip using Wiener-Hopf technique. Assuming that the thickness is small compared with the wavelength, the original problem is replaced by a strip of zero thickness satisfying the approximate boundary conditions [32], [35]. Introducing the Fourier transform for the unknown scattered field and applying boundary conditions in the transform domain, the problem is formulated in terms of the Wiener-Hopf equations, which are solved exactly via the factorization and decomposition procedure. However, the solution is formal in the sense that branch-cut integrals with unknown integrands are involved. By using a rigorous asymptotic method [36], [37] together with a special function introduced by authors [38], [39], we have derived a high-frequency solution for Wiener-Hopf equations, which is described in terms of an infinite asymptotic series. Taking the Fourier inverse of the solution in the transform domain and applying the saddle point method, the scattered far field in the real space is derived. Numerical examples of the RCS are shown for various physical parameters, and scattering characteristics of the strip are discussed in detail.

In Chapter 3, we shall consider the same geometry for the material strip, and analyze the E-polarized plane wave diffraction via a method similar to that developed in Chapter 2 for H polarization. Some differences can be seen in the scattering characteristics depending on the incident polarization [40].

In Chapter 4, concluding remarks are given, where the main results obtained in this work are summarized.

The time factor is assumed to be $e^{-i\omega t}$ and suppressed throughout this dissertation

2. WIENER-HOPF ANALYSIS OF THE PLANE WAVE DIFFRACTION BY A THIN MATERIAL STRIP: THE CASE OF H POLATIZATION

2.1. Introduction

In this chapter, we shall consider the same problem as in Volakis [29], and analyze the H-polarized plane wave diffraction by a thin material strip with the aid of the Wiener-Hopf technique together with approximate boundary conditions. It is known that the approximate boundary conditions presented by Senior and Volakis [29] are valid under the condition that the absolute value of the complex refractive index of the medium is not too large. On the other hand, Bleszynski *et al*. [35] developed a different type of approximate boundary conditions, which is valid for the case where the absolute value of the complex refractive index is large. The main purpose of this paper is to use the two different approximate boundary conditions in [29] and [35] to extend the range of applicability of the Wiener-Hopf solution to the diffraction by a material strip, so that it becomes applicable to the strip having various material constants.

Introducing the Fourier transform of the scattered field and applying approximate boundary conditions in the transform domain, the problem is formulated in terms of the simultaneous Wiener-Hopf equations, which are solved exactly via the factorization and decomposition procedure. However, the solution is formal since branch-cut integrals with unknown integrands are involved. By using a rigorous asymptotic method [36], [37] together with a special function newly introduced in this paper, we shall derive a high-frequency solution of the Wiener-Hopf equations, which is expressed in terms of an infinite asymptotic series and accounts for all the higher order multiple diffraction effects rigorously. It is shown that the higher-order multiple diffraction is expressed in terms of the special function mentioned above. Our solution is valid for the strip width greater than about the incident wavelength and requires numerical inversion of an appropriate matrix equation. The scattered field in the real space is evaluated asymptotically by taking the Fourier inverse of the solution in the transform domain and applying the saddle point method. It is to be noted that our final solution is uniformly valid in incidence and observation angles. Numerical examples of the RCS are presented for various physical parameters and far field scattering characteristics of the strip are discussed in detail. Some comparisons with Volakis [29] are also given. This paper provides an important generalization of the results presented in [38].

2.2. Formulation of the Problem

We consider the diffraction of an H-polarized plane wave by a thin material strip as shown in Fig. 2.1, where the relative permittivity and permeability of the strip are denoted by ε_r and μ_r, respectively. Let the total magnetic field $\phi^t(x,z)[\equiv H_y^t(x,z)]$ be

$$\phi^t(x,z) = \phi^i(x,z) + \phi(x,z), \tag{2.1}$$

where $\phi^i(x,z)$ is the incident field given by

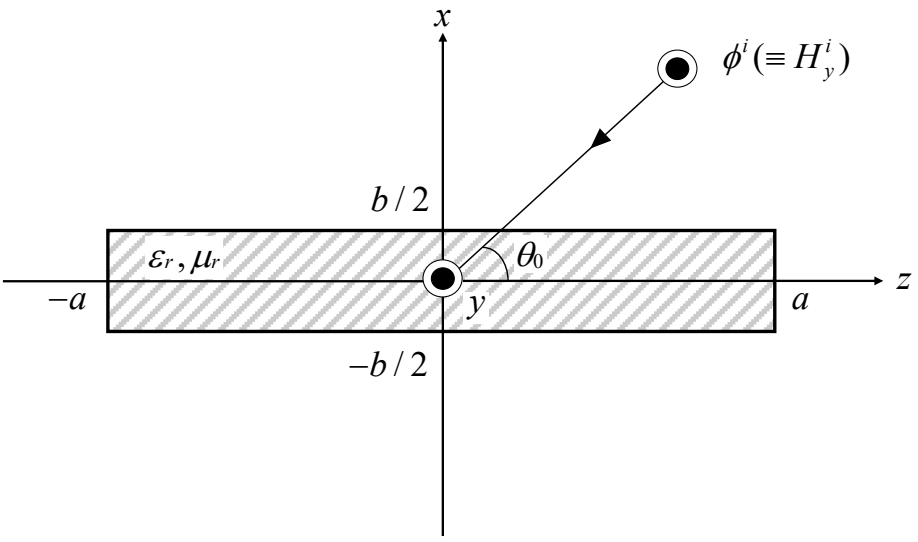

Fig. 2.1 Geometry of the problem.

$$\phi^i(x,z) = e^{-ik(x\sin\theta_0 + z\cos\theta_0)}, \quad 0 < \theta_0 < \pi/2 \tag{2.2}$$

with $k[=\omega(\varepsilon_0\mu_0)^{1/2}]$ being the free-space wavenumber. The term $\phi(x,z)$ is the unknown scattered field and satisfies the two-dimensional Helmholtz equation:

$$\left(\frac{\partial^2}{\partial x^2} + \frac{\partial^2}{\partial z^2} + k^2\right)\phi(x,z) = 0. \tag{2.3}$$

Nonzero components of the scattered electromagnetic fields are derived from the following relation:

$$(H_y, E_x, E_z) = \left(\phi, \frac{1}{i\omega\varepsilon_0}\frac{\partial\phi}{\partial z}, \frac{i}{\omega\varepsilon_0}\frac{\partial\phi}{\partial x}\right). \tag{2.4}$$

If the strip thickness is small compared with the wavelength, the material strip is approximately replaced by a strip of zero thickness satisfying the second order impedance boundary conditions [32]. On the strip surface, the total electromagnetic field satisfies the approximate boundary conditions as given by

$$E_z^t(+0,z) + E_z^t(-0,z) = 2R_e[H_y^t(+0,z) - H_y^t(-0,z)], \tag{2.5}$$

$$\left[\frac{1}{R_m} + \frac{1}{\tilde{R}_e}\left(1 + \frac{1}{k^2}\frac{\partial^2}{\partial x^2}\right)\right][H_y^t(+0,z) + H_y^t(-0,z)] = 2[E_z^t(+0,z) - E_z^t(-0,z)], \tag{2.6}$$

where

$$R_e = \frac{iZ_0}{kb(\varepsilon_r - 1)}, \quad \tilde{R}_e = \frac{iY_0\varepsilon_r}{kb(\varepsilon_r - 1)}, \quad R_m = \frac{iY_0}{kb(\mu_r - 1)} \tag{2.7}$$

with Z_0 and Y_0 being the intrinsic impedance and admittance of free space, respectively. It is verified by Senior and Volakis [41] using numerical experimentation that the approximate boundary conditions as given by (2.5)-(2.7) are valid for $b \le 0.1\lambda$.

For convenience of analysis, we assume the medium to be slightly lossy as in

$$k = k_1 + ik_2, \quad 0 < k_2 \ll k_1. \tag{2.8}$$

The solution for real k is obtained by letting $k_2 \to +0$ at the end of analysis. It follows from the radiation condition that

$$\phi(x,z) = O\left(e^{-k_2|z|\cos\theta_0}\right), \quad |z| \to \infty. \tag{2.9}$$

We now define the Fourier transform $\Phi(x,\alpha)$ of the scattered field $\phi(x,z)$ with respect to z as

$$\Phi(x,\alpha) = (2\pi)^{-1/2}\int_{-\infty}^{\infty}\phi(x,z)e^{i\alpha z}dz, \tag{2.10}$$

where $\alpha(\equiv \mathrm{Re}\,\alpha + i\,\mathrm{Im}\,\alpha) = \sigma + i\tau$. In view of (2.9), it is found that $\Phi(x,\alpha)$ is regular in the strip $|\tau| < k_2\cos\theta_0$ of the complex α-plane. Introducing the Fourier integrals as

$$\Phi_{\pm}(x,\alpha) = \pm(2\pi)^{-1/2}\int_{\pm a}^{\pm\infty}\phi(x,z)e^{i\alpha(z\mp a)}dz, \tag{2.11}$$

$$\Phi_1(x,\alpha) = (2\pi)^{-1/2}\int_{-a}^{a}\phi(x,z)e^{i\alpha z}dz, \tag{2.12}$$

we can express $\Phi(x,\alpha)$ as

$$\Phi(x,\alpha) = e^{-i\alpha a}\Phi_-(x,\alpha) + \Phi_1(x,\alpha) + e^{i\alpha a}\Phi_+(x,\alpha). \tag{2.13}$$

In (2.11), $\Phi_+(x,\alpha)$ and $\Phi_-(x,\alpha)$ are regular in the half-planes $\tau > -k_2\cos\theta_0$ and $\tau < k_2\cos\theta_0$, respectively, whereas $\Phi_1(x,\alpha)$ is an entire function. The derivative of (2.11) with respect to x is defined by

$$\Phi'_{\pm}(x,\alpha) = \pm(2\pi)^{-1/2}\int_{\pm a}^{\pm\infty}\frac{\partial\phi(x,z)}{\partial x}e^{i\alpha(z\mp a)}dz, \tag{2.14}$$

$$\Phi''_{\pm}(x,\alpha) = \pm(2\pi)^{-1/2}\int_{\pm a}^{\pm\infty}\frac{\partial^2\phi(x,z)}{\partial x^2}e^{i\alpha(z\mp a)}dz. \tag{2.15}$$

Taking the Fourier transform of the two-dimensional Helmholtz equation, we find that

$$(d^2/dx^2 - \gamma^2)\Phi(x,\alpha) = 0 \tag{2.16}$$

for any α in the strip $|\tau| < k_2\cos\theta_0$, where $\gamma = (\alpha^2 - k^2)^{1/2}$. Since γ is a double-valued function of α, we choose a proper branch of γ such that γ reduces to $-ik$

when $\alpha = 0$. According to the choice of this branch, we can show that $\mathrm{Re}\gamma > 0$ for any α in the strip $|\tau| < k_2 \cos\theta_0$. Equation (2.16) is the transformed wave equation. Because $\mathrm{Re}\gamma > 0$ for any α in $|\tau| < k_2 \cos\theta_0$ according to the choice of brunch cuts, the solution of (2.16) can be written as

$$\begin{aligned} \Phi(x,\alpha) &= A(\alpha)e^{-\gamma x}, \quad x > 0, \\ &= B(\alpha)e^{\gamma x}, \quad x < 0. \end{aligned} \tag{2.17}$$

By imposing the condition that $\Phi(x,\alpha)$ be bounded as $|x| \to \infty$.

The electromagnetic surface currents on the strip can be described

$$I_e(z) = H_y^t(+0,z) - H_y^t(-0,z), \tag{2.18}$$

$$I_m(z) = E_z^t(+0,z) - E_z^t(-0,z). \tag{2.19}$$

where $I_e(z)$ and $I_m(z)$ are magnetic and electric surface currents on the strip, respectively. From (2.1), $I_e(z)$ and $I_m(z)$ can be expressed that

$$\begin{aligned} I_e(z) &= [\phi^i(+0,z) + \phi(+0,z) - \phi^i(-0,z) - \phi(-0,z)] \\ &= \phi(+0,z) - \phi(-0,z), \end{aligned} \tag{2.20}$$

$$I_m(z) = \frac{i}{\omega\varepsilon_0}\left[\left.\frac{\partial\phi(x,z)}{\partial x}\right|_{x=+0} - \left.\frac{\partial\phi(x,z)}{\partial x}\right|_{x=-0}\right]. \tag{2.21}$$

Using (2.1), (2.2), (2.5) and (2.18), we find that

$$\begin{aligned} 2R_e I_e(z) &= \frac{i}{\omega\varepsilon_0}\left[\left.\frac{\partial}{\partial x}\phi^t(x,z)\right|_{x=+0} + \left.\frac{\partial}{\partial x}\phi^t(x,z)\right|_{x=-0}\right] \\ &= 2Z_0 \sin\theta_0 e^{-ikz\cos\theta_0} + \frac{i}{\omega\varepsilon_0}\left[\left.\frac{\partial\phi(x,z)}{\partial x}\right|_{x=+0} + \left.\frac{\partial\phi(x,z)}{\partial x}\right|_{x=-0}\right]. \end{aligned} \tag{2.22}$$

Taking into account (2.1), (2.2), (2.4), and (2.19) and setting $x = \pm 0$, (2.5) can be expressed that

$$\begin{aligned} I_m(z) &= \left(\frac{1}{R_m} + \frac{\cos^2\theta_0}{\tilde{R}_e}\right)e^{-ikz\cos\theta_0} \\ &\quad + \left[\frac{1}{2R_m} + \frac{1}{2\tilde{R}_e}\left(1 + \frac{1}{k^2}\frac{\partial^2}{\partial x^2}\right)\right][\phi(x,z)|_{x=+0} + \phi(x,z)|_{x=-0}]. \end{aligned} \tag{2.23}$$

Multiplying both sides of the (2.22) and (2.23) by $(2\pi)^{-1/2}e^{i\alpha z}$ and integrating with respect to z over the range $(-a,a)$, we obtain that

$$J_e(\alpha)=\frac{1}{Y_0R_e}\frac{\sin\theta_0}{(2\pi)^{1/2}i}\frac{e^{i(\alpha-k\cos\theta_0)a}-e^{-i(\alpha-k\cos\theta_0)a}}{(\alpha-k\cos\theta_0)}$$
$$+\frac{i}{2kY_0R_e}[\Phi_1'(+0,\alpha)+\Phi_1'(-0,\alpha)], \tag{2.24}$$

where

$$J_e(\alpha)=(2\pi)^{-1/2}\int_{-a}^{a}I_e(z)e^{i\alpha z}dz, \tag{2.25}$$

$$\Phi_1'(\pm0,\alpha)=\left.\frac{d\Phi_1(x,\alpha)}{dx}\right|_{x=\pm0}=(2\pi)^{-1/2}\int_{-a}^{a}\left.\frac{\partial\phi(x,z)}{\partial x}\right|_{x=\pm0}e^{i\alpha z}dz. \tag{2.26}$$

Similarly from (2.23), we have

$$J_m(\alpha)=\frac{1}{(2\pi)^{1/2}i}\left(\frac{1}{R_m}+\frac{\cos^2\theta_0}{\tilde{R}_e}\right)\frac{e^{i(\alpha-k\cos\theta_0)a}-e^{-i(\alpha-k\cos\theta_0)a}}{(\alpha-k\cos\theta_0)}$$
$$+\left(\frac{1}{2R_m}+\frac{1}{2\tilde{R}_e}\right)[\Phi_1(+0,\alpha)+\Phi_1(-0,\alpha)]$$
$$+\frac{1}{2\tilde{R}_ek^2}[\Phi_1''(+0,\alpha)+\Phi_1''(-0,\alpha)], \tag{2.27}$$

where

$$J_m(\alpha)=(2\pi)^{-1/2}\int_{-a}^{a}I_m(z)e^{i\alpha z}dz, \tag{2.28}$$

$$\Phi_1(\pm0,\alpha)=(2\pi)^{-1/2}\int_{-a}^{a}\phi(\pm0,z)e^{i\alpha z}dz, \tag{2.29}$$

$$\Phi_1''(\pm0,\alpha)=\left.\frac{d^2\Phi_1(x,\alpha)}{dx^2}\right|_{x=\pm0}=(2\pi)^{-1/2}\int_{-a}^{a}\left.\frac{\partial^2\phi(x,z)}{\partial x^2}\right|_{x=\pm0}e^{i\alpha z}dz. \tag{2.30}$$

In (2.17), we set $x=\pm0$ and apply the expression of (2.13), we obtain that

$$A(\alpha)=e^{-i\alpha a}\Phi_-(+0,\alpha)+\Phi_1(+0,\alpha)+e^{i\alpha a}\Phi_+(+0,\alpha), \tag{2.31}$$
$$B(\alpha)=e^{-i\alpha a}\Phi_-(-0,\alpha)+\Phi_1(-0,\alpha)+e^{i\alpha a}\Phi_+(-0,\alpha). \tag{2.32}$$

We differentiate (2.17) with respect to x and set $x=\pm0$, we obtain that

$$-\gamma A(\alpha) = e^{-i\alpha a}\Phi'_{-}(+0,\alpha) + \Phi'_{1}(+0,\alpha) + e^{i\alpha a}\Phi'_{+}(+0,\alpha), \tag{2.33}$$

$$\gamma B(\alpha) = e^{-i\alpha a}\Phi'_{-}(-0,\alpha) + \Phi'_{1}(-0,\alpha) + e^{i\alpha a}\Phi'_{+}(-0,\alpha). \tag{2.34}$$

We calculate the second order derivative of (2.17) twice with respect to x and set $x = \pm 0$, we obtain that

$$\gamma^2 A(\alpha) = e^{-i\alpha a}\Phi''_{-}(+0,\alpha) + \Phi''_{1}(+0,\alpha) + e^{i\alpha a}\Phi''_{+}(+0,\alpha), \tag{2.35}$$

$$\gamma^2 B(\alpha) = e^{-i\alpha a}\Phi''_{-}(-0,\alpha) + \Phi''_{1}(-0,\alpha) + e^{i\alpha a}\Phi''_{+}(-0,\alpha). \tag{2.36}$$

Taking into account the boundary condition for tangential scattered fields

$$\left.\begin{aligned} &\phi(+0,z) = \phi(-0,z)[\equiv \phi(0,z)], \\ &\left.\frac{\partial\phi(x,z)}{\partial x}\right|_{x=+0} = \left.\frac{\partial\phi(x,z)}{\partial x}\right|_{x=-0}\left[\equiv \left.\frac{\partial\phi(x,z)}{\partial x^2}\right|_{x=0}\right], \\ &\left.\frac{\partial^2\phi(x,z)}{\partial x^2}\right|_{x=+0} = \left.\frac{\partial^2\phi(x,z)}{\partial x^2}\right|_{x=-0}\left[\equiv \left.\frac{\partial^2\phi(x,z)}{\partial x^2}\right|_{x=0}\right] \end{aligned}\right\} \tag{2.37}$$

for $|z| > a$, we find that

$$\left.\begin{aligned} &\Phi_{\pm}(+0,\alpha) = \Phi_{\pm}(-0,\alpha) \equiv \Phi_{\pm}(0,\alpha), \\ &\Phi'_{\pm}(+0,\alpha) = \Phi'_{\pm}(-0,\alpha) \equiv \Phi'_{\pm}(0,\alpha), \\ &\Phi''_{\pm}(+0,\alpha) = \Phi''_{\pm}(-0,\alpha) \equiv \Phi''_{\pm}(0,\alpha) \end{aligned}\right\} \tag{2.38}$$

Then, we see from (2.31), (2.32), (2.35), (2.36) and (2.38) that

$$A(\alpha) + B(\alpha) = 2[e^{-i\alpha a}\Phi_{-}(0,\alpha) + e^{i\alpha a}\Phi_{+}(0,\alpha)] + \Phi_{1}(+0,\alpha) + \Phi_{1}(-0,\alpha), \tag{2.39}$$

$$A(\alpha) - B(\alpha) = \Phi_{1}(+0,\alpha) - \Phi_{1}(-0,\alpha), \tag{2.40}$$

$$\gamma^2[A(\alpha) + B(\alpha)] = 2[e^{-i\alpha a}\Phi''_{-}(0,\alpha) + e^{i\alpha a}\Phi''_{+}(0,\alpha)] + \Phi''_{1}(+0,\alpha) + \Phi''_{1}(-0,\alpha), \tag{2.41}$$

$$\gamma^2[A(\alpha) - B(\alpha)] = \Phi''_{1}(+0,\alpha) - \Phi''_{1}(-0,\alpha). \tag{2.42}$$

Here, we see from (2.39) and (2.41) that

$$\Phi_{1}(+0,\alpha) + \Phi_{1}(-0,\alpha) = [A(\alpha) + B(\alpha)] - 2[e^{-i\alpha a}\Phi_{-}(0,\alpha) + e^{i\alpha a}\Phi_{+}(0,\alpha)], \tag{2.43}$$

$$\Phi''_{1}(+0,\alpha) + \Phi''_{1}(-0,\alpha) = \gamma^2[A(\alpha) + B(\alpha)] - 2[e^{-i\alpha a}\Phi''_{-}(0,\alpha) + e^{i\alpha a}\Phi''_{+}(0,\alpha)]. \tag{2.44}$$

Substituting (2.43) and (2.44) into (2.27), we can obtain that

$$\left(\frac{1}{2R_m}+\frac{1}{2\tilde{R}_e}+\frac{\gamma^2}{2\tilde{R}_e k^2}\right)[A(\alpha)+B(\alpha)]=\mathrm{e}^{-\mathrm{i}\alpha a}U_{-}(\alpha)+\mathrm{e}^{\mathrm{i}\alpha a}U_{(+)}(\alpha)+J_m(\alpha), \quad (2.45)$$

where

$$U_{\substack{(+)\\(-)}}(\alpha)=\tilde{\Phi}_{\pm}(\alpha)\mp\frac{A_{1,2}}{\alpha-k\cos\theta_0}, \quad (2.46)$$

$$\tilde{\Phi}_{\pm}(\alpha)=\left(\frac{1}{R_m}+\frac{1}{\tilde{R}_e}\right)\Phi_{\pm}(0,\alpha)+\frac{1}{\tilde{R}_e k^2}\frac{d^2\Phi_{\pm}(0,\alpha)}{dx^2}, \quad (2.47)$$

$$A_{1,2}=\frac{1}{(2\pi)^{1/2}i}\left(\frac{1}{R_m}+\frac{\cos^2\theta_0}{\tilde{R}_e}\right)e^{\mp ika\cos\theta_0}. \quad (2.48)$$

Similarly (2.33) and (2.34), we see that

$$\begin{aligned}-\gamma[A(\alpha)-B(\alpha)]=2[&e^{-i\alpha a}\Phi'_{-}(0,\alpha)+e^{i\alpha a}\Phi'_{+}(0,\alpha)]\\&+\Phi'_1(+0,\alpha)+\Phi'_1(-0,\alpha),\end{aligned} \quad (2.49)$$

$$-\gamma[A(\alpha)+B(\alpha)]=\Phi'_1(+0,\alpha)-\Phi'_1(-0,\alpha). \quad (2.50)$$

We find from (2.49) and (2.24) that

$$-\gamma[A(\alpha)-B(\alpha)]=-2ikY_0R_eJ_e(\alpha)+2V_{-}(\alpha)e^{-i\alpha a}+2V_{(+)}(\alpha)e^{i\alpha a}, \quad (2.51)$$

where

$$V_{\substack{(+)\\(-)}}(\alpha)=\Phi'_{\pm}(\alpha)\mp\frac{B_{1,2}}{\alpha-k\cos\theta_0}, \quad (2.52)$$

$$\Phi'_{\pm}(\alpha)=\frac{d\Phi_{\pm}(0,\alpha)}{dx}, \quad (2.53)$$

$$B_{1,2}=-\frac{k\sin\theta_0}{(2\pi)^{1/2}}e^{\mp ika\cos\theta_0}. \quad (2.54)$$

Taking into account (2.12), (2.20) and (2.25), (2.40) can be expressed that

$$A(\alpha)-B(\alpha)=\Phi_1(+0,\alpha)-\Phi_1(-0,\alpha)=J_e(\alpha). \quad (2.55)$$

Similarly from (2.21), (2.26) and (2.28), (2.50) can be obtained that

$$A(\alpha)+B(\alpha)=-\frac{1}{\gamma}[\Phi'_1(+0,\alpha)-\Phi'_1(-0,\alpha)]=\frac{ikY_0}{\gamma}J_m(\alpha). \quad (2.56)$$

It is seen from (2.55) and (2.56) that

$$A(\alpha)=\frac{1}{2}\left[J_e(\alpha)+\frac{\mathrm{i}kY_0}{\gamma}J_m(\alpha)\right], \tag{2.57}$$

$$B(\alpha)=-\frac{1}{2}\left[J_e(\alpha)-\frac{\mathrm{i}kY_0}{\gamma}J_m(\alpha)\right]. \tag{2.58}$$

Substituting (2.45) and (2.51) into (2.56) and (2.55), we obtain that

$$\left(\frac{1}{2R_m}+\frac{1}{2\tilde{R}_e}+\frac{\gamma^2}{2\tilde{R}_e k^2}\right)\frac{ikY_0}{\gamma}J_m(\alpha)=e^{-i\alpha a}U_-(\alpha)+e^{i\alpha a}U_{(+)}(\alpha)+J_m(\alpha), \tag{2.59}$$

$$-\gamma J_e(\alpha)=-2ikY_0R_eJ_e(\alpha)+2V_-(\alpha)e^{-i\alpha a}+2V_{(+)}(\alpha)e^{i\alpha a}. \tag{2.60}$$

We derive, after some manipulations, that

$$-M(\alpha)J_m(\alpha)=e^{-i\alpha a}U_-(\alpha)+e^{i\alpha a}U_{(+)}(\alpha), \tag{2.61}$$

$$-K(\alpha)J_e(\alpha)=2[e^{-i\alpha a}V_-(\alpha)+e^{i\alpha a}V_{(+)}(\alpha)], \tag{2.62}$$

where

$$M(\alpha)=1-\frac{ikY_0}{2\gamma}\left[\frac{1}{R_m}+\frac{1}{\tilde{R}_e}\left(1+\frac{\gamma^2}{k^2}\right)\right], \tag{2.63}$$

$$K(\alpha)=\gamma-2ikY_0R_e. \tag{2.64}$$

Equations (2.61) and (2.62) are the Wiener-Hopf equations satisfied by unknown spectral functions, where $J_m(\alpha)$ and $J_e(\alpha)$ are the Fourier transform of magnetic and electric surface currents on the strip, respectively. In the above notation, the subscripts '+' and '−' imply that the functions are regular in upper $(\tau>-k_2\cos\theta_0)$ and lower $(\tau<k_2\cos\theta_0)$ half-planes, respectively, whereas the subscript '(+)' implies that the functions are regular in $\tau>-k_2\cos\theta_0$ except for a simple pole at $\alpha=k\cos\theta_0$. We shall henceforth use these conventions for indicating the region of regularity in the α-plane.

2.3. Factorization of the Kernel Functions

In this section, we shall factorize the kernel functions $M(\alpha)$ and $K(\alpha)$ defined by (2.63) and (2.64) with the aid of Noble's approach [12]. The factorization is to split $M(\alpha)$ and $K(\alpha)$ into the multiplication form as in

$$M(\alpha)=M_{+}(\alpha)M_{-}(\alpha)=M_{+}(\alpha)M_{+}(-\alpha), \tag{2.65}$$

$$K(\alpha)=K_{+}(\alpha)K_{-}(\alpha)=K_{+}(\alpha)K_{+}(-\alpha), \tag{2.66}$$

where $M_{\pm}(\alpha)$ and $K_{\pm}(\alpha)$ are regular and nonzero in $\tau \gtrless \mp k_2\cos\theta_0$. In order to factorize $M(\alpha)$ and $K(\alpha)$, let us introduce the auxiliary functions $N_n(\alpha)$ as [39]

$$N_n(\alpha)=1+\frac{i}{k\delta_n}\gamma, \quad n=1,2,3, \tag{2.67}$$

where

$$\delta_{1,2}=-\frac{\tilde{R}_e}{Y_0}\left\{1\pm\left[1+\frac{Y_0^2}{\tilde{R}_e}\left(\frac{1}{R_m}+\frac{1}{\tilde{R}_e}\right)\right]^{1/2}\right\}, \tag{2.68}$$

$$\delta_3=2Y_0R_e. \tag{2.69}$$

Substituting (2.67) into (2.61) and (2.64), respectively, it follows that

$$M(\alpha)=\frac{kY_0}{2i}\left(\frac{1}{R_m}+\frac{1}{\tilde{R}_e}\right)\frac{N_1(\alpha)N_2(\alpha)}{\gamma}, \tag{2.70}$$

$$K(\alpha)=-2ikY_0R_eN_3(\alpha). \tag{2.71}$$

Assuming that $N_n(\alpha)$ in (2.67) can be factorized as

$$N_n(\alpha)=N_{n+}(\alpha)N_{n-}(\alpha)=N_{n+}(\alpha)N_{n+}(-\alpha), \tag{2.72}$$

where $N_{n\pm}(\alpha)$ is regular and nonzero in $\tau \gtrless \mp k_2\cos\theta_0$, and the split functions $N_{n\pm}(\alpha)$ are expressed as follows:

$$N_{n\pm}(\alpha)=N_n^{1/2}(0)\exp\left\{\int_0^{\alpha}\frac{d}{d\beta}[\ln N_{n\pm}(\beta)]\,d\beta\right\}, \tag{2.73}$$

where

$$N_n(0)=1+i\frac{1}{k\delta_n}\gamma\bigg|_{\alpha=0}=1+\frac{1}{\delta_n} \tag{2.74}$$

with

$$\gamma\big|_{\alpha=0}=(\alpha^2-k^2)^{1/2}\big|_{\alpha=0}=-i(k^2-\alpha^2)^{1/2}\big|_{\alpha=0}=-ik. \tag{2.75}$$

We can show that $N_n(\alpha)$ in (2.67) can be written as

$$\frac{d}{d\alpha}[\ln N_n(\alpha)] = \frac{N_n'(\alpha)}{N_n(\alpha)} = \frac{\alpha}{\alpha^2 + k^2(\delta_n^2 - 1)}\left(\frac{\mathrm{i}k\delta_n}{\gamma} + 1\right)$$
$$= \frac{1}{2}\left(\frac{1}{\alpha - id_n} + \frac{1}{\alpha + id_n}\right) + \frac{ik\delta_n}{2}\left(\frac{1}{\alpha - id_n} + \frac{1}{\alpha + id_n}\right)L(\alpha), \quad (2.76)$$

where

$$L(\alpha) = \frac{1}{\gamma} = (\alpha^2 - k^2)^{-1/2}, \quad (2.77)$$

$$d_n = k(\delta_n^2 - 1)^{1/2}. \quad (2.78)$$

According to [12], (2.77) can be decomposed as

$$L(\alpha) = L_+(\alpha) + L_-(\alpha) = L_+(\alpha) + L_+(-\alpha), \quad (2.79)$$

where

$$L_\pm(\alpha) = \frac{1}{\pi\gamma}\arccos(\pm\alpha / k) = -i\frac{1}{\pi\gamma}\ln\left(\frac{\pm\alpha - \gamma}{k}\right). \quad (2.80)$$

In (2.80), $L_\pm(\alpha)$ is regular and nonzero in $\tau \gtrless \mp k_2$, respectively.

We find from (2.76) and (2.79) that

$$\frac{d}{d\alpha}[\ln N_{n\pm}(\alpha)] = -\frac{ik\delta_n}{2}\left[\frac{L_\pm(id_n)}{\alpha - id_n} + \frac{L_\mp(id_n)}{\alpha + id_n}\right] + ik\delta_n\frac{\alpha L_\pm(\alpha)}{\alpha^2 + d_n^2}, \quad (2.81)$$

where

$$L_\pm(id_n) = \frac{1}{k\delta_n}\left\{\frac{i}{2} \pm \frac{\ln[\delta_n + (\delta_n^2 - 1)^{1/2}]}{\pi}\right\}. \quad (2.82)$$

Setting $\alpha = \beta$ in (2.81) and integrating both side of (2.81) with respect to β over $(0, \alpha)$, we obtain that

$$\int_0^\alpha \frac{d[\ln N_n(\beta)]}{d\beta} d\beta = ik\delta_n \int_0^\alpha \frac{\beta L_+(\beta)}{\beta^2 + d_n^2} d\beta - \frac{ik\delta_n}{2} L_+(id_n) \int_0^\alpha \frac{1}{\beta - id_n} d\beta$$
$$- \frac{ik\delta_n}{2} L_-(id_n) \int_0^\alpha \frac{1}{\beta + id_n} d\beta$$
$$= ik\delta_n \int_0^\alpha \frac{\beta L_+(\beta)}{\beta^2 + d_n^2} d\beta$$
$$- \frac{ik\delta_n}{2} \left[L_+(id_n) \ln\left(\frac{\alpha - id_n}{-id_n} \right) + L_-(id_n) \ln\left(\frac{\alpha + id_n}{id_n} \right) \right]. \quad (2.83)$$

Substituting (2.83) into (2.73), we derive after some manipulations, that

$$N_{n\pm}(\alpha) = \left(1 + \frac{1}{\delta_n} \right)^{1/2} \exp\left\{ -\frac{\delta_n}{\pi} \int_{\pi/2}^{\arccos(\pm\alpha/k)} \frac{t \cos t}{\sin^2 t - \delta_n^2} dt \right.$$
$$\pm \frac{i}{2\pi} \ln[\delta_n + (\delta_n^2 - 1)^{1/2}] \ln\left[\frac{ik(\delta_n^2 - 1)^{1/2} + \alpha}{ik(\delta_n^2 - 1)^{1/2} - \alpha} \right]$$
$$\left. + \frac{1}{4} \ln\left[1 + \frac{\alpha^2}{k^2(\delta_n^2 - 1)} \right] \right\} \quad (2.84)$$

as $n = 1, 2, 3.$ Using (2.84), we find that the split functions $M_\pm(\alpha)$ and $K_\pm(\alpha)$ are expressed as

$$M_\pm(\alpha) = \left[\frac{kY_0}{2} \left(\frac{1}{R_m} + \frac{1}{\tilde{R}_e} \right) \right]^{1/2} \frac{N_{1\pm}(\alpha) N_{2\pm}(\alpha)}{(k \pm \alpha)^{1/2}}, \quad (2.85)$$

$$K_\pm(\alpha) = (2kY_0 R_e)^{1/2} e^{-i\pi/4} N_{3\pm}(\alpha), \quad (2.86)$$

where $M_\pm(\alpha)$ and $K_\pm(\alpha)$ are regular and nonzero in the half-plane $\tau \gtrless \mp k_2 \cos\theta_0$, and show an algebraic behavior at infinity.

2.4. Formal Solution

Multiplying both sides of (2.61) by $e^{\pm i\alpha a} / M_\mp(\alpha)$, we obtain that

$$-e^{-i\alpha a} J_m(\alpha) M_-(\alpha) = e^{-2i\alpha a} \frac{U_-(\alpha)}{M_+(\alpha)} + \frac{U_{(+)}(\alpha)}{M_+(\alpha)}, \quad (2.87)$$

$$-e^{i\alpha a} J_m(\alpha) M_+(\alpha) = e^{2i\alpha a} \frac{U_{(+)}(\alpha)}{M_-(\alpha)} + \frac{U_-(\alpha)}{M_-(\alpha)}. \quad (2.88)$$

Since $-e^{\mp i\alpha a}J_m(\alpha)$ is an entire function, the left-hand sides of (2.87) and (2.88) are regular in the upper $(\tau > -k_2\cos\theta_0)$ and the lower $(\tau < k_2\cos\theta_0)$ half-plane, respectively. In the right-hand sides of (2.87) and (2.88), the terms of $e^{-2i\alpha a}U_-(\alpha)/M_+(\alpha)$, $U_{(+)}(\alpha)/M_+(\alpha)$, and $e^{2i\alpha a}U_{(+)}(\alpha)/M_-(\alpha)$ are regular in the strip $|\tau| < k_2\cos\theta_0$, and the term $U_-(\alpha)/M_-(\alpha)$ is regular in the lower $(\tau < k_2\cos\theta_0)$ half-plane. Hence, in accordance with the Wiener-Hopf procedure, we must decompose the terms on the right-hand sides of (2.87) and (2.88) which are regular in strip $|\tau| < k_2\cos\theta_0$ into the sum of two functions regular in the half planes $\tau \gtrless \mp k_2\cos\theta_0$.

Applying the edge condition [42] and the fundamental theorem on the asymptotic behavior of the Fourier integral, we find that

$$\left.\begin{aligned} U_{(\pm)}(\alpha) &= O(\alpha^{-3/2}), \\ M_{\pm}(\alpha) &= O(\alpha^{1/2}) \end{aligned}\right\} \tag{2.89}$$

as $\alpha \to \infty$. Wee see from (2.89) that the first terms of the right-hand sides of (2.87) and (2.88) are $O(|\sigma|^{-2})$ uniformly in τ as $|\sigma| \to \infty$ in the strip $|\tau| < k_2\cos\theta_0$. Applying the standard decomposition theorem based on Cauchy's integral formula [5], wee obtain that

$$e^{-2i\alpha a}\frac{U_-(\alpha)}{M_+(\alpha)} = \frac{1}{2\pi i}\int_{C_1}\frac{e^{-2i\beta a}U_-(\beta)}{M_+(\beta)(\beta-\alpha)}d\beta - \frac{1}{2\pi i}\int_{C_2}\frac{e^{-2i\beta a}U_-(\beta)}{M_+(\beta)(\beta-\alpha)}d\beta, \tag{2.90}$$

$$e^{2i\alpha a}\frac{U_{(+)}(\alpha)}{M_-(\alpha)} = \frac{1}{2\pi i}\int_{C_1}\frac{e^{2i\beta a}U_{(+)}(\beta)}{M_-(\beta)(\beta-\alpha)}d\beta - \frac{1}{2\pi i}\int_{C_2}\frac{e^{2i\beta a}U_{(+)}(\beta)}{M_-(\beta)(\beta-\alpha)}d\beta, \tag{2.91}$$

where C_1 and C_2 are the infinite integration paths parallel to the real axis, as shown in Fig. 2.2. In (2.87), $U_{(+)}(\alpha)/M_+(\alpha)$ is regular in the upper $(\tau > -k_2\cos\theta_0)$ half-plane except $\alpha = k\cos\theta_0$, and we decompose $U_{(+)}(\alpha)/M_+(\alpha)$ that

$$\frac{U_{(+)}(\alpha)}{M_+(\alpha)} = H_+^a(\alpha) + H_-^b(\alpha), \tag{2.92}$$

where

$$\left.\begin{aligned} H_+^a(\alpha) &= \frac{U_{(+)}(\alpha)}{M_+(\alpha)} + \frac{A_1}{M_+(k\cos\theta_0)(\alpha - k\cos\theta_0)}, \\ H_-^b(\alpha) &= -\frac{A_1}{M_+(k\cos\theta_0)(\alpha - k\cos\theta_0)}. \end{aligned}\right\} \tag{2.93}$$

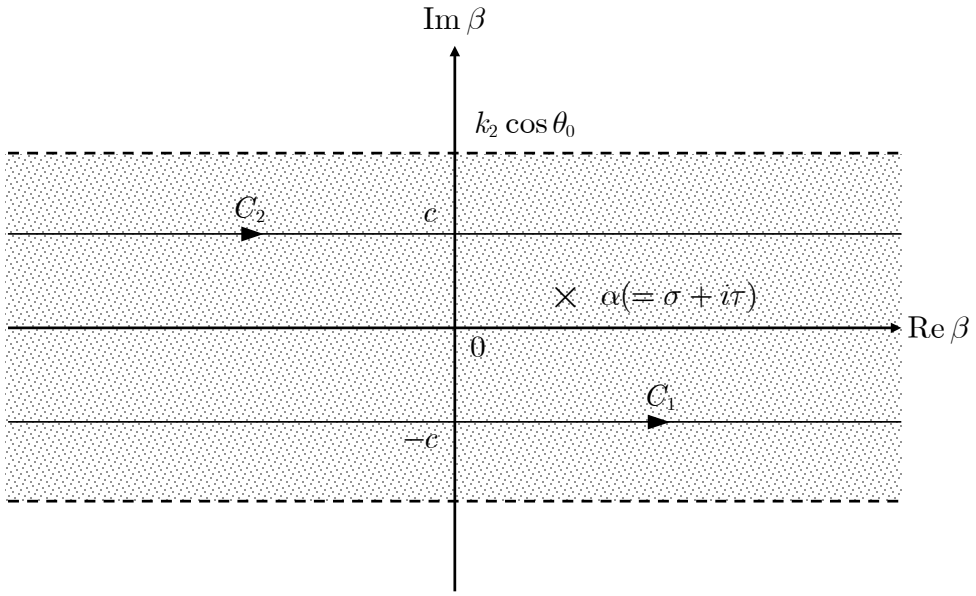

Fig. 2.2 Integral paths C_1 and C_2 for decomposition $(0 < \tau < c < k_2 \cos\theta_0)$.

Substituting the decomposition result of (2.90)-(2.93) into (2.87) and (2.88), we can express that

$$-e^{-i\alpha a} M_-(\alpha) J_m(\alpha) - H_-^b(\alpha) + \frac{1}{2\pi i}\int_{C_2} \frac{e^{-2i\beta a} U_-(\beta)}{M_+(\beta)(\beta-\alpha)} d\beta$$
$$= H_+^a(\alpha) + \frac{1}{2\pi i}\int_{C_1} \frac{e^{-2i\beta a} U_-(\beta)}{M_+(\beta)(\beta-\alpha)} d\beta, \tag{2.94}$$

$$\frac{U_-(\alpha)}{M_-(\alpha)} - \frac{1}{2\pi i}\int_{C_2} \frac{e^{2i\beta a} U_{(+)}(\beta)}{M_-(\beta)(\beta-\alpha)} d\beta$$
$$= -e^{i\alpha a} M_+(\alpha) J_m(\alpha) - \frac{1}{2\pi i}\int_{C_1} \frac{e^{2i\beta a} U_{(+)}(\beta)}{M_-(\beta)(\beta-\alpha)} d\beta, \tag{2.95}$$

where the left-hand and the right-hand sides of (2.94) and (2.95) are regular in the lower $(\tau < k_2 \cos\theta_0)$ and the upper $(\tau > -k_2 \cos\theta_0)$ half-plane, respectively, and both sides have a common strip of regularity in the strip $|\tau| < k_2 \cos\theta_0$. Hence, argument of the analytic continuation shows that there exists an entire function, denoted by $P(\alpha)$, which coincides with the left-hand and the right-hand sides of (2.94) and (2.95) are regular in the lower $(\tau < k_2 \cos\theta_0)$ and the upper $(\tau > -k_2 \cos\theta_0)$ half-plane, respectively. Taking into account (2.89) and the asymptotic behavior of the split functions, we see that the integrals in (2.94) and (2.95) are $o(1)$ as $\alpha \to \infty$. Therefore, it is seen from the Liouville's theorem that $P(\alpha) \equiv 0$. Thus, we obtain that

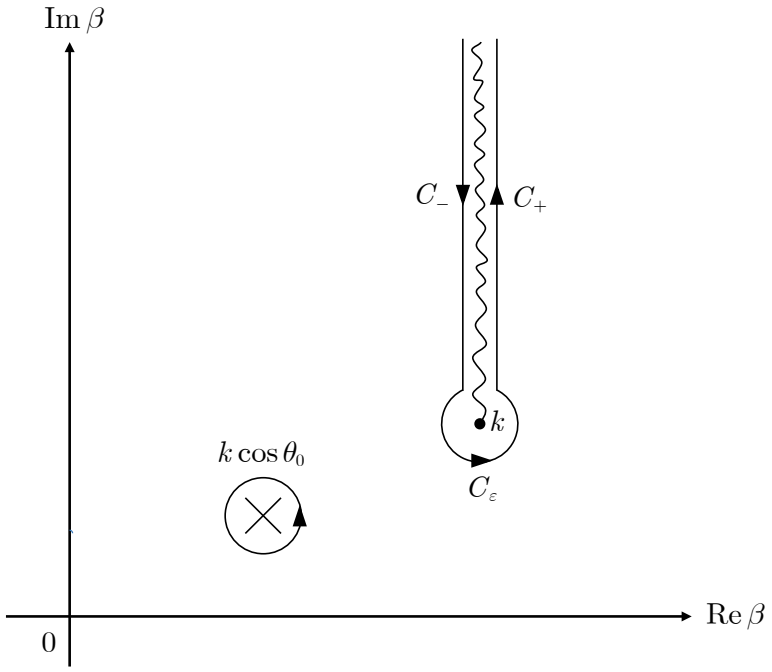

Fig. 2.3 Integral path $C(=C_- + C_\varepsilon + C_+)$.

$$\frac{U_{(+)}(\alpha)}{M_+(\alpha)} + \frac{A_1}{M_+(k\cos\theta_0)(\alpha - k\cos\theta_0)} + \frac{1}{2\pi i}\int_{C_1} \frac{e^{-2i\beta a}U_-(\beta)}{M_+(\beta)(\beta-\alpha)}d\beta = 0, \qquad (2.96)$$

$$\frac{U_-(\alpha)}{M_-(\alpha)} - \frac{1}{2\pi \mathrm{i}}\int_{C_2} \frac{\mathrm{e}^{2\mathrm{i}\beta a}U_{(+)}(\beta)}{M_-(\beta)(\beta-\alpha)}\mathrm{d}\beta = 0. \qquad (2.97)$$

Equations (2.96) and (2.97) are a set of two coupled integral equations for $U_{(+)}(\alpha)$ and $U_-(\alpha)$. However, they may be decoupled in a following manner. Seting $\alpha \to -\alpha$ in (2.97) and making a change of variable $\beta \to -\beta$ in (2.96), we derive, after the manipulations of the sum and difference of the resultant equations, that

$$\frac{U^{s,d}_{(+)}(\alpha)}{M_+(\alpha)} = -\frac{A_1}{M_+(k\cos\theta_0)(\alpha - k\cos\theta_0)} \pm \frac{1}{2\pi i}\int_{C_2} \frac{e^{2i\beta a}U^{s,d}_{(+)}(\beta)}{M_-(\beta)(\beta+\alpha)}d\beta, \qquad (2.98)$$

where

$$\begin{aligned} U^{s,d}_{(+)}(\alpha) &= U_{(+)}(\alpha) \pm U_-(-\alpha) \\ &= \tilde{\Phi}^{s,d}_+(\alpha) - \frac{A_1}{(\alpha - k\cos\theta_0)} \mp \frac{A_2}{(\alpha + k\cos\theta_0)} \end{aligned} \qquad (2.99)$$

with

$$\tilde{\Phi}_{+}^{s,d}(\alpha) = \tilde{\Phi}_{+}(\alpha) \pm \tilde{\Phi}_{-}(-\alpha). \tag{2.100}$$

It is verified from (2.99) that the singularities associated with the integral in (2.98) for $\mathrm{Im}\,\beta > c$ $(0 < |\tau| < c < k_2 \cos\theta_0)$ have a simple pole at $\beta = k\cos\theta_0$ and a branch point at $\beta = k$. We now choose a branch cut emanating from $\beta = k$ as a straight line that is parallel to the imaginary axis and goes to infinity in the upper half-plane. Then evaluating the integral by enclosing the contour into the upper half-plane, yields

$$U_{(+)}^{s,d}(\alpha) = M_{+}(\alpha)\left[-\frac{A_1}{M_{+}(k\cos\theta_0)(\alpha - k\cos\theta_0)} \right.$$
$$\left. \mp \frac{A_2}{M_{-}(k\cos\theta_0)(\alpha + k\cos\theta_0)} \pm u_{s,d}(\alpha) \right], \tag{2.101}$$

where

$$u_{s,d}(\alpha) = \frac{1}{2\pi i}\int_C \frac{e^{2i\beta a} U_{(+)}^{s,d}(\beta)}{M_{-}(\beta)(\beta + \alpha)} d\beta. \tag{2.102}$$

In (2.102), C is the contour composed of a portion C_ε of a circle with radius $\varepsilon \ll 1$ centered at $\beta = k$ and semi-infinite straight paths $C_{\pm}$ along the branch cut, as shown in Fig. 2.3. We find that the contribution from C_ε tends to zero by letting $\varepsilon \to 0$. On the other hand, the contributions from $C_{\pm}$ can be combined to yield a single branch-cut integral by noting that

$$(\beta^2 - k^2)^{1/2}\Big|_{\beta \in C_+} = -(\beta^2 - k^2)^{1/2}\Big|_{\beta \in C_-}. \tag{2.103}$$

After letting $\varepsilon \to 0$ and $1/M_{-}(\beta) \to M_{+}(\beta)/M(\beta)$, we obtain, making some arrangements, that

$$u_{s,d}(\alpha) = \frac{1}{\pi i}\int_k^{k+i\infty} \frac{e^{2i\beta a}(\beta - k)^{1/2}}{\beta + \alpha} U_{(+)}^{s,d}(\beta) F_{+}(\beta) d\beta, \tag{2.104}$$

where

$$F_{+}(\beta) = \frac{ikY_0}{2} \frac{[1/R_m + \beta^2/(\tilde{R}_e k^2)](\beta + k)^{1/2} M_{+}(\beta)}{\beta^2 - k^2 + k^2 Y_0^2 [1/R_m + \beta^2/(\tilde{R}_e k^2)]^2/4}. \tag{2.105}$$

In (2.104), the contour is the one running parallel to the imaginary axis on the right-hand side of the brunch-cut. Substituting (2.104) into (2.101) and solving for $U_{(+)}(\alpha)$, we obtain that

$$U_{(+)}(\alpha)=M_{+}(\alpha)\left[-\frac{A_1}{M_{+}(k\cos\theta_0)(\alpha-k\cos\theta_0)}-\frac{u_{s,d}(\alpha)-u_{s,d}(\alpha)}{2}\right], \tag{2.106}$$

$$U_{-}(\alpha)=M_{-}(\alpha)\left[\frac{A_2}{M_{-}(k\cos\theta_0)(\alpha-k\cos\theta_0)}+\frac{u_{s,d}(-\alpha)+u_{s,d}(-\alpha)}{2}\right]. \tag{2.107}$$

Equation (2.62) can be solved in a similar manner. We multiply both sides of (2.62) by $e^{\pm i\alpha a}/K_{\mp}(\alpha)$. Applying the edge condition and the fundamental theorem on the asymptotic behavior of the Fourier integral, we find that

$$\left.\begin{aligned} V_{(\pm)}(\alpha)&=O(\alpha^{-1/2}),\\ K_{\pm}(\alpha)&=O(\alpha^{1/2}) \end{aligned}\right\} \tag{2.108}$$

as $\alpha\to\infty$. Decomposing the resultant equations and making some manipulations, we obtain that

$$\frac{V_{(+)}(\alpha)}{K_{+}(\alpha)}+\frac{B_1}{K_{+}(k\cos\theta_0)(\alpha-k\cos\theta_0)}+\frac{1}{2\pi i}\int_{C_1}\frac{e^{-2i\beta a}V_{-}(\beta)}{K_{+}(\beta)(\beta-\alpha)}d\beta=0, \tag{2.109}$$

$$\frac{V_{-}(\alpha)}{K_{-}(\alpha)}-\frac{1}{2\pi i}\int_{C_2}\frac{e^{2i\beta a}V_{(+)}(\beta)}{K_{-}(\beta)(\beta-\alpha)}d\beta=0. \tag{2.110}$$

where C_1 and C_2 are the infinite integration paths shown in Fig. 2.1. A similar procedure can be also be applied to (2.109) and (2.110). Omitting the details, we obtain that

$$\begin{aligned} V_{(+)}^{s,d}(\alpha)=K_{+}(\alpha)\Bigg[&-\frac{B_1}{K_{+}(k\cos\theta_0)(\alpha-k\cos\theta_0)}\\ &\mp\frac{B_2}{K_{-}(k\cos\theta_0)(\alpha+k\cos\theta_0)}\pm v_{s,d}(\alpha)\Bigg], \end{aligned} \tag{2.111}$$

where

$$V_{(+)}^{s,d}(\alpha)=V_{(+)}(\alpha)\pm V_{-}(-\alpha), \tag{2.112}$$

$$v_{s,d}(\alpha)=\frac{1}{\pi i}\int_{k}^{k+i\infty}\frac{e^{2i\beta a}(\beta-k)^{1/2}}{\beta+\alpha}V_{(+)}^{s,d}(\beta)T_{+}(\beta)d\beta, \tag{2.113}$$

$$T_+(\beta)=\frac{(\beta+k)^{1/2}K_+(\beta)}{\beta^2-k^2+4k^2Y_0^2R_e^2}. \tag{2.114}$$

Substituting (2.111) into (2.112) and solving for $V_{(\pm)}(\alpha)$, we obtain that

$$V_{(+)}(\alpha)=K_+(\alpha)\left[-\frac{B_1}{K_+(k\cos\theta_0)(\alpha-k\cos\theta_0)}-\frac{v_{s,d}(\alpha)-v_{s,d}(\alpha)}{2}\right], \tag{2.115}$$

$$V_-(\alpha)=K_-(\alpha)\left[\frac{B_2}{K_-(k\cos\theta_0)(\alpha-k\cos\theta_0)}+\frac{v_{s,d}(-\alpha)+v_{s,d}(-\alpha)}{2}\right]. \tag{2.116}$$

Equations (2.106), (2.107), (2.115) and (2.116) the exact solutions to the Wiener-Hopf equations (2.61) and (2.62), respectively, but they are formal in the sense that the branch-cut integrals with unknown integrands $u_{s,d}(\alpha)$ and $v_{s,d}(\alpha)$ are involved. Accordingly, it is required to develop approximation procedures for these integrals to derive explicit solutions.

2.5. Asymptotic Solution of a Certain Integral Equation in the Complex Plane

In this section, we shall consider a certain integral equation in the complex plane that often arises in the Wiener-Hopf analysis of canonical scattering problems, and discuss a method of solution in detail. The results obtained in this section will provide a generalization of the method developed in our previous papers [38].

The Wiener-Hopf analysis often leads to the following exact solution in the complex plane:

$$f(\alpha)=h(\alpha)\left[g(\alpha)+\frac{C}{\pi i}\int_k^{k+i\infty}e^{i\beta l}\frac{(\beta-k)^{\nu}G(\beta)f(\beta)}{\beta+\alpha}d\beta\right]. \tag{2.117}$$

In (2.117), $f(\alpha)$ is the unknown function to be determined, and all the other quantities are known constants or functions.

Let $f(\beta)$ be a function of a complex variable β satisfying the following conditions:

(i) *$f(\beta)$ is an analytic function of β regular in $|\beta-k|<\varepsilon<\infty$, where $k=k_1+ik_2$ with $k_1>0$, $k_2>0$, and $\varepsilon\neq 0$.*

(ii) *$f(\beta)$ satisfies $O[(\beta-k)^{\delta}]$ for any β such that $|\beta-k|\geq R$ with $\varepsilon<R<\infty$, where δ is some real constant.*

(iii) $f(\beta)$ *is a continuous function of* β *on any bounded part of the semi-infinite straight path from* k *to* $k+i\infty$ *in the* β*-plane.*

Let α be a complex variable such that $|\alpha+k|>0$ and $-\pi/2<\arg(\alpha+k)<3\pi/2,$ and introduce

$$F_m^{\nu}(l,\alpha)=\frac{1}{\pi i}\int_k^{k+i\infty}e^{i\beta l}\frac{(\beta-k)^{\nu}G(\beta)f(\beta)}{(\beta+\alpha)^m}d\beta \tag{2.118}$$

for $l>0,\ \mathrm{Re}\,\nu>-1,$ and positive integer $m,$ where $\arg(\beta-k)=\pi/2.$ In (2.118), $G(\beta)$ is regular in the neighborhood of $\beta=k,$ and shows an algebraic behavior as $\beta\to\infty$ in the upper half-plane.

We define the region in the α-plane as follows:

$$D=\left\{\alpha:|\alpha+k|>0,-\pi/2<\arg(\alpha+k)<3\pi/2\right\}. \tag{2.119}$$

Then it is shown that the function $F_m^{\nu}(l,\alpha)$ defined by (2.118) is uniformly convergent in any bounded closed region in D and hence, regular in D. We can prove the following theorem on the asymptotic expansion of $F_m^{\nu}(l,\alpha)$ for large l:

Theorem. *The function* $F_m^{\nu}(l,\alpha)$ *has an asymptotic expansion*

$$F_m^{\nu}(l,\alpha)\sim\frac{e^{ikl}}{\pi}\sum_{n=0}^{\infty}f_n\frac{i^{\nu-m+n}}{l^{\nu-m+n+1}}\Gamma_m^g[\nu+n+1,-i(\alpha+k)l] \tag{2.120}$$

as $l\to\infty,$ *where*

$$f_n=\frac{1}{n!}\frac{d^nf(\beta)}{d\beta^n}\bigg|_{\beta=k}. \tag{2.121}$$

In (2.120), $\Gamma_m^g(\cdot,\cdot)$ *is the special function defined by*

$$\Gamma_m^g(u,w)=\int_0^{\infty}\frac{t^{u-1}e^{-t}}{(t+w)^m}G(k+it/l)dt \tag{2.122}$$

for $\mathrm{Re}\,u>0,\ |w|>0,\ |\arg w|<\pi,$ *and positive integer* $m.$

The above theorem reduces to the results obtained in [37], [38] by setting $G(\beta)\equiv1.$

Using the function $F_m^{\nu}(l,\alpha),$ (2.118) can be written as

$$f(\alpha)=h(\alpha)[g(\alpha)+CF_1^{\nu}(l,\alpha)], \tag{2.123}$$

where it is assumed that $f(\alpha)$ satisfies the conditions (i)-(iii), and $g(\alpha)$ and $h(\alpha)$

are regular in region Δ contained in D. Then we can apply Theorem to derive an asymptotic expansion of $F_1^{\nu}(l,\alpha)$ for large l. Thus we obtain from (2.123) that

$$f(\alpha) \sim h(\alpha)\left[g(\alpha) + C\sum_{n=0}^{\infty} f_n \xi_{0n}^{g}(\nu,l,\alpha) \right] \tag{2.124}$$

as $l \to \infty$, where f_n is defined by (2.121), and

$$\xi_{0n}^{g}(\nu,l,\alpha) = \frac{e^{ikl}}{\pi} \frac{i^{n+\nu-1}}{l^{n+\nu}} \Gamma_1^{g}[\nu+n+1, -i(\alpha+k)l]. \tag{2.125}$$

Equation (2.124) is the asymptotic solution of the integral equation (2.123) for large l, where an infinite number of unknowns f_n with $n = 0,1,2,\cdots$ are contained. Hence, it is required to derive matrix equations for these unknowns in an appropriate manner.

Setting $\alpha = k$ in (2.124), and using the notation (2.121), we find that

$$f_0 \sim h(k)\left[g(k) + C\sum_{n=0}^{\infty} f_n \xi_{0n}^{g}(\nu,l,k) \right]. \tag{2.126}$$

We now differentiate both sides of (2.124) m times $(m = 1,2,3,\cdots)$ with respect to α by taking into account the regularity of $F_m^{\nu}(l,\alpha)$ in D, and setting $\alpha = k$ in the resultant equation, we obtain that

$$f_m \sim \sum_{p=0}^{m} \frac{h^{(m-p)}(k)}{p!(m-p)!}\left[g^{(p)}(k) + C\sum_{n=0}^{\infty} f_n \xi_{pn}^{g}(\nu,l,k) \right] \tag{2.127}$$

for $m = 1,2,3,\cdots$,

$$h^{(m-p)}(k) = \left. \frac{d^{m-p}h(\alpha)}{d\alpha^{m-p}} \right|_{\alpha=k}, \tag{2.128}$$

$$g^{(p)}(k) = \left. \frac{d^{p}g(\alpha)}{d\alpha^{p}} \right|_{\alpha=k}, \tag{2.129}$$

$$\xi_{pn}^{g}(\nu,l,k) = \frac{e^{ikl}}{\pi}(-1)^p p! \frac{i^{n-p+\nu-1}}{l^{n-p+\nu}} \Gamma_{p+1}(\nu+n+1, -2ikl). \tag{2.130}$$

Hence it follows from (2.126) and (2.127) that

$$f_m - C\sum_{n=0}^{\infty} A_{mn} f_n \sim B_m, \quad m = 0,1,2,\cdots \tag{2.131}$$

for large l, where

$$A_{mn} = \sum_{p=0}^{m} \frac{h^{(m-p)}(k)\xi_{pn}^{g}(\nu,l,k)}{p!(m-p)!}, \tag{2.132}$$

$$B_m = \sum_{p=0}^{m} \frac{h^{(m-p)}(k)g^{(p)}(k)}{p!(m-p)!}. \tag{2.133}$$

Equation (2.131) provides the desired matrix equation for determining the unknowns f_n with $n = 0,1,2,\cdots$ in (2.124), and it is valid for large l.

2.6. High-Frequency Asymptotic Solutions

In this section, we shall apply the method established in the previous section to solve (2.101) and (2.111) asymptotically. In order to eliminate the singularities of $U_{(+)}^{s,d}(\alpha)$ (2.101) at $\alpha = k\cos\theta_0$, we introduce the auxiliary functions $\tilde{\Phi}_{+}^{s,d}(\alpha)$ as

$$\tilde{\Phi}_{+}^{s,d}(\alpha) = U_{(+)}^{s,d}(\alpha) + \frac{A_1}{\alpha - k\cos\theta_0} \pm \frac{A_2}{\alpha + k\cos\theta_0}, \tag{2.134}$$

where $\tilde{\Phi}_{+}^{s,d}(\alpha)$ is regular in the upper half-plane $\tau > -k_2\cos\theta_0$. Substituting (2.134) into (2.101) and carrying out some manipulation, we describe that

$$\tilde{\Phi}_{+}^{s,d}(\alpha) = M_{+}(\alpha)[\chi_{us,ud}(\alpha) + C_{s,d}F_{s,d}^{u}(\alpha)], \tag{2.135}$$

$$\chi_{us,ud}(\alpha) = A_1[P_1(\alpha) \pm \eta_{f2}(\alpha)] + A_2[\eta_{f1}(\alpha) \pm P_2(\alpha)], \tag{2.136}$$

$$C_{s,d} = \pm 1, \tag{2.137}$$

$$F_{s,d}^{u}(\alpha) = \frac{1}{\pi i}\int_{k}^{k+i\infty} \frac{e^{2i\beta a}(\beta - k)^{1/2}}{\beta + \alpha}\tilde{\Phi}_{+}^{s,d}(\beta)F_{+}(\beta)d\beta \tag{2.138}$$

with

$$P_{1,2}(\alpha) = \frac{1}{\alpha \mp k\cos\theta_0}\left[\frac{1}{M_{+}(\alpha)} - \frac{1}{M_{\pm}(k\cos\theta_0)}\right], \tag{2.139}$$

$$\eta_{f1,f2}(\alpha)=\frac{\xi_{00}^{f}(\alpha)-\xi_{00}^{f}(\pm k\cos\theta_0)}{\alpha\mp k\cos\theta_0}, \tag{2.140}$$

$$\xi_{00}^{f}(\alpha)=\frac{e^{2ika}}{\pi}\frac{i^{-1/2}}{(2a)^{1/2}}\Gamma_1^{f}[3/2,-2i(\alpha+k)a]. \tag{2.141}$$

In (2.141), $\Gamma_m^f(\cdot,\cdot)$ is the special function defined by

$$\Gamma_m^{f}(u,w)=\int_0^{\infty}\frac{t^{u-1}e^{-t}}{(t+w)^m}F_{+}[k+it/(2a)]dt \tag{2.142}$$

for $\mathrm{Re}\,u>0,\ |w|>0,\ |\arg w|<\pi,$ and positive integer $m,$ which accounts for multiple diffraction effects.

Applying Theorem in Section 2.5, we can obtain a high-frequency asymptotic expansion of (2.135) with the result that

$$\tilde{\Phi}_{+}^{s,d}(\alpha)\sim M_{+}(\alpha)\left[\chi_{us,ud}(\alpha)+C_{s,d}\sum_{n=0}^{N}f_n^{us,ud}\xi_{0n}^{f}(\alpha)\right] \tag{2.143}$$

for $ka\to\infty$, where N denotes the truncation number of the infinite asymptotic series, and

$$f_n^{us,ud}=\frac{1}{n!}\frac{d^n\tilde{\Phi}_{+}^{s,d}(\alpha)}{d\alpha^n}\bigg|_{\alpha=k}, \tag{2.144}$$

$$\xi_{0n}^{f}(\alpha)=\frac{e^{2ika}}{\pi}\frac{i^{n-1/2}}{(2a)^{n+1/2}}\Gamma_1^{f}[3/2+n,-2i(\alpha+k)a]. \tag{2.145}$$

Taking into account (2.131) and carrying out some manipulations, the unknowns $f_n^{us,ud}$ in (2.144) is determined by solving the matrix equation

$$f_m^{us,ud}-C_{s,d}\sum_{n=0}^{N}A_{mn}^{u}f_n^{us,ud}\sim B_m^{us,ud} \tag{2.146}$$

for $m=0,1,2,\cdots,N,$ where

$$A_{mn}^{u}=\sum_{p=0}^{m}\frac{M_{+}^{(m-p)}(k)\xi_{pn}^{f}(k)}{p!(m-p)!}, \tag{2.147}$$

$$B_m^{us,ud}=\sum_{p=0}^{m}\frac{M_{+}^{(m-p)}(k)\chi_{us,ud}^{(p)}(k)}{p!(m-p)!} \tag{2.148}$$

with

$$M_+^{(m-p)}(k)=\left.\frac{d^{m-p}M_+(\alpha)}{d\alpha^{m-p}}\right|_{\alpha=k}, \tag{2.149}$$

$$\xi_{pn}^f(k)=\frac{e^{2ika}}{\pi}(-1)^p\,p!\frac{i^{n-p-1/2}}{(2a)^{n-p+1/2}}\Gamma_{p+1}^f(3/2+n,-4ika), \tag{2.150}$$

$$\chi_{us,ud}^{(p)}(k)=\left.\frac{d^p\chi_{us,ud}(\alpha)}{d\alpha^p}\right|_{\alpha=k}. \tag{2.151}$$

Making use of the above results and carrying out further manipulations, we finally arrive at an explicit asymptotic solution to the Wiener-Hopf equation (2.61) with the result that

$$U_{(+)}(\alpha)\sim M_+(\alpha)\left[-\frac{A_1}{M_\pm(k\cos\theta_0)(\alpha-k\cos\theta_0)}+A_2\eta_{f1}(\alpha)\right.$$
$$\left.+\frac{1}{2}\sum_{n=0}^{N}(f_n^{us}\mp f_n^{ud})\xi_{0n}^f(\alpha)\right], \tag{2.152}$$

$$U_-(\alpha)\sim M_-(\alpha)\left[\mp\frac{A_2}{M_-(k\cos\theta_0)(\alpha-k\cos\theta_0)}+A_1\eta_{f2}(-\alpha)\right.$$
$$\left.+\frac{1}{2}\sum_{n=0}^{N}(f_n^{us}+f_n^{ud})\xi_{0n}^f(-\alpha)\right] \tag{2.153}$$

as $ka\to\infty$.

A similar procedure may also be applied to (2.115) and (2.116) for a high-frequency solution. Omitting the details, we can obtain

$$V_{(+)}(\alpha)\sim K_+(\alpha)\left[-\frac{B_1}{K_\pm(k\cos\theta_0)(\alpha-k\cos\theta_0)}+B_2\eta_{t1}(\alpha)\right.$$
$$\left.+\frac{1}{2}\sum_{n=0}^{N}(f_n^{vs}\mp f_n^{vd})\xi_{0n}^t(\alpha)\right], \tag{2.154}$$

$$V_-(\alpha)\sim K_-(\alpha)\left[\mp\frac{B_2}{K_-(k\cos\theta_0)(\alpha-k\cos\theta_0)}+B_1\eta_{t2}(-\alpha)\right.$$
$$\left.+\frac{1}{2}\sum_{n=0}^{N}(f_n^{vs}+f_n^{vd})\xi_{0n}^t(-\alpha)\right] \tag{2.155}$$

for $ka\to\infty$, where

$$\eta_{t1,t2}(\alpha)=\frac{\xi_{00}^{t}(\alpha)-\xi_{00}^{t}(\pm k\cos\theta_0)}{\alpha\mp k\cos\theta_0}, \tag{2.156}$$

$$f_n^{vs,vd}=\frac{1}{n!}\frac{d^n\Phi_+'^{s,d}(\alpha)}{d\alpha^n}\bigg|_{\alpha=k}, \tag{2.157}$$

$$\xi_{0n}^{t}(\alpha)=\frac{e^{2ika}}{\pi}\frac{i^{n-1/2}}{(2a)^{n+1/2}}\Gamma_1^t[3/2+n,-2i(\alpha+k)a], \tag{2.158}$$

$$B_m^{us,ud}=\sum_{p=0}^{m}\frac{M_+^{(m-p)}(k)\chi_{us,ud}^{(p)}(k)}{p!(m-p)!} \tag{2.159}$$

with

$$\Phi_+'^{s,d}(\alpha)=V_{(+)}^{s,d}(\alpha)+\frac{B_1}{\alpha-k\cos\theta_0}\pm\frac{B_2}{\alpha+k\cos\theta_0}, \tag{2.160}$$

$$\Gamma_m^t(u,w)=\int_0^\infty\frac{t^{u-1}e^{-t}}{(t+w)^m}T_+[k+it/(2a)]dt. \tag{2.161}$$

Equations (2.152)-(2.155) provide complete, high-frequency asymptotic solutions to the Wiener-Hopf equations. It is to be noted that the above results rigorously take into account the multiple diffraction between the edges of the strip.

2.7. Scattered Far Field

Using the boundary condition, the scattered field in the Fourier transform domain is expressed as

$$\Phi(x,\alpha)=\hat{\Phi}(\alpha)e^{-\gamma|x|}, \tag{2.162}$$

where

$$\hat{\Phi}(\alpha)=-ikY_0\frac{e^{-i\alpha a}U_-(\alpha)+e^{i\alpha a}U_{(+)}(\alpha)}{2\gamma M(\alpha)}\mp\frac{e^{-i\alpha a}V_-(\alpha)+e^{i\alpha a}V_{(+)}(\alpha)}{K(\alpha)},\ x\gtrless 0. \tag{2.163}$$

The scattered field $\phi(x,z)$ in the real space is obtained by taking the inverse Fourier transform of (2.162) according to the formula

$$\phi(x,z)=(2\pi)^{-1/2}\int_{-\infty+ic}^{\infty+ic}\Phi(\alpha)e^{-i\alpha z}d\alpha, \tag{2.164}$$

where c is a constant such that $0<|c|<k_2\cos\theta_0$. Substituting (2.162) into (2.164),

an integral representation of the scattered field $\phi(x,z)$ is found to be

$$\phi(x,z) = (2\pi)^{-1/2} \int_{-\infty+ic}^{\infty+ic} \Phi(\alpha) e^{-\gamma|x| - i\alpha z} d\alpha. \tag{2.165}$$

It is seen from (2.57) and (2.58) that (2.163) can be written as

$$\hat{\Phi}(\alpha) = \frac{1}{2}\left[\pm J_e(\alpha) + \frac{\mathrm{i}kY_0}{\gamma} J_m(\alpha) \right], \tag{2.166}$$

where $J_e(\alpha)$ and $J_m(\alpha)$ are entire functions. This shows that singularities of the integrand of (2.165) are only branch points at $\alpha = \pm k$. Introducing the cylindrical coordinate (ρ,θ) centered at the origin as

$$x = \rho \sin\theta, \quad z = \rho\cos\theta, \quad -\pi < \theta < \pi \tag{2.167}$$

and applying the saddle point method, we derive a far field asymptotic expression with the result that

$$\phi(\rho,\theta) \sim \pm\hat{\Phi}(-k\cos\theta) k \sin\theta \frac{e^{i(k\rho - \pi/4)}}{(k\rho)^{1/2}}, \quad x \gtrless 0 \tag{2.168}$$

as $k\rho \to \infty$. Equation (2.168) is uniformly valid for arbitrary incidence and observation angles.

2.8. Alternative Approach

In this section, we shall consider the same diffraction problem as in the previous sections, and carry out the Wiener-Hopf analysis by using approximate boundary conditions [35] valid for $|M| (= |\varepsilon_r \mu_r|^{1/2}) \gg 1$:

$$H_y^t(+0,z) + H_y^t(-0,z) = 2Q[E_z^t(+0,z) - E_z^t(-0,z)], \tag{2.169}$$

$$E_z^t(+0,z) + E_z^t(-0,z) = 2R[H_y^t(+0,z) - H_y^t(-0,z)], \tag{2.170}$$

where

$$\left.\begin{aligned} R &= \frac{iZ_0}{2} \frac{\mu_r^{1/2}}{\varepsilon_r^{1/2}} \cot[kb(\varepsilon_r\mu_r)^{1/2}/2], \\ Q &= \frac{i}{2Z_0} \frac{\varepsilon_r^{1/2}}{\mu_r^{1/2}} \cot[kb(\varepsilon_r\mu_r)^{1/2}/2]. \end{aligned}\right\} \tag{2.171}$$

Since the method is similar to that followed in the above sections, only the main results

will be summarized.

Solving (2.16) and taking into account (2.169) and (2.170) as in above discussions, we obtain that

$$-M^1(\alpha)J_m^1(\alpha) = e^{-i\alpha a}U_-^1(\alpha) + e^{i\alpha a}U_{(+)}^1(\alpha), \tag{2.172}$$

$$-K^1(\alpha)J_e^1(\alpha) = 2[e^{-i\alpha a}V_-^1(\alpha) + e^{i\alpha a}V_{(+)}^1(\alpha)], \tag{2.173}$$

where

$$M^1(\alpha) = M_+^1(\alpha)M_-^1(\alpha) = Q - \frac{ikY_0}{2\gamma}, \tag{2.174}$$

$$K^1(\alpha) = K_+^1(\alpha)K_-^1(\alpha) = \gamma - 2ikY_0R, \tag{2.175}$$

$$J_m^1(\alpha) = \frac{i}{kY_0}\left[\frac{d\Phi_1(+0,\alpha)}{dx} - \frac{d\Phi_1(-0,\alpha)}{dx}\right], \tag{2.176}$$

$$J_e^1(\alpha) = \Phi_1(+0,\alpha) - \Phi_1(-0,\alpha), \tag{2.177}$$

$$U_{(+)}^1(\alpha) = \Phi_\pm(\alpha) \mp \frac{A_{1,2}^1}{\alpha - k\cos\theta_0}, \tag{2.178}$$

$$V_{(+)}^1(\alpha) = \Phi'_\pm(\alpha) \mp \frac{B_{1,2}^1}{\alpha - k\cos\theta_0} \tag{2.179}$$

with

$$A_{1,2}^1 = \frac{1}{(2\pi)^{1/2}i}e^{\mp ika\cos\theta_0}, \tag{2.180}$$

$$B_{1,2}^1 = -\frac{k\sin\theta_0}{(2\pi)^{1/2}}e^{\mp ika\cos\theta_0}, \tag{2.181}$$

$$M_\pm^1(\alpha) = \left(\frac{kY_0}{2}\right)^{1/2}\frac{N_{1\pm}^1(\alpha)}{(k\pm\alpha)^{1/2}}, \tag{2.182}$$

$$K_\pm^1(\alpha) = (2kY_0R)^{1/2}e^{-i\pi/4}N_{2\pm}^1(\alpha), \tag{2.183}$$

$$N_{n\pm}^{1}(\alpha)=(1+\delta_{1n}^{-1})^{1/2}\exp\left\{-\frac{\delta_{1n}}{\pi}\int_{\pi/2}^{\arccos(\pm\alpha/k)}\frac{t\cos t}{\sin^2 t-\delta_{1n}^2}dt\right.$$
$$\pm\ln[\delta_{1n}+(\delta_{1n}^2-1)^{1/2}]\frac{i}{2\pi}\ln\left[\frac{ik(\delta_{1n}^2-1)^{1/2}+\alpha}{ik(\delta_{1n}^2-1)^{1/2}-\alpha}\right]$$
$$\left.+\frac{1}{4}\ln\left[1+\frac{\alpha^2}{k^2(\delta_{1n}^2-1)}\right]\right\},\quad n=1,2, \tag{2.184}$$

where

$$\delta_{11}=\frac{Y_0}{2Q},\quad \delta_{12}=2Y_0R. \tag{2.185}$$

Equations (2.172) and (2.173) are the Wiener-Hopf equations satisfied by unknown spectral functions.

Applying the asymptotic method established [37], [38], we can derive a high-frequency representation of (2.178) for large ka with the result that

$$U_{(\pm)}^{1}(\alpha)\sim M_{\pm}^{1}(\alpha)\left[\mp\frac{A_{1,2}^{1}}{M_{\pm}^{1}(k\cos\theta_0)(\alpha-k\cos\theta_0)}+A_{2,1}^{1}\eta_{f1,f2}^{1}(\pm\alpha)\right.$$
$$\left.+\frac{1}{2}\sum_{n=0}^{N}(f_n^{1us}\mp f_n^{1ud})\xi_{0n}^{1f}(\pm\alpha)\right] \tag{2.186}$$

for $ka\to\infty$, where

$$f_n^{1us,1ud}=\frac{1}{n!}\frac{d^n\Phi_{+}^{s,d}(\alpha)}{d\alpha^n}\bigg|_{\alpha=k}, \tag{2.187}$$

$$\eta_{f1,f2}^{1}(\alpha)=\frac{\xi_{00}^{1f}(\alpha)-\xi_{00}^{1f}(\pm k\cos\theta_0)}{\alpha\mp k\cos\theta_0} \tag{2.188}$$

with

$$\Phi_{+}^{s,d}(\alpha)=\Phi_{+}(\alpha)\pm\Phi_{-}(-\alpha), \tag{2.189}$$

$$\xi_{0n}^{1f}(\alpha)=\frac{e^{2ika}}{\pi}\frac{i^{n-1/2}}{(2a)^{n+1/2}}\Gamma_1^{1f}[3/2+n,-2i(\alpha+k)a], \tag{2.190}$$

$$\Gamma_m^{1f}(u,w)=\int_0^{\infty}\frac{t^{u-1}e^{-t}}{(t+w)^m}F_{+}^{1}[k+it/(2a)]dt, \tag{2.191}$$

$$F_{+}^{1}(\beta)=\frac{2ikY_0(\beta+k)^{1/2}M_{+}^{1}(\beta)}{4(\beta^2-k^2)Q^2+k^2Y_0^2}. \tag{2.192}$$

Equation (2.186) provides complete, high-frequency asymptotic solutions to the Wiener-Hopf equations.

A similar procedure may also be applied to (2.179) for a high-frequency solution as follows:

A similar procedure may also be applied to (3.179) for a high-frequency solution as follows:

$$V_{(+)}^{1}(\alpha)\sim K_{\pm}^{1}(\alpha)\left[\mp\frac{B_{1,2}^{1}}{K_{\pm}^{1}(k\cos\theta_0)(\alpha-k\cos\theta_0)}+B_{2,1}^{1}\eta_{t1,t2}^{1}(\pm\alpha)\right.$$
$$\left.+\frac{1}{2}\sum_{n=0}^{N}(f_n^{1vs}\mp f_n^{1vd})\xi_{0n}^{1t}(\pm\alpha)\right] \tag{2.193}$$

for $ka\to\infty$, where

$$f_n^{1vs,1vd}=\frac{1}{n!}\frac{d^n\Phi_{+}^{\prime s,d}(\alpha)}{d\alpha^n}\bigg|_{\alpha=k}, \tag{2.194}$$

$$\eta_{t1,t2}^{1}(\alpha)=\frac{\xi_{00}^{1t}(\alpha)-\xi_{00}^{1t}(\pm k\cos\theta_0)}{\alpha\mp k\cos\theta_0} \tag{2.195}$$

with

$$\Phi_{+}^{\prime}(\alpha)=\Phi_{+}^{\prime}(\alpha)\pm\Phi_{-}^{\prime}(-\alpha), \tag{2.196}$$

$$\xi_{0n}^{1t}(\alpha)=\frac{e^{2ika}}{\pi}\frac{i^{n-1/2}}{(2a)^{n+1/2}}\Gamma_1^{1t}[3/2+n,-2i(\alpha+k)a], \tag{2.197}$$

$$\Gamma_m^{1t}(u,w)=\int_0^{\infty}\frac{t^{u-1}e^{-t}}{(t+w)^m}T_{+}^{1}[k+it/(2a)]dt, \tag{2.198}$$

$$T_{+}^{1}(\beta)=\frac{(\beta+k)^{1/2}K_{+}^{1}(\beta)}{\beta^2-k^2+4k^2Y_0^2R^2}. \tag{2.199}$$

Introducing the cylindrical coordinate $x=\rho\sin\theta,\quad z=\rho\cos\theta$ for $-\pi<\theta<\pi$ and applying the saddle point method, we derive a far field asymptotic expression with the result that

$$\phi(\rho,\theta) \sim \pm\hat{\Phi}^1(-k\cos\theta)k\sin\theta\frac{e^{i(k\rho-\pi/4)}}{(k\rho)^{1/2}}, \quad x \gtrless 0 \tag{2.200}$$

as $k\rho \to \infty$, where

$$\hat{\Phi}^1(\alpha) = -ikY_0\frac{e^{-i\alpha a}U_-^1(\alpha)+e^{i\alpha a}U_{(+)}^1(\alpha)}{2\gamma M^1(\alpha)} \mp \frac{e^{-i\alpha a}V_-^1(\alpha)+e^{i\alpha a}V_{(+)}^1(\alpha)}{K^1(\alpha)}, x \gtrless 0. \tag{2.201}$$

Equation (2.200) is uniformly valid for arbitrary incidence and observation angles.

2.9. Numerical Results and Discussion

In this section, we shall present numerical results on the RCS for H polarization, and discuss far field scattering characteristics of the strip in detail. The normalized RCS per unit length is defined by

$$\frac{\sigma}{\lambda} = \lim_{\rho\to\infty}\left(k\rho\left|\frac{\phi}{\phi^i}\right|^2\right) \tag{2.202}$$

with λ being the free-space wavelength. All the results are plotted in decibels [dB] by computing $10\log_{10}(\sigma/\lambda)$.

In computing (2.202), we have used the high-frequency asymptotic expressions as given by (2.152)-(2.155) for $U_{(\pm)}(\alpha)$ and $V_{(\pm)}(\alpha)$, where the truncation number N for the asymptotic series is contained. Let $\sigma^{(N)}$ and $\sigma^{(N+1)}$ be the RCS with the truncation numbers being N and $N+1$, respectively. In numerical computation, we have employed the convergence criteria $\left|\sigma^{(N+1)}-\sigma^{(N)}\right| < 10^{-3}$ in order to determine the desired truncation number N. By careful numerical investigation, we have verified that the choice of $N=3$ satisfies the aforementioned convergence criteria and hence provides sufficiently accurate solutions.

Figure 2.4 shows the normalized RCS as a function of observation angle θ, where the strip width is $2a = \lambda, 5\lambda, 10\lambda$, the strip thickness is $b = 0.01\lambda$, 0.04λ, 0.07λ, 0.10λ, and the incidence angle θ_0 is fixed as $60°$. As an example of existing lossy materials, we have chosen the ferrite with $\varepsilon_r = 12.0 + i0$ and $\mu_r = 1.4 + i4.5$ in numerical computation [43]. It is seen from the figure that the RCS shows noticeable peaks along the reflected and incident shadow boundaries at $\theta = 120°$ and $\theta = -120°$, respectively. We observe by comparing the results for $2a = \lambda$, 5λ, and 10λ that the RCS shows sharp oscillation for larger strip width $2a$. We also notice that, for fixed $2a$, the RCS level becomes larger with an increase of the strip thickness b except in the neighborhood of the reflected shadow boundary at $\theta = 120°$. Scattering characteristics near $\theta = 120°$ need some considerations. We see that, for $b = 0.04\lambda$, 0.07λ, 0.10λ, the RCS level around $\theta = 120°$ becomes lower with an increase of the

strip thickness. This is because, ferrite is an electromagnetic wave absorber and hence, the RCS reduction around the specular reflection direction becomes noticeable for larger strip thickness b.

Figure 2.5 shows the normalized RCS as a function of incidence angle θ_0, where the strip width is $2a = \lambda, 5\lambda, 10\lambda$, the strip thickness is $b = 0.01\lambda$, 0.04λ, 0.07λ, 0.10λ, and the same material parameters as in Fig. 2.4 have been chosen for computation. The truncation number is $N = 3$. It is obvious that the peaks at $\theta_0 = 90°$ in the figure correspond to the specular reflection from the strip. Comparing the RCS characteristics for $2a = \lambda$, 5λ, and 10λ, we observe that the RCS exhibits sharp oscillation for larger strip width $2a$. We also notice that, for fixed $2a$, the RCS level becomes larger with an increase of the strip thickness b except in the neighborhood of $\theta_0 = 90°$, whereas the RCS becomes lower with an increase of the strip thickness for $b = 0.04\lambda$, 0.07λ, 0.10λ, around $\theta_0 = 90°$. This is due to the electromagnetic energy absorption for the ferrite material with larger strip thickness b, as has been investigated above for the normalized RCS as a function of observation angle.

Let us now make comparison of the results obtained via a use of approximate boundary conditions by Senior and Volakis [29] ((2.5)-(2.7)) with those by Bleszynski *et al*. [35] ((2.169)-(2.171)). Figure 2.6 shows the normalized RCS as a function of incidence angle θ_0, where the strip dimension is $2a = 10\lambda$, $b = 0.01\lambda$, and the other parameters are same as in Fig. 2. We see from the figure that the two results are in excellent agreement. By careful numerical experimentation for the case of $\varepsilon_r = 12.0 + i0$, $\mu_r = 1.4 + i4.5$, we have verified that the second order impedance boundary conditions [29] given by ((2.5)-(2.7)) can be employed for $|M| < 20$ with good accuracy.

Figures 2.7 and 2.8 show the normalized RCS versus incidence angle θ_0 and versus the frequency parameter ka for H polarization, respectively. In the figures, the results obtained by Volakis [29] and Shapoval [44] are also plotted. It is observed from Figs. 2.7 and 2.8 that our results agree well with Shapoval's results. It is also seen from the Fig. 2.7 that our results agree reasonably well with Volakis's results over $40° < \theta_0 < 90°$, but there are some discrepancies for $0° < \theta_0 < 40°$. These discrepancies are perhaps due to the fact that Volakis's solution is derived on the basis of the solutions for the two independent half-planes and becomes less accurate at narrow strip width as in $2a = 1.7\lambda$. It is therefore inferred that Volakis's solution is not applicable at low frequencies and for near-gazing incidence ($\theta_0 \approx 0°$).

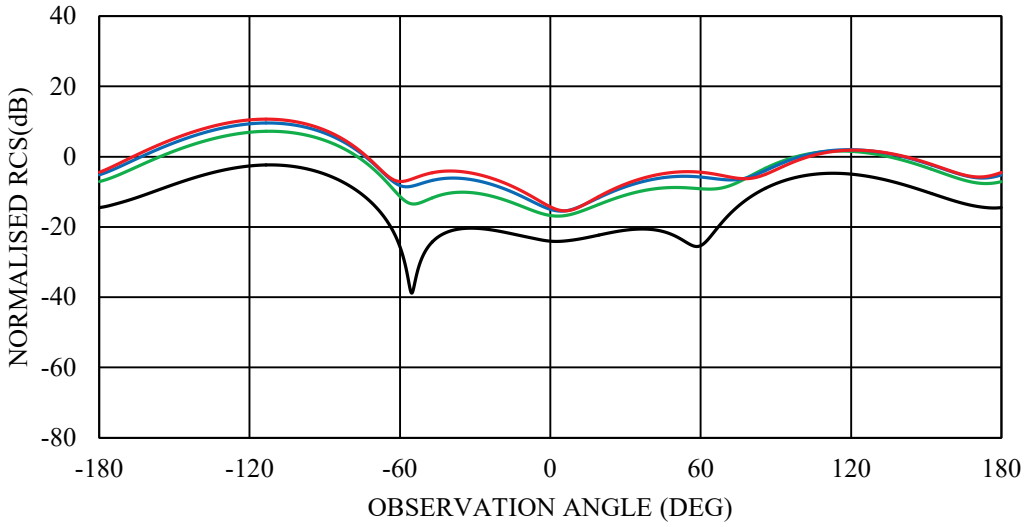

Fig. 2.4a Normalized RCS $\sigma^{(N)}/\lambda$ versus observation angle θ for H polarization, $\theta_0 = 60°$, $2a = \lambda$, $\varepsilon_r = 12.0 + i0$, $\mu_r = 1.4 + i4.5$, $N = 3$. ——: $b = 0.01\lambda$. ——: $b = 0.04\lambda$. ——: $b = 0.07\lambda$. ——: $b = 0.10\lambda$.

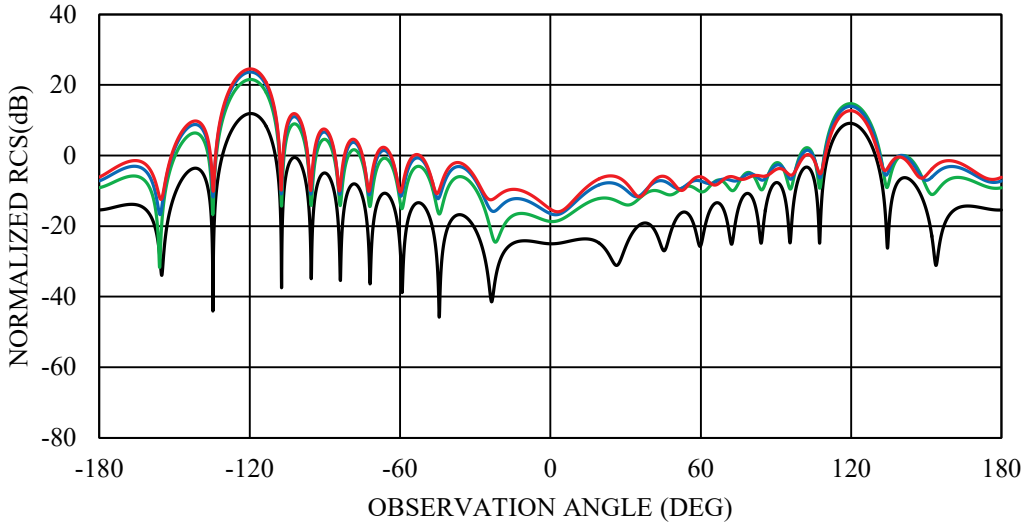

Fig. 2.4b Normalized RCS $\sigma^{(N)}/\lambda$ versus observation angle θ for H polarization, $\theta_0 = 60°$, $2a = 5\lambda$, $\varepsilon_r = 12.0 + i0$, $\mu_r = 1.4 + i4.5$, $N = 3$. ——: $b = 0.01\lambda$. ——: $b = 0.04\lambda$. ——: $b = 0.07\lambda$. ——: $b = 0.10\lambda$.

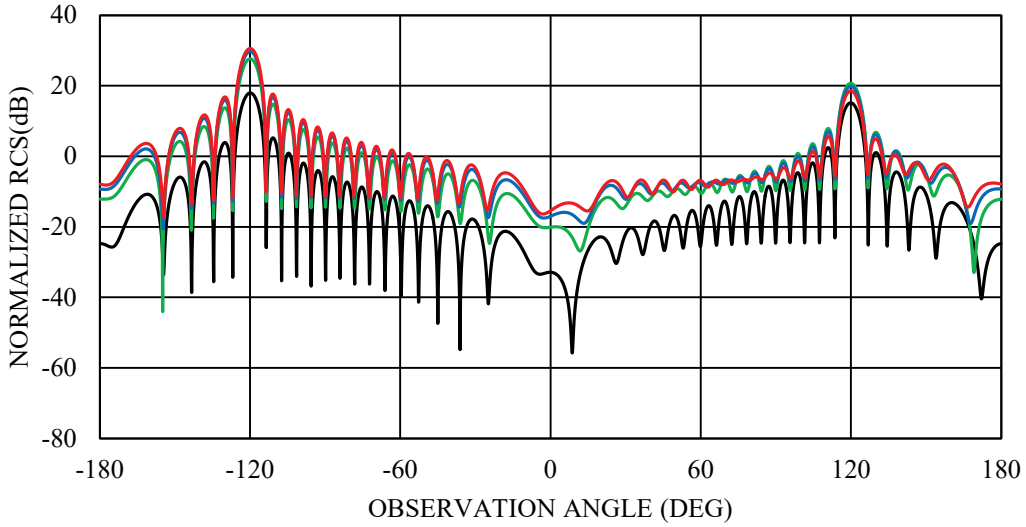

Fig. 2.4c Normalized RCS $\sigma^{(N)}/\lambda$ versus observation angle θ for H polarization, $\theta_0 = 60°$, $2a = 10\lambda$, $\varepsilon_r = 12.0 + i0$, $\mu_r = 1.4 + i4.5$, $N = 3$. ——: $b = 0.01\lambda$. ——: $b = 0.04\lambda$. ——: $b = 0.07\lambda$. ——: $b = 0.10\lambda$.

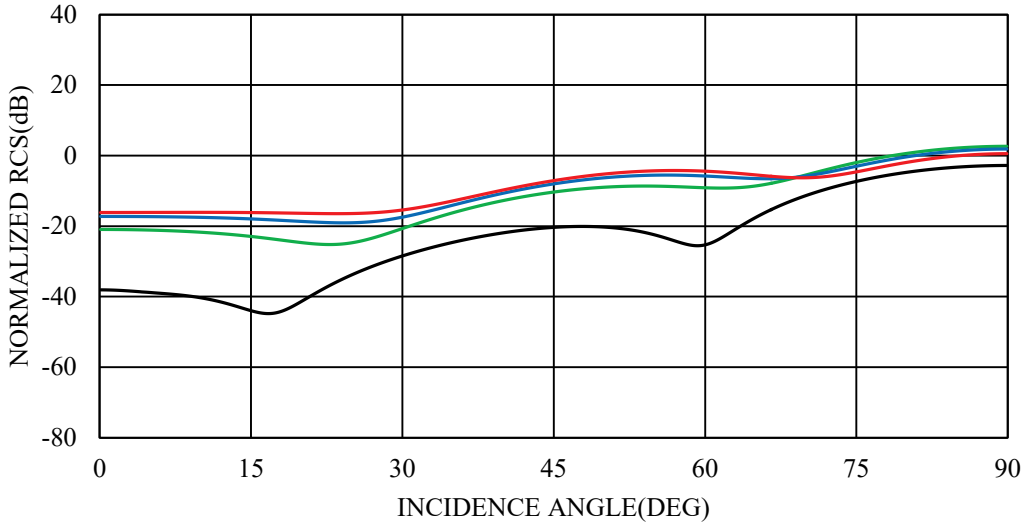

Fig. 2.5a Normalized RCS $\sigma^{(N)}/\lambda$ versus incidence angle θ_0 for H polarization, $2a = \lambda$, $\varepsilon_r = 12.0 + i0$, $\mu_r = 1.4 + i4.5$, $N = 3$. ——: $b = 0.01\lambda$. ——: $b = 0.04\lambda$. ——: $b = 0.07\lambda$. ——: $b = 0.10\lambda$.

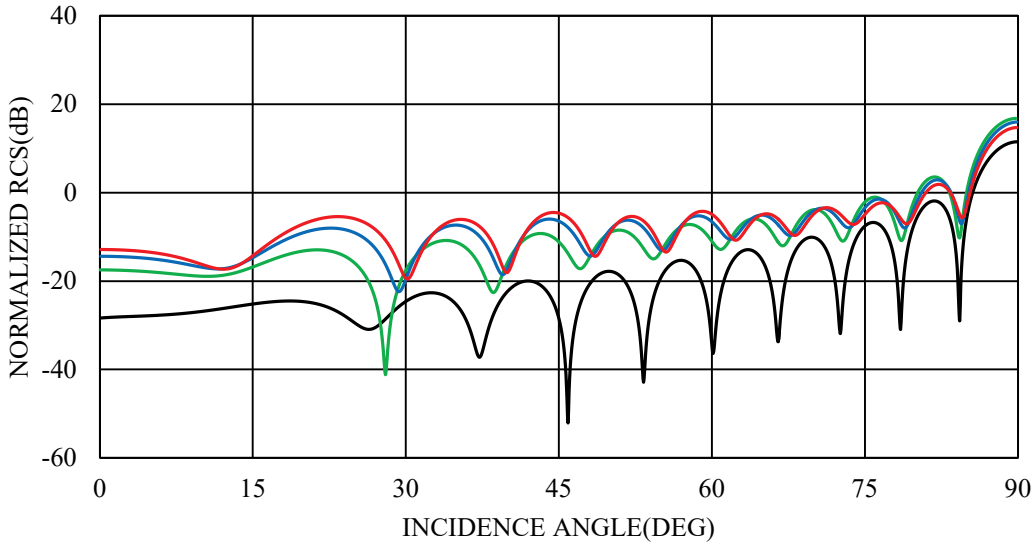

Fig. 2.5b Normalized RCS $\sigma^{(N)}/\lambda$ versus incidence angle θ_0 for H polarization, $2a=5\lambda$, $\varepsilon_r=12.0+i0$, $\mu_r=1.4+i4.5$, $N=3$. ——: $b=0.01\lambda$. ——: $b=0.04\lambda$. ——: $b=0.07\lambda$. ——: $b=0.10\lambda$.

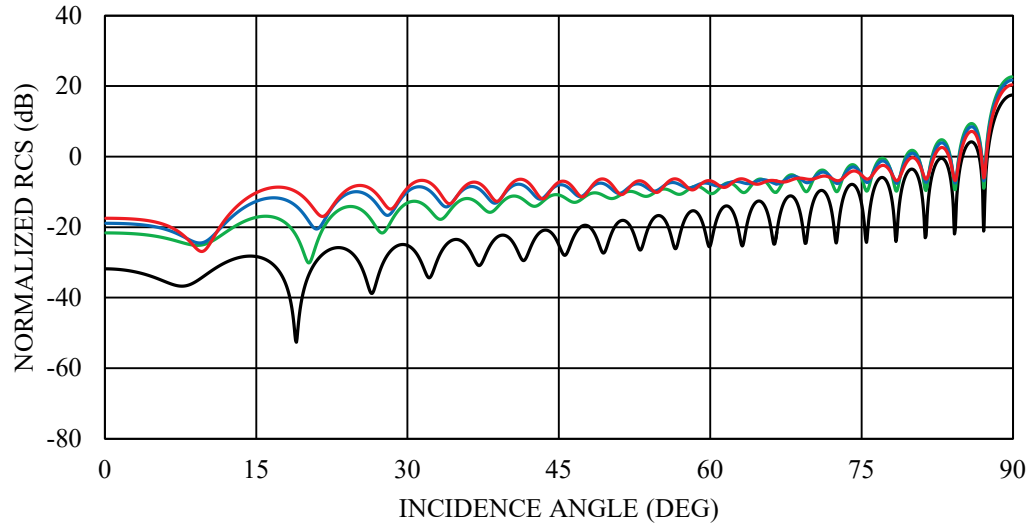

Fig. 2.5c Normalized RCS $\sigma^{(N)}/\lambda$ versus incidence angle θ_0 for H polarization, $2a=10\lambda$, $\varepsilon_r=12.0+i0$, $\mu_r=1.4+i4.5$, $N=3$. ——: $b=0.01\lambda$. ——: $b=0.04\lambda$. ——: $b=0.07\lambda$. ——: $b=0.10\lambda$.

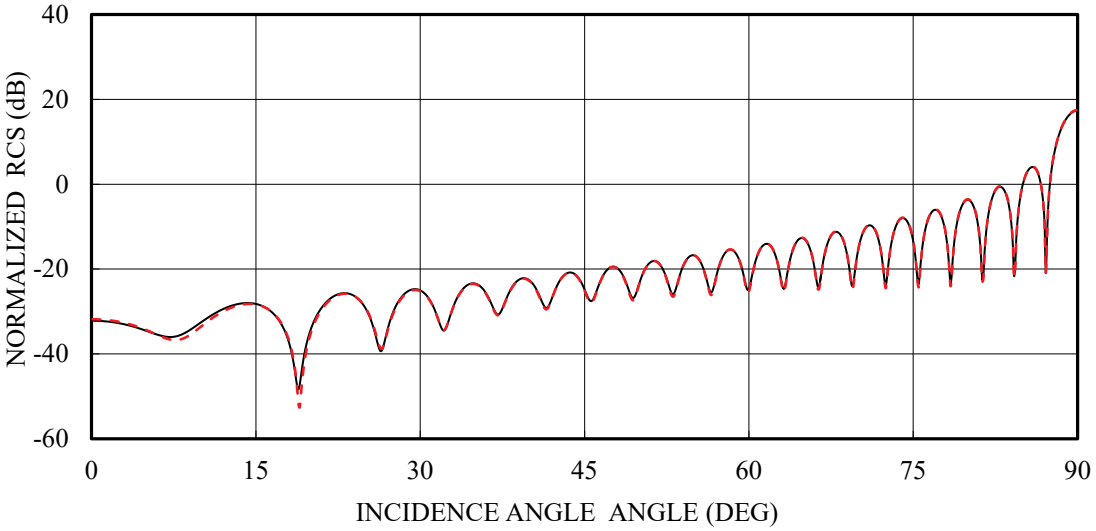

Fig. 2.6 Comparison of the normalized RCS $\sigma^{(N)}/\lambda$ versus incidence angle θ_0 between two different approximate boundary conditions for H polarization, $2a=10\lambda$, $b=0.01\lambda$, $\varepsilon_r=12.0+i0$, $\mu_r=1.4+i4.5$, $N=3$. ——: approximate boundary conditions [32]. - - - -: approximate boundary conditions [35].

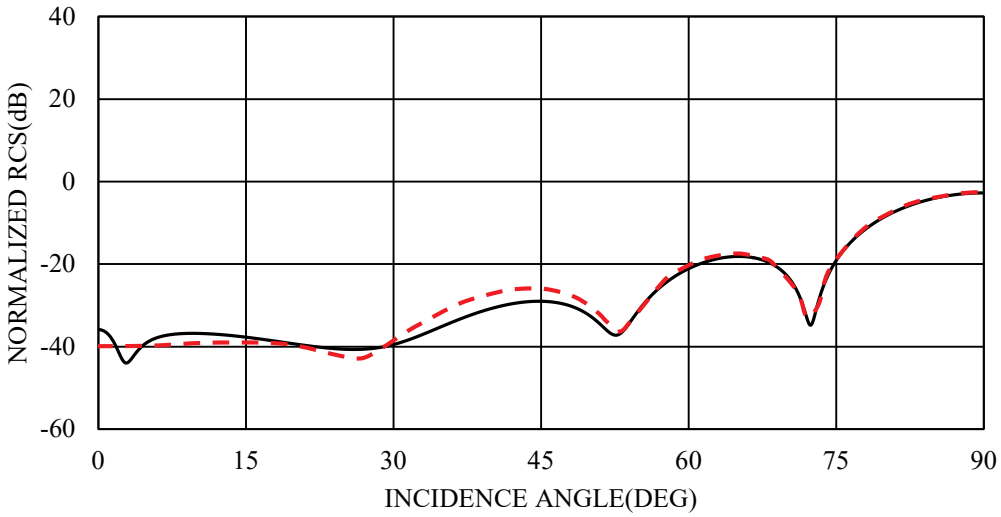

Fig. 2.7 Normalized RCS $\sigma^{(N)}/\lambda$ versus incidence angle θ_0 for H polarization, $2a=1.7\lambda$, $b=0.01\lambda$, $\varepsilon_r=7.4+i1.11$, $\mu_r=1.4+i0.672$, $N=3$. ——: this paper. - - - -: Volakis [29].

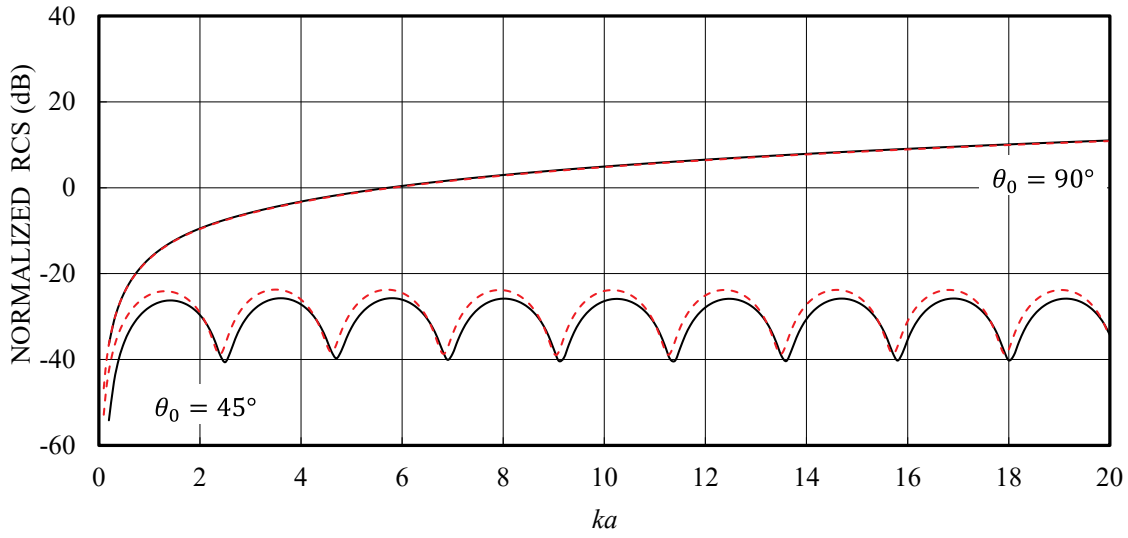

Fig. 2.8 Normalized RCS $\sigma^{(N)}/\lambda$ versus frequency parameter ka for H polarization, $\theta_0 = 45°, 90°$, $b = 0.025\lambda$, $\varepsilon_r = 4 + i0.4$, $\mu_r = 1$, $N = 3$, and its comparison with Shapoval [44]. ——— : this paper. - - - - : Shapoval [44].

2.10. Summary

In this chapter, we have analyzed the diffraction by a thin material strip for the H-polarized plane wave incidence using the Wiener-Hopf technique combined with the perturbation method together with approximate boundary conditions [32], [35].

Assuming that the strip thickness and width are small and large compared with the wavelength, respectively, our final solution is obtained. Taking the inverse Fourier transform and applying the saddle point method, we have derived a far field asymptotic expression of the scattered field, which is shown to be valid for arbitrary incidence and observation angles.

Based on the results, we have carried out numerical computation of the far field intensity and investigated the effect of the strip in detail. Some comparisons with the other existing method have also been provided.

3. WIENER-HOPF ANALYSIS OF THE PLANE WAVE DIFFRACTION BY A THIN MATERIAL STRIP: THE CASE OF E POLATIZATION

3.1 Introduction

In Chapter 3, we shall consider the same grating geometry as in Chapter 2, and analyze the diffraction problem for the E-polarized plane wave incidence. The method of solution presented in Chapter 3 for E polarization is similar to, but more complicated than, the analysis carried out for the H-polarized case. Representative numerical examples of the far field intensity are shown for various physical parameters, and scattering characteristics of the grating are discussed in detail [40]. The results are also compared with our analysis for the H-polarized case.

3.2 Formulation of the Problem

We consider the diffraction of an E-polarized plane wave by a thin material strip as shown in Fig. 3.1, where the relative permittivity and permeability of the strip are denoted by ε_r and μ_r, respectively. Let the total electric field $\phi^t(x,z)[\equiv E_y^t(x,z)]$ be

$$\phi^t(x,z) = \phi^i(x,z) + \phi(x,z), \tag{3.1}$$

where $\phi^i(x,z)$ is the incident field given by

$$\phi^i(x,z) = e^{-ik(x\sin\theta_0 + z\cos\theta_0)}, \quad 0 < \theta_0 < \pi/2 \tag{3.2}$$

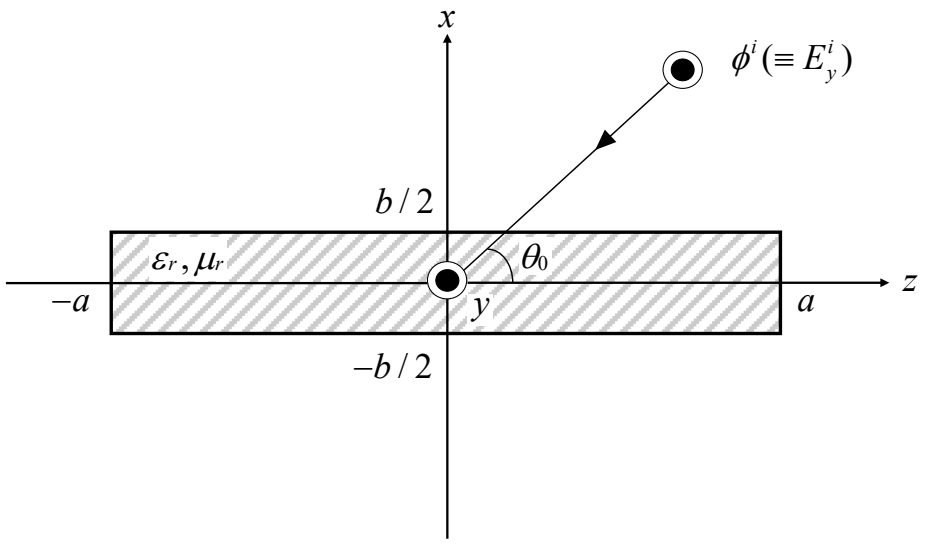

Fig. 3.1 Geometry of the problem.

with $k[=\omega(\varepsilon_0\mu_0)^{1/2}]$ being the free-space wavenumber. The term $\phi(x,z)$ is the unknown scattered field and satisfies the two-dimensional Helmholtz equation:

$$\left(\frac{\partial^2}{\partial x^2}+\frac{\partial^2}{\partial z^2}+k^2\right)\phi(x,z)=0. \tag{3.3}$$

Nonzero components of the scattered electromagnetic fields are derived from the following relation:

$$(E_y,H_x,H_z)=\left(\phi,\frac{i}{\omega\mu_0}\frac{\partial\phi}{\partial z},\frac{1}{i\omega\mu_0}\frac{\partial\phi}{\partial x}\right). \tag{3.4}$$

If the strip thickness is small compared with the wavelength, the material strip is approximately replaced by a strip of zero thickness satisfying the second order impedance boundary conditions [29]. On the strip surface, the total electromagnetic field satisfies the approximate boundary conditions as given by

$$H_z^t(+0,z)+H_z^t(-0,z)=-2R_m[E_y^t(+0,z)-E_y^t(-0,z)], \tag{3.5}$$

$$\left[\frac{1}{R_e}+\frac{1}{\tilde{R}_m}\left(1+\frac{1}{k^2}\frac{\partial^2}{\partial x^2}\right)\right][E_y^t(+0,z)+E_y^t(-0,z)]=-2[H_z^t(+0,z)-H_z^t(-0,z)], \tag{3.6}$$

where

$$R_e=\frac{iZ_0}{kb(\varepsilon_r-1)},\quad R_m=\frac{iY_0}{kb(\mu_r-1)},\quad \tilde{R}_m=\frac{iZ_0\mu_r}{kb(\mu_r-1)} \tag{3.7}$$

with Z_0 and Y_0 being the intrinsic impedance and admittance of free space, respectively. It is verified by Senior and Volakis [29] using numerical experimentation that the approximate boundary conditions as given by (3.5)-(3.7) are valid for $b\le 0.1\lambda$.

For convenience of analysis, we assume the medium to be slightly lossy as in

$$k=k_1+ik_2,\quad 0<k_2\ll k_1. \tag{3.8}$$

The solution for real k is obtained by letting $k_2\to+0$ at the end of analysis. It follows from the radiation condition that

$$\phi(x,z)=O\left(e^{-k_2|z|\cos\theta_0}\right),\quad |z|\to\infty. \tag{3.9}$$

We now define the Fourier transform $\Phi(x,\alpha)$ of the scattered field $\phi(x,z)$ with

respect to z as

$$\Phi(x,\alpha) = (2\pi)^{-1/2}\int_{-\infty}^{\infty}\phi(x,z)e^{i\alpha z}dz, \tag{3.10}$$

where $\alpha(\equiv \mathrm{Re}\,\alpha + i\,\mathrm{Im}\,\alpha) = \sigma + i\tau$. In view of (3.9), it is found that $\Phi(x,\alpha)$ is regular in the strip $|\tau| < k_2\cos\theta_0$ of the complex α-plane. Introducing the Fourier integrals as

$$\Phi_{\pm}(x,\alpha) = \pm(2\pi)^{-1/2}\int_{\pm a}^{\pm\infty}\phi(x,z)e^{i\alpha(z\mp a)}dz, \tag{3.11}$$

$$\Phi_1(x,\alpha) = (2\pi)^{-1/2}\int_{-a}^{a}\phi(x,z)e^{i\alpha z}dz, \tag{3.12}$$

we can express $\Phi(x,\alpha)$ as

$$\Phi(x,\alpha) = e^{-i\alpha a}\Phi_{-}(x,\alpha) + \Phi_1(x,\alpha) + e^{i\alpha a}\Phi_{+}(x,\alpha). \tag{3.13}$$

In (3.13), $\Phi_{+}(x,\alpha)$ and $\Phi_{-}(x,\alpha)$ are regular in the half-planes $\tau > -k_2\cos\theta_0$ and $\tau < k_2\cos\theta_0$, respectively, whereas $\Phi_1(x,\alpha)$ is an entire function. The derivative of (3.11) with respect to x is defined by

$$\Phi'_{\pm}(x,\alpha) = \pm(2\pi)^{-1/2}\int_{\pm a}^{\pm\infty}\frac{\partial\phi(x,z)}{\partial x}e^{i\alpha(z\mp a)}dz, \tag{3.14}$$

$$\Phi''_{\pm}(x,\alpha) = \pm(2\pi)^{-1/2}\int_{\pm a}^{\pm\infty}\frac{\partial^2\phi(x,z)}{\partial x^2}e^{i\alpha(z\mp a)}dz. \tag{3.15}$$

Taking the Fourier transform of the two-dimensional Helmholtz equation, we find that

$$(d^2/dx^2 - \gamma^2)\Phi(x,\alpha) = 0 \tag{3.16}$$

for any α in the strip $|\tau| < k_2\cos\theta_0$, where $\gamma = (\alpha^2 - k^2)^{1/2}$. Since γ is a double-valued function of α, we choose a proper branch of γ such that γ reduces to $-ik$ when $\alpha = 0$. According to the choice of this branch, we can show that $\mathrm{Re}\,\gamma > 0$ for any α in the strip $|\tau| < k_2\cos\theta_0$. Equation (3.16) is the transformed wave equation. Because $\mathrm{Re}\,\gamma > 0$ for any α in $|\tau| < k_2\cos\theta_0$ according to the choice of brunch cuts, the solution of (3.16) can be written as

$$\begin{aligned}\Phi(x,\alpha) &= A(\alpha)e^{-\gamma x}, \quad x > 0,\\ &= B(\alpha)e^{\gamma x}, \quad x < 0.\end{aligned} \tag{3.17}$$

By imposing the condition that $\Phi(x,\alpha)$ be bounded as $|x| \to \infty$.

The electromagnetic surface currents on the strip can be described

$$I_e(z) = H_z^t(+0,z) - H_z^t(-0,z), \tag{3.18}$$

$$I_m(z) = E_y^t(+0,z) - E_y^t(-0,z). \tag{3.19}$$

where $I_e(z)$ and $I_m(z)$ are magnetic and electric surface currents on the strip, respectively. From (3.1), $I_e(z)$ and $I_m(z)$ can be expressed that

$$I_e(z) = \frac{1}{i\omega\mu_0}\left[\left.\frac{\partial\phi(x,z)}{\partial x}\right|_{x=+0} - \left.\frac{\partial\phi(x,z)}{\partial x}\right|_{x=-0}\right], \tag{3.20}$$

$$I_m(z) = \phi(+0,z) - \phi(-0,z). \tag{3.21}$$

Using (3.1), (3.2), (3.5) and (3.18), we find that

$$\begin{aligned} 2R_m I_m(z) &= -\frac{1}{i\omega\mu_0}\left[\left.\frac{\partial}{\partial x}\phi^t(x,z)\right|_{x=+0} + \left.\frac{\partial}{\partial x}\phi^t(x,z)\right|_{x=-0}\right] \\ &= 2Y_0\sin\theta_0 e^{-ikz\cos\theta_0} + \frac{i}{\omega\mu_0}\left[\left.\frac{\partial\phi(x,z)}{\partial x}\right|_{x=+0} + \left.\frac{\partial\phi(x,z)}{\partial x}\right|_{x=-0}\right]. \end{aligned} \tag{3.22}$$

Taking into account (3.1), (3.2), (3.4), and (3.19) and setting $x = \pm 0$, (3.5) can be expressed that

$$\begin{aligned} I_m(z) &= \left(\frac{1}{R_m} + \frac{\cos^2\theta_0}{\tilde{R}_e}\right)e^{-ikz\cos\theta_0} \\ &\quad + \left[\frac{1}{2R_m} + \frac{1}{2\tilde{R}_e}\left(1 + \frac{1}{k^2}\frac{\partial^2}{\partial x^2}\right)\right][\phi(x,z)|_{x=+0} + \phi(x,z)|_{x=-0}]. \end{aligned} \tag{3.23}$$

Multiplying both sides of the (3.22) and (3.23) by $(2\pi)^{-1/2}e^{i\alpha z}$ and integrating with respect to z over the range $(-a,a)$, we obtain that

$$\begin{aligned} J_m(\alpha) &= \frac{1}{Z_0 R_m}\frac{\sin\theta_0}{(2\pi)^{1/2} i}\frac{e^{i(\alpha - k\cos\theta_0)a} - e^{-i(\alpha - k\cos\theta_0)a}}{(\alpha - k\cos\theta_0)} \\ &\quad + \frac{i}{2kZ_0 R_m}[\Phi_1'(+0,\alpha) + \Phi_1'(-0,\alpha)], \end{aligned} \tag{3.24}$$

where

$$J_m(\alpha) = (2\pi)^{-1/2}\int_{-a}^{a} I_m(z)e^{i\alpha z}dz, \tag{3.25}$$

$$\Phi_1'(\pm 0,\alpha)=\left.\frac{d\Phi_1(x,\alpha)}{dx}\right|_{x=\pm 0}=(2\pi)^{-1/2}\int_{-a}^{a}\left.\frac{\partial\phi(x,z)}{\partial x}\right|_{x=\pm 0}e^{i\alpha z}dz. \tag{3.26}$$

Similarly from (3.23), we have

$$\begin{aligned}J_e(\alpha)=&-\frac{1}{(2\pi)^{1/2}i}\left(\frac{1}{R_e}+\frac{\cos^2\theta_0}{\tilde{R}_m}\right)\frac{e^{i(\alpha-k\cos\theta_0)a}-e^{-i(\alpha-k\cos\theta_0)a}}{(\alpha-k\cos\theta_0)}\\&+\left(\frac{1}{2R_e}+\frac{1}{2\tilde{R}_m}\right)[\Phi_1(+0,\alpha)+\Phi_1(-0,\alpha)]\\&+\frac{1}{2\tilde{R}_m k^2}[\Phi_1''(+0,\alpha)+\Phi_1''(-0,\alpha)],\end{aligned} \tag{3.27}$$

where

$$J_e(\alpha)=(2\pi)^{-1/2}\int_{-a}^{a}I_e(z)e^{i\alpha z}dz, \tag{3.28}$$

$$\Phi_1(\pm 0,\alpha)=(2\pi)^{-1/2}\int_{-a}^{a}\phi(\pm 0,z)e^{i\alpha z}dz, \tag{3.29}$$

$$\Phi_1''(\pm 0,\alpha)=\left.\frac{d^2\Phi_1(x,\alpha)}{dx^2}\right|_{x=\pm 0}=(2\pi)^{-1/2}\int_{-a}^{a}\left.\frac{\partial^2\phi(x,z)}{\partial x^2}\right|_{x=\pm 0}e^{i\alpha z}dz. \tag{3.30}$$

In (3.17), we set $x=\pm 0$ and apply the expression of (3.13), we obtain that

$$A(\alpha)=e^{-i\alpha a}\Phi_-(+0,\alpha)+\Phi_1(+0,\alpha)+e^{i\alpha a}\Phi_+(+0,\alpha), \tag{3.31}$$

$$B(\alpha)=e^{-i\alpha a}\Phi_-(-0,\alpha)+\Phi_1(-0,\alpha)+e^{i\alpha a}\Phi_+(-0,\alpha). \tag{3.32}$$

We differentiate (3.17) with respect to x and set $x=\pm 0,$ we obtain that

$$-\gamma A(\alpha)=e^{-i\alpha a}\Phi_-'(+0,\alpha)+\Phi_1'(+0,\alpha)+e^{i\alpha a}\Phi_+'(+0,\alpha), \tag{3.33}$$

$$\gamma B(\alpha)=e^{-i\alpha a}\Phi_-'(-0,\alpha)+\Phi_1'(-0,\alpha)+e^{i\alpha a}\Phi_+'(-0,\alpha). \tag{3.34}$$

We calculate the second order derivative of (3.17) twice with respect to x and set $x=\pm 0,$ we obtain that

$$\gamma^2 A(\alpha)=e^{-i\alpha a}\Phi_-''(+0,\alpha)+\Phi_1''(+0,\alpha)+e^{i\alpha a}\Phi_+''(+0,\alpha), \tag{3.35}$$

$$\gamma^2 B(\alpha)=e^{-i\alpha a}\Phi_-''(-0,\alpha)+\Phi_1''(-0,\alpha)+e^{i\alpha a}\Phi_+''(-0,\alpha). \tag{3.36}$$

Taking into account the boundary condition for tangential scattered fields

$$\left.\begin{aligned}
&\phi(+0,z)=\phi(-0,z)[\equiv\phi(0,z)],\\
&\left.\frac{\partial\phi(x,z)}{\partial x}\right|_{x=+0}=\left.\frac{\partial\phi(x,z)}{\partial x}\right|_{x=-0}\left[\equiv\left.\frac{\partial\phi(x,z)}{\partial x^2}\right|_{x=0}\right],\\
&\left.\frac{\partial^2\phi(x,z)}{\partial x^2}\right|_{x=+0}=\left.\frac{\partial^2\phi(x,z)}{\partial x^2}\right|_{x=-0}\left[\equiv\left.\frac{\partial^2\phi(x,z)}{\partial x^2}\right|_{x=0}\right]
\end{aligned}\right\} \tag{3.37}$$

for $|z|>a$, we find that

$$\left.\begin{aligned}
&\Phi_{\pm}(+0,\alpha)=\Phi_{\pm}(-0,\alpha)\equiv\Phi_{\pm}(0,\alpha),\\
&\Phi'_{\pm}(+0,\alpha)=\Phi'_{\pm}(-0,\alpha)\equiv\Phi'_{\pm}(0,\alpha),\\
&\Phi''_{\pm}(+0,\alpha)=\Phi''_{\pm}(-0,\alpha)\equiv\Phi''_{\pm}(0,\alpha).
\end{aligned}\right\} \tag{3.38}$$

Then, we see from (3.31), (3.32), (3.35), (3.36) and (3.38) that

$$A(\alpha)+B(\alpha)=2[e^{-i\alpha a}\Phi_{-}(0,\alpha)+e^{i\alpha a}\Phi_{+}(0,\alpha)]+\Phi_1(+0,\alpha)+\Phi_1(-0,\alpha), \tag{3.39}$$

$$A(\alpha)-B(\alpha)=\Phi_1(+0,\alpha)-\Phi_1(-0,\alpha), \tag{3.40}$$

$$\gamma^2[A(\alpha)+B(\alpha)]=2[e^{-i\alpha a}\Phi''_{-}(0,\alpha)+e^{i\alpha a}\Phi''_{+}(0,\alpha)]+\Phi''_1(+0,\alpha)+\Phi''_1(-0,\alpha), \tag{3.41}$$

$$\gamma^2[A(\alpha)-B(\alpha)]=\Phi''_1(+0,\alpha)-\Phi''_1(-0,\alpha). \tag{3.42}$$

Here, we see from (3.39) and (3.41) that

$$\Phi_1(+0,\alpha)+\Phi_1(-0,\alpha)=[A(\alpha)+B(\alpha)]-2[e^{-i\alpha a}\Phi_{-}(0,\alpha)+e^{i\alpha a}\Phi_{+}(0,\alpha)], \tag{3.43}$$

$$\Phi''_1(+0,\alpha)+\Phi''_1(-0,\alpha)=\gamma^2[A(\alpha)+B(\alpha)]-2[e^{-i\alpha a}\Phi''_{-}(0,\alpha)+e^{i\alpha a}\Phi''_{+}(0,\alpha)]. \tag{3.44}$$

Substituting (3.43) and (3.44) into (3.27), we can obtain that

$$\left(\frac{1}{2R_e}+\frac{1}{2\tilde{R}_m}+\frac{\gamma^2}{2\tilde{R}_m k^2}\right)[A(\alpha)+B(\alpha)]=e^{-i\alpha a}U_{-}(\alpha)+e^{i\alpha a}U_{(+)}(\alpha)+J_e(\alpha). \tag{3.45}$$

where

$$U_{\underset{-}{(+)}}(\alpha)=\tilde{\Phi}_{\pm}(\alpha)\mp\frac{A_{1,2}}{\alpha-k\cos\theta_0}, \tag{3.46}$$

$$\tilde{\Phi}_{\pm}(\alpha)=\left(\frac{1}{R_e}+\frac{1}{\tilde{R}_m}\right)\Phi_{\pm}(0,\alpha)+\frac{1}{\tilde{R}_m k^2}\frac{d^2\Phi_{\pm}(0,\alpha)}{dx^2}, \tag{3.47}$$

$$A_{1,2}=\frac{1}{(2\pi)^{1/2}i}\left(\frac{1}{R_e}+\frac{\cos^2\theta_0}{\tilde{R}_m}\right)e^{\mp ika\cos\theta_0}, \tag{3.48}$$

Similarly (3.33) and (3.34), we see that

$$\begin{aligned}-\gamma[A(\alpha)-B(\alpha)]=2[&e^{-i\alpha a}\Phi'_{-}(0,\alpha)+e^{i\alpha a}\Phi'_{+}(0,\alpha)]\\&+\Phi'_1(+0,\alpha)+\Phi'_1(-0,\alpha),\end{aligned} \tag{3.49}$$

$$-\gamma[A(\alpha)+B(\alpha)]=\Phi'_1(+0,\alpha)-\Phi'_1(-0,\alpha). \tag{3.50}$$

We find from (3.49) and (3.24) that

$$-\gamma[A(\alpha)-B(\alpha)]=-2ikZ_0R_mJ_m(\alpha)+2V_{-}(\alpha)e^{-i\alpha a}+2V_{(+)}(\alpha)e^{i\alpha a}. \tag{3.51}$$

where

$$V_{(\pm)}(\alpha)=\Phi'_{\pm}(\alpha)\mp\frac{B_{1,2}}{\alpha-k\cos\theta_0}, \tag{3.52}$$

$$\Phi'_{\pm}(\alpha)=\frac{d\Phi_{\pm}(0,\alpha)}{dx}, \tag{3.53}$$

$$B_{1,2}=-\frac{k\sin\theta_0}{(2\pi)^{1/2}}e^{\mp ika\cos\theta_0}. \tag{3.54}$$

Taking into account (3.12), (3.20) and (3.25), (3.40) can be expressed that

$$A(\alpha)-B(\alpha)=\Phi_1(+0,\alpha)-\Phi_1(-0,\alpha)=J_e(\alpha). \tag{3.55}$$

Similarly from (3.21), (3.26) and (3.28), (3.50) can be obtained that

$$A(\alpha)+B(\alpha)=-\frac{1}{\gamma}[\Phi'_1(+0,\alpha)-\Phi'_1(-0,\alpha)]=\frac{ikZ_0}{\gamma}J_e(\alpha). \tag{3.56}$$

It is seen from (3.55) and (3.56) that

$$A(\alpha)=\frac{1}{2}\left[J_m(\alpha)-\frac{\mathrm{i}kZ_0}{\gamma}J_e(\alpha)\right], \tag{3.57}$$

$$B(\alpha)=-\frac{1}{2}\left[J_m(\alpha)-\frac{\mathrm{i}kZ_0}{\gamma}J_e(\alpha)\right]. \tag{3.58}$$

Substituting (3.45) and (3.51) into (3.56) and (3.55), we obtain that

$$-\left(\frac{1}{2R_e}+\frac{1}{2\tilde{R}_m}+\frac{\gamma^2}{2\tilde{R}_m k^2}\right)\frac{ikZ_0}{\gamma}J_e(\alpha)=e^{-i\alpha a}U_-(\alpha)+e^{i\alpha a}U_{(+)}(\alpha)-J_e(\alpha), \tag{3.59}$$

$$-\gamma J_m(\alpha)=-2ikZ_0R_mJ_m(\alpha)+2V_-(\alpha)e^{-i\alpha a}+2V_{(+)}(\alpha)e^{i\alpha a}. \tag{3.60}$$

We derive, after some manipulations, that

$$M(\alpha)J_e(\alpha)=e^{-i\alpha a}U_-(\alpha)+e^{i\alpha a}U_{(+)}(\alpha), \tag{3.61}$$

$$-K(\alpha)J_m(\alpha)=2[e^{-i\alpha a}V_-(\alpha)+e^{i\alpha a}V_{(+)}(\alpha)], \tag{3.62}$$

where

$$M(\alpha)=1-\frac{ikZ_0}{2\gamma}\left[\frac{1}{R_e}+\frac{1}{\tilde{R}_m}\left(1+\frac{\gamma^2}{k^2}\right)\right], \tag{3.63}$$

$$K(\alpha)=\gamma-2ikZ_0R_m, \tag{3.64}$$

Equations (3.61) and (3.62) are the Wiener-Hopf equations satisfied by unknown spectral functions, where $J_m(\alpha)$ and $J_e(\alpha)$ are the Fourier transform of magnetic and electric surface currents on the strip, respectively. In the above notation, the subscripts '+' and '−' imply that the functions are regular in upper $(\tau>-k_2\cos\theta_0)$ and lower $(\tau<k_2\cos\theta_0)$ half-planes, respectively, whereas the subscript '(+)' implies that the functions are regular in $\tau>-k_2\cos\theta_0$ except for a simple pole at $\alpha=k\cos\theta_0$. We shall henceforth use these conventions for indicating the region of regularity in the α-plane.

3.3. Factorization of the Kernel Functions

In this section, we shall factorize the kernel functions $M(\alpha)$ and $K(\alpha)$ defined by (3.63) and (3.64) with the aid of Noble's approach [12]. The factorization is to split $M(\alpha)$ and $K(\alpha)$ into the multiplication form as in

$$M(\alpha)=M_+(\alpha)M_-(\alpha)=M_+(\alpha)M_+(-\alpha), \tag{3.65}$$

$$K(\alpha)=K_+(\alpha)K_-(\alpha)=K_+(\alpha)K_+(-\alpha), \tag{3.66}$$

where $M_\pm(\alpha)$ and $K_\pm(\alpha)$ are regular and nonzero in $\tau\gtrless\mp k_2\cos\theta_0$. In order to

factorize $M(\alpha)$ and $K(\alpha)$, let us introduce the auxiliary functions $N_n(\alpha)$ as

$$N_n(\alpha) = 1 + \frac{i}{k\delta_n}\gamma, \quad n = 1,2,3, \tag{3.67}$$

where

$$\delta_{1,2} = -\frac{\tilde{R}_m}{Z_0}\left\{1 \pm \left[1 + \frac{Z_0^2}{\tilde{R}_m}\left(\frac{1}{R_e} + \frac{1}{\tilde{R}_m}\right)\right]^{1/2}\right\}, \tag{3.68}$$

$$\delta_3 = 2Z_0 R_m. \tag{3.69}$$

Substituting (3.67) into (3.61) and (3.64), respectively, it follows that

$$M(\alpha) = \frac{kZ_0}{2i}\left(\frac{1}{R_e} + \frac{1}{\tilde{R}_m}\right)\frac{N_1(\alpha)N_2(\alpha)}{\gamma}, \tag{3.70}$$

$$K(\alpha) = -2ikZ_0 R_m N_3(\alpha). \tag{3.71}$$

Assuming that $N_n(\alpha)$ in (3.67) can be factorized as

$$N_n(\alpha) = N_{n+}(\alpha)N_{n-}(\alpha) = N_{n+}(\alpha)N_{n+}(-\alpha), \tag{3.72}$$

where $N_{n\pm}(\alpha)$ is regular and nonzero in $\tau \gtrless \mp k_2 \cos\theta_0$, and the split functions $N_{n\pm}(\alpha)$ are expressed as follows:

$$N_{n\pm}(\alpha) = N_n^{1/2}(0)\exp\left\{\int_0^\alpha \frac{d}{d\beta}[\ln N_{n\pm}(\beta)]\,d\beta\right\}, \tag{3.73}$$

where

$$N_n(0) = 1 + i\frac{1}{k\delta_n}\gamma\bigg|_{\alpha=0} = 1 + \frac{1}{\delta_n} \tag{3.74}$$

with

$$\gamma\big|_{\alpha=0} = (\alpha^2 - k^2)^{1/2}\big|_{\alpha=0} = -i(k^2 - \alpha^2)^{1/2}\big|_{\alpha=0} = -ik. \tag{3.75}$$

We can show that $N_n(\alpha)$ in (3.67) can be written as

$$\frac{d}{d\alpha}[\ln N_n(\alpha)] = \frac{N_n'(\alpha)}{N_n(\alpha)} = \frac{\alpha}{\alpha^2 + k^2(\delta_n^2 - 1)}\left(\frac{\mathrm{i}k\delta_n}{\gamma} + 1\right)$$
$$= \frac{1}{2}\left(\frac{1}{\alpha - id_n} + \frac{1}{\alpha + id_n}\right) + \frac{ik\delta_n}{2}\left(\frac{1}{\alpha - id_n} + \frac{1}{\alpha + id_n}\right)L(\alpha), \quad (3.76)$$

where

$$L(\alpha) = \frac{1}{\gamma} = (\alpha^2 - k^2)^{-1/2}, \quad (3.77)$$

$$d_n = k(\delta_n^2 - 1)^{1/2}. \quad (3.78)$$

According to [12], (3.77) can be decomposed as

$$L(\alpha) = L_+(\alpha) + L_-(\alpha) = L_+(\alpha) + L_+(-\alpha), \quad (3.79)$$

where

$$L_\pm(\alpha) = \frac{1}{\pi\gamma}\arccos(\pm\alpha / k) = -i\frac{1}{\pi\gamma}\ln\left(\frac{\pm\alpha - \gamma}{k}\right). \quad (3.80)$$

In (3.80), $L_\pm(\alpha)$ is regular and nonzero in $\tau \gtrless \mp k_2$, respectively.

We find from (3.76) and (3.79) that

$$\frac{d}{d\alpha}[\ln N_{n\pm}(\alpha)] = -\frac{ik\delta_n}{2}\left[\frac{L_\pm(id_n)}{\alpha - id_n} + \frac{L_\mp(id_n)}{\alpha + id_n}\right] + ik\delta_n\frac{\alpha L_\pm(\alpha)}{\alpha^2 + d_n^2}, \quad (3.81)$$

where

$$L_\pm(id_n) = \frac{1}{k\delta_n}\left\{\frac{i}{2} \pm \frac{\ln[\delta_n + (\delta_n^2 - 1)^{1/2}]}{\pi}\right\}. \quad (3.82)$$

Setting $\alpha = \beta$ in (3.81) and integrating both side of (3.81) with respect to β over $(0, \alpha)$, we obtain that

$$\int_0^{\alpha}\frac{d[\ln N_n(\beta)]}{d\beta}d\beta = ik\delta_n\int_0^{\alpha}\frac{\beta L_+(\beta)}{\beta^2+d_n^2}d\beta - \frac{ik\delta_n}{2}L_+(id_n)\int_0^{\alpha}\frac{1}{\beta-id_n}d\beta$$
$$-\frac{ik\delta_n}{2}L_-(id_n)\int_0^{\alpha}\frac{1}{\beta+id_n}d\beta$$
$$= ik\delta_n\int_0^{\alpha}\frac{\beta L_+(\beta)}{\beta^2+d_n^2}d\beta$$
$$-\frac{ik\delta_n}{2}\left[L_+(id_n)\ln\left(\frac{\alpha-id_n}{-id_n}\right)+L_-(id_n)\ln\left(\frac{\alpha+id_n}{id_n}\right)\right] \qquad (3.83)$$

Substituting (3.83) into (3.73), we derive after some manipulations, that

$$N_{n\pm}(\alpha) = \left(1+\frac{1}{\delta_n}\right)^{1/2}\exp\left\{-\frac{\delta_n}{\pi}\int_{\pi/2}^{\arccos(\pm\alpha/k)}\frac{t\cos t}{\sin^2 t-\delta_n^2}dt\right.$$
$$\pm\frac{i}{2\pi}\ln[\delta_n+(\delta_n^2-1)^{1/2}]\ln\left[\frac{ik(\delta_n^2-1)^{1/2}+\alpha}{ik(\delta_n^2-1)^{1/2}-\alpha}\right]$$
$$\left.+\frac{1}{4}\ln\left[1+\frac{\alpha^2}{k^2(\delta_n^2-1)}\right]\right\} \qquad (3.84)$$

as $n = 1,2,3.$ Using (3.84), we find that the split functions $M_{\pm}(\alpha)$ and $K_{\pm}(\alpha)$ are expressed as

$$M_{\pm}(\alpha) = \left[\frac{kZ_0}{2}\left(\frac{1}{R_e}+\frac{1}{\tilde{R}_m}\right)\right]^{1/2}\frac{N_{1\pm}(\alpha)N_{2\pm}(\alpha)}{(k\pm\alpha)^{1/2}}, \qquad (3.85)$$

$$K_{\pm}(\alpha) = (2kZ_0R_m)^{1/2}e^{-i\pi/4}N_{3\pm}(\alpha), \qquad (3.86)$$

where $M_{\pm}(\alpha)$ and $K_{\pm}(\alpha)$ are regular and nonzero in the half-plane $\tau \gtrless \mp k_2\cos\theta_0$, and show an algebraic behavior at infinity.

3.4. Formal Solution of the Wiener-Hopf Equations

Multiplying both sides of (3.61) by $e^{\pm i\alpha a}/M_{\mp}(\alpha)$, we obtain that

$$e^{-i\alpha a}J_e(\alpha)M_-(\alpha) = e^{-2i\alpha a}\frac{U_-(\alpha)}{M_+(\alpha)}+\frac{U_{(+)}(\alpha)}{M_+(\alpha)}, \qquad (3.87)$$

$$e^{i\alpha a}J_e(\alpha)M_+(\alpha)=e^{2i\alpha a}\frac{U_{(+)}(\alpha)}{M_-(\alpha)}+\frac{U_-(\alpha)}{M_-(\alpha)}. \tag{3.88}$$

Since $e^{\mp i\alpha a}J_e(\alpha)$ is an entire function, the left-hand sides of (3.87) and (3.88) are regular in the upper $(\tau>-k_2\cos\theta_0)$ and the lower $(\tau<k_2\cos\theta_0)$ half-plane, respectively. In the right-hand sides of (3.87) and (3.88), the terms of $e^{-2i\alpha a}U_-(\alpha)/M_+(\alpha)$, $U_{(+)}(\alpha)/M_+(\alpha)$, and $e^{2i\alpha a}U_{(+)}(\alpha)/M_-(\alpha)$ are regular in the strip $|\tau|<k_2\cos\theta_0$, and the term $U_-(\alpha)/M_-(\alpha)$ is regular in the lower $(\tau<k_2\cos\theta_0)$ half-plane. Hence, in accordance with the Wiener-Hopf procedure, we must decompose the terms on the right-hand sides of (3.87) and (3.88) which are regular in strip $|\tau|<k_2\cos\theta_0$ into the sum of two functions regular in the half planes $\tau\gtrless\mp k_2\cos\theta_0$.

Applying the edge condition [42] and the fundamental theorem on the asymptotic behavior of the Fourier integral, we find that

$$\left.\begin{aligned}U_{(+)}(\alpha)&=O(\alpha^{-3/2}),\\ M_{\pm}(\alpha)&=O(\alpha^{1/2})\end{aligned}\right\} \tag{3.89}$$

as $\alpha\to\infty$. Wee see from (3.89) that the first terms of the right-hand sides of (3.87) and (3.88) are $O(|\sigma|^{-2})$ uniformly in τ as $|\sigma|\to\infty$ in the strip $|\tau|<k_2\cos\theta_0$. Applying the standard decomposition theorem based on Cauchy's integral formula , we obtain that

$$e^{-2i\alpha a}\frac{U_-(\alpha)}{M_+(\alpha)}=\frac{1}{2\pi i}\int_{C_1}\frac{e^{-2i\beta a}U_-(\beta)}{M_+(\beta)(\beta-\alpha)}d\beta-\frac{1}{2\pi i}\int_{C_2}\frac{e^{-2i\beta a}U_-(\beta)}{M_+(\beta)(\beta-\alpha)}d\beta, \tag{3.90}$$

$$e^{2i\alpha a}\frac{U_{(+)}(\alpha)}{M_-(\alpha)}=\frac{1}{2\pi i}\int_{C_1}\frac{e^{2i\beta a}U_{(+)}(\beta)}{M_-(\beta)(\beta-\alpha)}d\beta-\frac{1}{2\pi i}\int_{C_2}\frac{e^{2i\beta a}U_{(+)}(\beta)}{M_-(\beta)(\beta-\alpha)}d\beta, \tag{3.91}$$

where C_1 and C_2 are the infinite integration paths parallel to the real axis, as shown in Fig. 3.2. In (3.87), $U_{(+)}(\alpha)/M_+(\alpha)$ is regular in the upper $(\tau>-k_2\cos\theta_0)$ half-plane except $\alpha=k\cos\theta_0$, and we decompose $U_{(+)}(\alpha)/M_+(\alpha)$ that

$$\frac{U_{(+)}(\alpha)}{M_+(\alpha)}=H_+^a(\alpha)+H_-^b(\alpha), \tag{3.92}$$

where

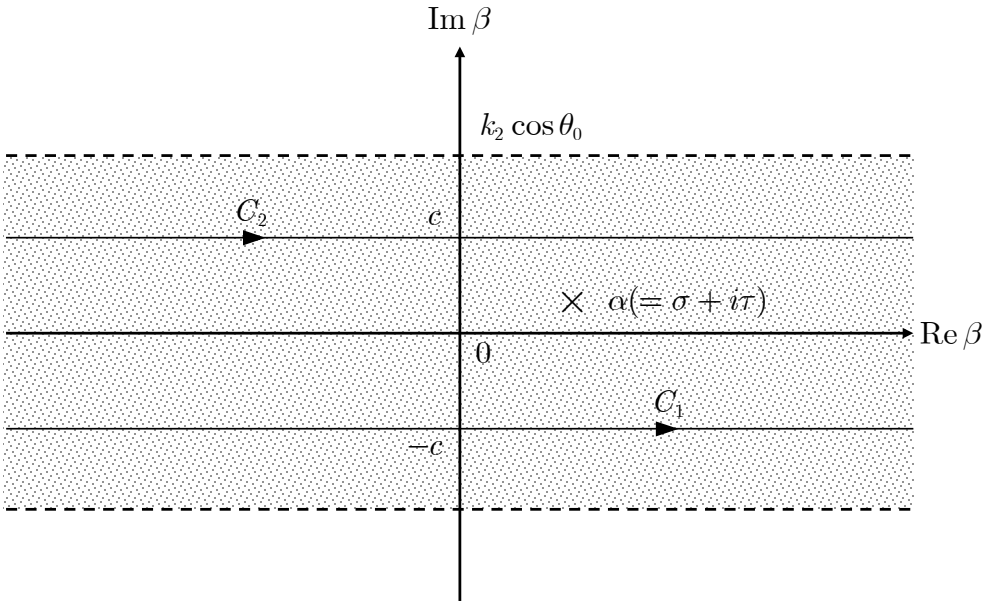

Fig. 3.2 Integral paths C_1 and C_2 for decomposition $(0<\tau<c<k_2\cos\theta_0)$.

$$\left.\begin{aligned} H_+^a(\alpha) &= \frac{U_{(+)}(\alpha)}{M_+(\alpha)} + \frac{A_1}{M_+(k\cos\theta_0)(\alpha - k\cos\theta_0)}, \\ H_-^b(\alpha) &= -\frac{A_1}{M_+(k\cos\theta_0)(\alpha - k\cos\theta_0)}. \end{aligned}\right\} \tag{3.93}$$

Substituting the decomposition result of (3.90)-(3.93) into (3.87) and (3.88), we can express that

$$\begin{aligned} & e^{-i\alpha a} M_-(\alpha) J_e(\alpha) - H_-^b(\alpha) + \frac{1}{2\pi i}\int_{C_2} \frac{e^{-2i\beta a} U_-(\beta)}{M_+(\beta)(\beta-\alpha)} d\beta \\ &= H_+^a(\alpha) + \frac{1}{2\pi i}\int_{C_1} \frac{e^{-2i\beta a} U_-(\beta)}{M_+(\beta)(\beta-\alpha)} d\beta, \end{aligned} \tag{3.94}$$

$$\begin{aligned} & \frac{U_-(\alpha)}{M_-(\alpha)} - \frac{1}{2\pi i}\int_{C_2} \frac{e^{2i\beta a} U_{(+)}(\beta)}{M_-(\beta)(\beta-\alpha)} d\beta \\ &= e^{i\alpha a} M_+(\alpha) J_e(\alpha) - \frac{1}{2\pi i}\int_{C_1} \frac{e^{2i\beta a} U_{(+)}(\beta)}{M_-(\beta)(\beta-\alpha)} d\beta, \end{aligned} \tag{3.95}$$

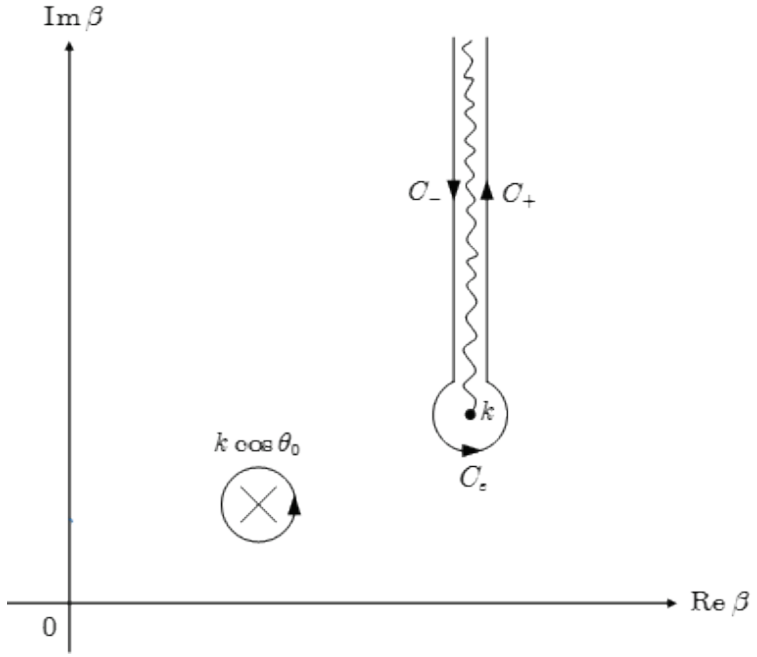

Fig. 3.3 Integral path $C(=C_- + C_\varepsilon + C_+)$.

where the left-hand and the right-hand sides of (3.94) and (3.95) are regular in the lower $(\tau < k_2 \cos\theta_0)$ and the upper $(\tau > -k_2 \cos\theta_0)$ half-plane, respectively, and both sides have a common strip of regularity in the strip $|\tau| < k_2 \cos\theta_0$. Hence, argument of the analytic continuation shows that there exists an entire function, denoted by $P(\alpha)$, which coincides with the left-hand and the right-hand sides of (3.94) and (3.95) are regular in the lower $(\tau < k_2 \cos\theta_0)$ and the upper $(\tau > -k_2 \cos\theta_0)$ half-plane, respectively. Taking into account (3.89) and the asymptotic behavior of the split functions, we see that the integrals in (3.94) and (3.95) are $o(1)$ as $\alpha \to \infty$. Therefore, it is seen from the Liouville's theorem that $P(\alpha) \equiv 0$. Thus, we obtain that

$$\frac{U_{(+)}(\alpha)}{M_+(\alpha)} + \frac{A_1}{M_+(k\cos\theta_0)(\alpha - k\cos\theta_0)} + \frac{1}{2\pi i}\int_{C_1} \frac{e^{-2i\beta a} U_-(\beta)}{M_+(\beta)(\beta - \alpha)} d\beta = 0, \qquad (3.96)$$

$$\frac{U_-(\alpha)}{M_-(\alpha)} - \frac{1}{2\pi \mathrm{i}}\int_{C_2} \frac{\mathrm{e}^{2\mathrm{i}\beta a} U_{(+)}(\beta)}{M_-(\beta)(\beta - \alpha)} \mathrm{d}\beta = 0. \qquad (3.97)$$

Equations (3.96) and (3.97) are a set of two coupled integral equations for $U_{(+)}(\alpha)$ and $U_-(\alpha)$. However, they may be decoupled in a following manner. Seting $\alpha \to -\alpha$

in (3.97) and making a change of variable $\beta \to -\beta$ in (3.96), we derive, after the manipulations of the sum and difference of the resultant equations, that

$$\frac{U_{(+)}^{s,d}(\alpha)}{M_+(\alpha)} = -\frac{A_1}{M_+(k\cos\theta_0)(\alpha - k\cos\theta_0)} \pm \frac{1}{2\pi i}\int_{C_2} \frac{e^{2i\beta a} U_{(+)}^{s,d}(\beta)}{M_-(\beta)(\beta+\alpha)} d\beta, \tag{3.98}$$

where

$$\begin{aligned} U_{(+)}^{s,d}(\alpha) &= U_{(+)}(\alpha) \pm U_-(-\alpha) \\ &= \tilde{\Phi}_+^{s,d}(\alpha) - \frac{A_1}{(\alpha - k\cos\theta_0)} \mp \frac{A_2}{(\alpha + k\cos\theta_0)} \end{aligned} \tag{3.99}$$

with

$$\tilde{\Phi}_+^{s,d}(\alpha) = \tilde{\Phi}_+(\alpha) \pm \tilde{\Phi}_-(-\alpha). \tag{3.100}$$

It is verified from (3.99) that the singularities associated with the integral in (3.98) for $\mathrm{Im}\,\beta > c \quad (0 < |\tau| < c < k_2 \cos\theta_0)$ have a simple pole at $\beta = k\cos\theta_0$ and a branch point at $\beta = k$. We now choose a branch cut emanating from $\beta = k$ as a straight line that is parallel to the imaginary axis and goes to infinity in the upper half-plane. Then evaluating the integral by enclosing the contour into the upper half-plane, yields

$$\begin{aligned} U_{(+)}^{s,d}(\alpha) = M_+(\alpha)\Bigg[&-\frac{A_1}{M_+(k\cos\theta_0)(\alpha - k\cos\theta_0)} \\ &\mp \frac{A_2}{M_-(k\cos\theta_0)(\alpha + k\cos\theta_0)} \pm u_{s,d}(\alpha)\Bigg], \end{aligned} \tag{3.101}$$

where

$$u_{s,d}(\alpha) = \frac{1}{2\pi i}\int_C \frac{e^{2i\beta a} U_{(+)}^{s,d}(\beta)}{M_-(\beta)(\beta+\alpha)} d\beta. \tag{3.102}$$

In (3.102), C is the contour composed of a portion C_ε of a circle with radius $\varepsilon \ll 1$ centered at $\beta = k$ and semi-infinite straight paths $C_\pm$ along the branch cut, as shown in Fig. 3.3. We find that the contribution from C_ε tends to zero by letting $\varepsilon \to 0$. On the other hand, the contributions from $C_\pm$ can be combined to yield a single branch-cut integral by noting that

$$(\beta^2 - k^2)^{1/2}\Big|_{\beta \in C_+} = -(\beta^2 - k^2)^{1/2}\Big|_{\beta \in C_-}. \tag{3.103}$$

After letting $\varepsilon \to 0$ and $1/M_{-}(\beta) \to M_{+}(\beta)/M(\beta)$, we obtain, making some arrangements, that

$$u_{s,d}(\alpha) = \frac{1}{\pi i}\int_{k}^{k+i\infty} \frac{e^{2i\beta a}(\beta-k)^{1/2}}{\beta+\alpha} U_{(+)}^{s,d}(\beta) F_{+}(\beta) d\beta, \tag{3.104}$$

where

$$F_{+}(\beta) = \frac{ikZ_0}{2} \frac{[1/R_e + \beta^2/(\tilde{R}_m k^2)](\beta+k)^{1/2} M_{+}(\beta)}{\beta^2 - k^2 + k^2 Z_0^2 [1/R_e + \beta^2/(\tilde{R}_m k^2)]^2/4}. \tag{3.105}$$

In (3.104), the contour is the one running parallel to the imaginary axis on the right-hand side of the brunch-cut. Substituting (3.104) into (3.101) and solving for $U_{(\pm)}(\alpha)$, we obtain that

$$U_{(+)}(\alpha) = M_{+}(\alpha)\left[-\frac{A_1}{M_{+}(k\cos\theta_0)(\alpha - k\cos\theta_0)} - \frac{u_{s,d}(\alpha) - u_{s,d}(\alpha)}{2} \right], \tag{3.106}$$

$$U_{-}(\alpha) = M_{-}(\alpha)\left[\frac{A_2}{M_{-}(k\cos\theta_0)(\alpha - k\cos\theta_0)} + \frac{u_{s,d}(-\alpha) + u_{s,d}(-\alpha)}{2} \right]. \tag{3.107}$$

Equation (3.62) can be solved in a similar manner. We multiply both sides of (3.62) by $e^{\pm i\alpha a}/K_{\mp}(\alpha)$. Applying the edge condition and the fundamental theorem on the asymptotic behavior of the Fourier integral, we find that

$$\left.\begin{aligned} V_{(\pm)}(\alpha) &= O(\alpha^{-1/2}), \\ K_{\pm}(\alpha) &= O(\alpha^{1/2}) \end{aligned}\right\} \tag{3.108}$$

as $\alpha \to \infty$. Decomposing the resultant equations and making some manipulations, we obtain that

$$\frac{V_{(+)}(\alpha)}{K_{+}(\alpha)} + \frac{B_1}{K_{+}(k\cos\theta_0)(\alpha - k\cos\theta_0)} + \frac{1}{2\pi i}\int_{C_1} \frac{e^{-2i\beta a} V_{-}(\beta)}{K_{+}(\beta)(\beta-\alpha)} d\beta = 0, \tag{3.109}$$

$$\frac{V_{-}(\alpha)}{K_{-}(\alpha)} - \frac{1}{2\pi i}\int_{C_2} \frac{e^{2i\beta a} V_{(+)}(\beta)}{K_{-}(\beta)(\beta-\alpha)} d\beta = 0. \tag{3.110}$$

where C_1 and C_2 are the infinite integration paths shown in Fig. 3.2. A similar procedure can be also be applied to (3.109) and (3.110). Omitting the details, we obtain that

$$V_{(+)}^{s,d}(\alpha) = K_+(\alpha)\Bigg[-\frac{B_1}{K_+(k\cos\theta_0)(\alpha - k\cos\theta_0)} \mp \frac{B_2}{K_-(k\cos\theta_0)(\alpha + k\cos\theta_0)} \pm v_{s,d}(\alpha)\Bigg], \tag{3.111}$$

where

$$V_{(+)}^{s,d}(\alpha) = V_{(+)}(\alpha) \pm V_-(-\alpha), \tag{3.112}$$

$$v_{s,d}(\alpha) = \frac{1}{\pi i}\int_k^{k+i\infty} \frac{e^{2i\beta a}(\beta - k)^{1/2}}{\beta + \alpha} V_{(+)}^{s,d}(\beta) T_+(\beta) d\beta, \tag{3.113}$$

$$T_+(\beta) = \frac{(\beta + k)^{1/2} K_+(\beta)}{\beta^2 - k^2 + 4k^2 Z_0^2 R_m^2}. \tag{3.114}$$

Substituting (3.111) into (3.112) and solving for $V_{(\pm)}(\alpha)$, we obtain that

$$V_{(+)}(\alpha) = K_+(\alpha)\Bigg[-\frac{B_1}{K_+(k\cos\theta_0)(\alpha - k\cos\theta_0)} - \frac{v_{s,d}(\alpha) - v_{s,d}(\alpha)}{2}\Bigg], \tag{3.115}$$

$$V_-(\alpha) = K_-(\alpha)\Bigg[\frac{B_2}{K_-(k\cos\theta_0)(\alpha - k\cos\theta_0)} + \frac{v_{s,d}(-\alpha) + v_{s,d}(-\alpha)}{2}\Bigg]. \tag{3.116}$$

Equations (3.106), (3.107), (3.115) and (3.116) the exact solutions to the Wiener-Hopf equations (3.61) and (3.62), respectively, but they are formal in the sense that the branch-cut integrals with unknown integrands $u_{s,d}(\alpha)$ and $v_{s,d}(\alpha)$ are involved. Accordingly, it is required to develop approximation procedures for these integrals to derive explicit solutions.

3.5. Asymptotic Solution of a Certain Integral Equation in the Complex Plane

In this section, we shall consider a certain integral equation in the complex plane that often arises in the Wiener-Hopf analysis of canonical scattering problems, and discuss a method of solution in detail. The results obtained in this section will provide a generalization of the method developed in our previous papers [38].

The Wiener-Hopf analysis often leads to the following exact solution in the complex plane:

$$f(\alpha)=h(\alpha)\left[g(\alpha)+\frac{C}{\pi i}\int_k^{k+i\infty}e^{i\beta l}\frac{(\beta-k)^{\nu}G(\beta)f(\beta)}{\beta+\alpha}d\beta\right]. \tag{3.117}$$

In (3.117), $f(\alpha)$ is the unknown function to be determined, and all the other quantities are known constants or functions.

Let $f(\beta)$ be a function of a complex variable β satisfying the following conditions:

(i) $f(\beta)$ *is an analytic function of* β *regular in* $|\beta-k|<\varepsilon<\infty$, *where* $k=k_1+ik_2$ *with* $k_1>0$, $k_2>0$, *and* $\varepsilon\not\approx 0$.

(ii) $f(\beta)$ *satisfies* $O[(\beta-k)^{\delta}]$ *for any* β *such that* $|\beta-k|\geq R$ *with* $\varepsilon<R<\infty$, *where* δ *is some real constant.*

(iii) $f(\beta)$ *is a continuous function of* β *on any bounded part of the semi-infinite straight path from* k *to* $k+i\infty$ *in the* β*-plane.*

Let α be a complex variable such that $|\alpha+k|>0$ and $-\pi/2<\arg(\alpha+k)<3\pi/2$, and introduce

$$F_m^{\nu}(l,\alpha)=\frac{1}{\pi i}\int_k^{k+i\infty}e^{i\beta l}\frac{(\beta-k)^{\nu}G(\beta)f(\beta)}{(\beta+\alpha)^m}d\beta \tag{3.118}$$

for $l>0$, $\mathrm{Re}\,\nu>-1$, and positive integer m, where $\arg(\beta-k)=\pi/2$. In (3.118), $G(\beta)$ is regular in the neighborhood of $\beta=k$, and shows an algebraic behavior as $\beta\to\infty$ in the upper half-plane.

We define the region in the α-plane as follows:

$$D=\left\{\alpha:|\alpha+k|>0,-\pi/2<\arg(\alpha+k)<3\pi/2\right\}. \tag{3.119}$$

Then it is shown that the function $F_m^{\nu}(l,\alpha)$ defined by (3.118) is uniformly convergent in any bounded closed region in D and hence, regular in D. We can prove the following theorem on the asymptotic expansion of $F_m^{\nu}(l,\alpha)$ for large l:

Theorem. *The function* $F_m^{\nu}(l,\alpha)$ *has an asymptotic expansion*

$$F_m^{\nu}(l,\alpha) \sim \frac{e^{ikl}}{\pi} \sum_{n=0}^{\infty} f_n \frac{i^{\nu-m+n}}{l^{\nu-m+n+1}} \Gamma_m^g[\nu+n+1, -i(\alpha+k)l] \tag{3.120}$$

as $l \to \infty$, *where*

$$f_n = \frac{1}{n!} \frac{d^n f(\beta)}{d\beta^n}\bigg|_{\beta=k}. \tag{3.121}$$

In (3.120), $\Gamma_m^g(\cdot,\cdot)$ *is the special function defined by*

$$\Gamma_m^g(u,w) = \int_0^{\infty} \frac{t^{u-1}e^{-t}}{(t+w)^m} G(k+it/l)dt \tag{3.122}$$

for $\mathrm{Re}\, u > 0, |w| > 0, |\arg w| < \pi$, *and positive integer* m.

The above theorem reduces to the results obtained in [38] by setting $G(\beta) \equiv 1$.

Using the function $F_m^{\nu}(l,\alpha)$, (3.118) can be written as

$$f(\alpha) = h(\alpha)[g(\alpha) + CF_1^{\nu}(l,\alpha)], \tag{3.123}$$

where it is assumed that $f(\alpha)$ satisfies the conditions (i)-(iii), and $g(\alpha)$ and $h(\alpha)$ are regular in region Δ contained in D. Then we can apply Theorem to derive an asymptotic expansion of $F_1^{\nu}(l,\alpha)$ for large l. Thus we obtain from (3.123) that

$$f(\alpha) \sim h(\alpha)\left[g(\alpha) + C\sum_{n=0}^{\infty} f_n \xi_{0n}^g(\nu,l,\alpha) \right] \tag{3.124}$$

as $l \to \infty$, where f_n is defined by (3.121), and

$$\xi_{0n}^g(\nu,l,\alpha) = \frac{e^{ikl}}{\pi} \frac{i^{n+\nu-1}}{l^{n+\nu}} \Gamma_1^g[\nu+n+1, -i(\alpha+k)l]. \tag{3.125}$$

Equation (3.124) is the asymptotic solution of the integral equation (3.123) for large l, where an infinite number of unknowns f_n with $n = 0,1,2,\cdots$ are contained. Hence, it is required to derive matrix equations for these unknowns in an appropriate manner.

Setting $\alpha = k$ in (3.124), and using the notation (3.121), we find that

$$f_0 \sim h(k)\left[g(k) + C\sum_{n=0}^{\infty} f_n \xi_{0n}^g(\nu,l,k) \right]. \tag{3.126}$$

We now differentiate both sides of (3.124) m times $(m=1,2,3,\cdots)$ with respect to α by taking into account the regularity of $F_m^v(l,\alpha)$ in D, and setting $\alpha=k$ in the resultant equation, we obtain that

$$f_m \sim \sum_{p=0}^{m} \frac{h^{(m-p)}(k)}{p!(m-p)!}\left[g^{(p)}(k) + C\sum_{n=0}^{\infty} f_n \xi_{pn}^{g}(v,l,k) \right] \tag{3.127}$$

for $m=1,2,3,\cdots,$

$$h^{(m-p)}(k) = \left.\frac{d^{m-p}h(\alpha)}{d\alpha^{m-p}}\right|_{\alpha=k}, \tag{3.128}$$

$$g^{(p)}(k) = \left.\frac{d^{p}g(\alpha)}{d\alpha^{p}}\right|_{\alpha=k}, \tag{3.129}$$

$$\xi_{pn}^{g}(v,l,k) = \frac{e^{ikl}}{\pi}(-1)^p\, p!\, \frac{i^{n-p+v-1}}{l^{n-p+v}}\Gamma_{p+1}(v+n+1,-2ikl). \tag{3.130}$$

Hence it follows from (3.126) and (3.127) that

$$f_m - C\sum_{n=0}^{\infty} A_{mn} f_n \sim B_m, \quad m=0,1,2,\cdots \tag{3.131}$$

for large l, where

$$A_{mn} = \sum_{p=0}^{m} \frac{h^{(m-p)}(k)\xi_{pn}^{g}(v,l,k)}{p!(m-p)!}, \tag{3.132}$$

$$B_m = \sum_{p=0}^{m} \frac{h^{(m-p)}(k)g^{(p)}(k)}{p!(m-p)!}. \tag{3.133}$$

Equation (3.131) provides the desired matrix equation for determining the unknowns f_n with $n=0,1,2,\cdots$ in (3.124), and it is valid for large l.

3.6. High-Frequency Asymptotic Solutions

In this section, we shall apply the method established in the previous section to solve (3.101) and (3.111) asymptotically. In order to eliminate the singularities of $U_{(+)}^{s,d}(\alpha)$ (3.101) at $\alpha = k\cos\theta_0$, we introduce the auxiliary functions $\tilde{\Phi}_{+}^{s,d}(\alpha)$ as

$$\tilde{\Phi}_{+}^{s,d}(\alpha) = U_{(+)}^{s,d}(\alpha) + \frac{A_1}{\alpha - k\cos\theta_0} \pm \frac{A_2}{\alpha + k\cos\theta_0}, \tag{3.134}$$

where $\tilde{\Phi}_{+}^{s,d}(\alpha)$ is regular in the upper half-plane $\tau > -k_2\cos\theta_0$. Substituting (3.134) into (3.101) and carrying out some manipulation, we describe that

$$\tilde{\Phi}_{+}^{s,d}(\alpha) = M_{+}(\alpha)[\chi_{us,ud}(\alpha) + C_{s,d}F_{s,d}^{u}(\alpha)], \tag{3.135}$$

$$\chi_{us,ud}(\alpha) = A_1[P_1(\alpha) \pm \eta_{f2}(\alpha)] + A_2[\eta_{f1}(\alpha) \pm P_2(\alpha)], \tag{3.136}$$

$$C_{s,d} = \pm 1, \tag{3.137}$$

$$F_{s,d}^{u}(\alpha) = \frac{1}{\pi i}\int_{k}^{k+i\infty} \frac{e^{2i\beta a}(\beta - k)^{1/2}}{\beta + \alpha}\tilde{\Phi}_{+}^{s,d}(\beta)F_{+}(\beta)d\beta \tag{3.138}$$

with

$$P_{1,2}(\alpha) = \frac{1}{\alpha \mp k\cos\theta_0}\left[\frac{1}{M_{+}(\alpha)} - \frac{1}{M_{\pm}(k\cos\theta_0)}\right], \tag{3.139}$$

$$\eta_{f1,f2}(\alpha) = \frac{\xi_{00}^{f}(\alpha) - \xi_{00}^{f}(\pm k\cos\theta_0)}{\alpha \mp k\cos\theta_0}, \tag{3.140}$$

$$\xi_{00}^{f}(\alpha) = \frac{e^{2ika}}{\pi}\frac{i^{-1/2}}{(2a)^{1/2}}\Gamma_1^{f}[3/2, -2i(\alpha + k)a]. \tag{3.141}$$

In (3.141), $\Gamma_m^{f}(\cdot,\cdot)$ is the special function defined by

$$\Gamma_m^{f}(u,w) = \int_0^{\infty} \frac{t^{u-1}e^{-t}}{(t+w)^m}F_{+}[k + it/(2a)]dt \tag{3.142}$$

for $\mathrm{Re}\,u > 0,\ |w| > 0,\ |\arg w| < \pi,$ and positive integer $m,$ which accounts for multiple diffraction effects.

Applying Theorem in Section 3.5, we can obtain a high-frequency asymptotic expansion of (3.135) with the result that

$$\tilde{\Phi}_{+}^{s,d}(\alpha) \sim M_{+}(\alpha)\left[\chi_{us,ud}(\alpha) + C_{s,d}\sum_{n=0}^{N} f_n^{us,ud}\xi_{0n}^{f}(\alpha)\right] \tag{3.143}$$

for $ka \to \infty$, where N denotes the truncation number of the infinite asymptotic series,

and

$$f_n^{us,ud} = \frac{1}{n!}\frac{d^n \tilde{\Phi}_+^{s,d}(\alpha)}{d\alpha^n}\bigg|_{\alpha=k}, \tag{3.144}$$

$$\xi_{0n}^f(\alpha) = \frac{e^{2ika}}{\pi}\frac{i^{n-1/2}}{(2a)^{n+1/2}}\Gamma_1^f[3/2+n, -2i(\alpha+k)a]. \tag{3.145}$$

Taking into account (3.131) and carrying out some manipulations, the unknowns $f_n^{us,ud}$ in (3.144) is determined by solving the matrix equation

$$f_m^{us,ud} - C_{s,d}\sum_{n=0}^{N} A_{mn}^u f_n^{us,ud} \sim B_m^{us,ud} \tag{3.146}$$

for $m = 0,1,2,\cdots,N,$ where

$$A_{mn}^u = \sum_{p=0}^{m}\frac{M_+^{(m-p)}(k)\xi_{pn}^f(k)}{p!(m-p)!}, \tag{3.147}$$

$$B_m^{us,ud} = \sum_{p=0}^{m}\frac{M_+^{(m-p)}(k)\chi_{us,ud}^{(p)}(k)}{p!(m-p)!} \tag{3.148}$$

with

$$M_+^{(m-p)}(k) = \frac{d^{m-p}M_+(\alpha)}{d\alpha^{m-p}}\bigg|_{\alpha=k}, \tag{3.149}$$

$$\xi_{pn}^f(k) = \frac{e^{2ika}}{\pi}(-1)^p p!\frac{i^{n-p-1/2}}{(2a)^{n-p+1/2}}\Gamma_{p+1}^f(3/2+n, -4ika), \tag{3.150}$$

$$\chi_{us,ud}^{(p)}(k) = \frac{d^p\chi_{us,ud}(\alpha)}{d\alpha^p}\bigg|_{\alpha=k}. \tag{3.151}$$

Making use of the above results and carrying out further manipulations, we finally arrive at an explicit asymptotic solution to the Wiener-Hopf equation (3.61) with the result that

$$U_{(+)}(\alpha) \sim M_+(\alpha)\bigg[-\frac{A_1}{M_\pm(k\cos\theta_0)(\alpha - k\cos\theta_0)} + A_2\eta_{f1}(\alpha) + \frac{1}{2}\sum_{n=0}^{N}(f_n^{us} \mp f_n^{ud})\xi_{0n}^f(\alpha)\bigg], \tag{3.152}$$

$$U_{-}(\alpha) \sim M_{-}(\alpha)\left[\mp \frac{A_2}{M_{-}(k\cos\theta_0)(\alpha - k\cos\theta_0)} + A_1\eta_{f2}(-\alpha) \right.$$
$$\left. + \frac{1}{2}\sum_{n=0}^{N}(f_n^{us} + f_n^{ud})\xi_{0n}^{f}(-\alpha) \right] \tag{3.153}$$

as $ka \to \infty$.

A similar procedure may also be applied to (3.115) and (3.116) for a high-frequency solution. Omitting the details, we can obtain

$$V_{(+)}(\alpha) \sim K_{+}(\alpha)\left[-\frac{B_1}{K_{\pm}(k\cos\theta_0)(\alpha - k\cos\theta_0)} + B_2\eta_{t1}(\alpha) \right.$$
$$\left. + \frac{1}{2}\sum_{n=0}^{N}(f_n^{vs} \mp f_n^{vd})\xi_{0n}^{t}(\alpha) \right], \tag{3.154}$$

$$V_{-}(\alpha) \sim K_{-}(\alpha)\left[\mp \frac{B_2}{K_{-}(k\cos\theta_0)(\alpha - k\cos\theta_0)} + B_1\eta_{t2}(-\alpha) \right.$$
$$\left. + \frac{1}{2}\sum_{n=0}^{N}(f_n^{vs} + f_n^{vd})\xi_{0n}^{t}(-\alpha) \right] \tag{3.155}$$

for $ka \to \infty$, where

$$\eta_{t1,t2}(\alpha) = \frac{\xi_{00}^{t}(\alpha) - \xi_{00}^{t}(\pm k\cos\theta_0)}{\alpha \mp k\cos\theta_0}, \tag{3.156}$$

$$f_n^{vs,vd} = \frac{1}{n!}\frac{d^n\Phi_{+}'^{s,d}(\alpha)}{d\alpha^n}\bigg|_{\alpha=k}, \tag{3.157}$$

$$\xi_{0n}^{t}(\alpha) = \frac{e^{2ika}}{\pi}\frac{i^{n-1/2}}{(2a)^{n+1/2}}\Gamma_1^{t}[3/2 + n, -2i(\alpha + k)a], \tag{3.158}$$

$$B_m^{us,ud} = \sum_{p=0}^{m}\frac{M_{+}^{(m-p)}(k)\chi_{us,ud}^{(p)}(k)}{p!(m-p)!} \tag{3.159}$$

with

$$\Phi_{+}'^{s,d}(\alpha) = V_{(+)}^{s,d}(\alpha) + \frac{B_1}{\alpha - k\cos\theta_0} \pm \frac{B_2}{\alpha + k\cos\theta_0}, \tag{3.160}$$

$$\Gamma_m^t(u,w)=\int_0^\infty \frac{t^{u-1}e^{-t}}{(t+w)^m}T_+[k+it/(2a)]dt. \tag{3.161}$$

Equations (3.152)-(3.155) provide complete, high-frequency asymptotic solutions to the Wiener-Hopf equations. It is to be noted that the above results rigorously take into account the multiple diffraction between the edges of the strip.

3.7 Scattered Far Field

Using the boundary condition, the scattered field in the Fourier transform domain is expressed as

$$\Phi(x,\alpha)=\hat{\Phi}(\alpha)e^{-\gamma|x|}, \tag{3.162}$$

where

$$\hat{\Phi}(\alpha)=-ikZ_0\frac{e^{-i\alpha a}U_-(\alpha)+e^{i\alpha a}U_{(+)}(\alpha)}{2\gamma M(\alpha)}\mp\frac{e^{-i\alpha a}V_-(\alpha)+e^{i\alpha a}V_{(+)}(\alpha)}{K(\alpha)},\quad x\gtrless 0. \tag{3.163}$$

The scattered field $\phi(x,z)$ in the real space is obtained by taking the inverse Fourier transform of (3.162) according to the formula

$$\phi(x,z)=(2\pi)^{-1/2}\int_{-\infty+ic}^{\infty+ic}\Phi(\alpha)e^{-i\alpha z}d\alpha, \tag{3.164}$$

where c is a constant such that $0<|c|<k_2\cos\theta_0$. Substituting (3.162) into (3.164), an integral representation of the scattered field $\phi(x,z)$ is found to be

$$\phi(x,z)=(2\pi)^{-1/2}\int_{-\infty+ic}^{\infty+ic}\Phi(\alpha)e^{-\gamma|x|-i\alpha z}d\alpha. \tag{3.165}$$

It is seen from (3.57) and (3.58) that (3.163) can be written as

$$\hat{\Phi}(\alpha)=\frac{1}{2}\left[\pm J_m(\alpha)-\frac{ikZ_0}{\gamma}J_e(\alpha)\right], \tag{3.166}$$

where $J_e(\alpha)$ and $J_m(\alpha)$ are entire functions. This shows that singularities of the integrand of (3.165) are only branch points at $\alpha=\pm k$. Introducing the cylindrical coordinate (ρ,θ) centered at the origin as

$$x=\rho\sin\theta,\quad z=\rho\cos\theta,\quad -\pi<\theta<\pi \tag{3.167}$$

and applying the saddle point method, we derive a far field asymptotic expression with the result that

$$\phi(\rho,\theta)\sim\pm\hat{\Phi}(-k\cos\theta)k\sin\theta\frac{e^{i(k\rho-\pi/4)}}{(k\rho)^{1/2}},\quad x\gtrless 0 \tag{3.168}$$

as $k\rho \to \infty$. Equation (3.168) is uniformly valid for arbitrary incidence and observation angles.

3.8 Alternative Approach

In this section, we shall consider the same diffraction problem as in the previous sections, and carry out the Wiener-Hopf analysis by using approximate boundary conditions [35] valid for $|M|(=|\varepsilon_r\mu_r|^{1/2}) \gg 1$:

$$E_y^t(+0,z) + E_y^t(-0,z) = -2R[H_z^t(+0,z) - H_z^t(-0,z)], \tag{3.169}$$

$$H_z^t(+0,z) + H_z^t(-0,z) = -2Q[E_y^t(+0,z) - E_y^t(-0,z)], \tag{3.170}$$

where

$$\left.\begin{aligned} R &= \frac{iZ_0}{2}\frac{\mu_r^{1/2}}{\varepsilon_r^{1/2}}\cot[kb(\varepsilon_r\mu_r)^{1/2}/2], \\ Q &= \frac{i}{2Z_0}\frac{\varepsilon_r^{1/2}}{\mu_r^{1/2}}\cot[kb(\varepsilon_r\mu_r)^{1/2}/2]. \end{aligned}\right\} \tag{3.171}$$

Since the method is similar to that followed in the above sections, only the main results will be summarized.

Solving (3.16) and taking into account (3.169) and (3.170) as in above discussions, we obtain that

$$M^1(\alpha)J_e^1(\alpha) = e^{-i\alpha a}U_-^1(\alpha) + e^{i\alpha a}U_{(+)}^1(\alpha), \tag{3.172}$$

$$K^1(\alpha)J_m^1(\alpha) = -2[e^{-i\alpha a}V_-^1(\alpha) + e^{i\alpha a}V_{(+)}^1(\alpha)], \tag{3.173}$$

where

$$M^1(\alpha) = M_+^1(\alpha)M_-^1(\alpha) = R - \frac{ikZ_0}{2\gamma}, \tag{3.174}$$

$$K^1(\alpha) = K_+^1(\alpha)K_-^1(\alpha) = \gamma - 2ikZ_0Q, \tag{3.175}$$

$$J_e^1(\alpha) = -\frac{i}{kZ_0}\left[\frac{d\Phi_1(+0,\alpha)}{dx} - \frac{d\Phi_1(-0,\alpha)}{dx}\right], \tag{3.176}$$

$$J_m^1(\alpha) = \Phi_1(+0,\alpha) - \Phi_1(-0,\alpha), \tag{3.177}$$

$$U_{(+)}^1(\alpha) = \Phi_\pm(\alpha) \mp \frac{A_{1,2}^1}{\alpha - k\cos\theta_0}, \tag{3.178}$$

$$V^1_{(\pm)}(\alpha) = \Phi'_{\pm}(\alpha) \mp \frac{B^1_{1,2}}{\alpha - k\cos\theta_0} \tag{3.179}$$

with

$$A^1_{1,2} = \frac{1}{(2\pi)^{1/2} i} e^{\mp ika\cos\theta_0}, \tag{3.180}$$

$$B^1_{1,2} = -\frac{k\sin\theta_0}{(2\pi)^{1/2}} e^{\mp ika\cos\theta_0}, \tag{3.181}$$

$$M^1_{\pm}(\alpha) = \left(\frac{kZ_0}{2}\right)^{1/2} \frac{N^1_{1\pm}(\alpha)}{(k\pm\alpha)^{1/2}}, \tag{3.182}$$

$$K^1_{\pm}(\alpha) = (2kZ_0Q)^{1/2} e^{-i\pi/4} N^1_{2\pm}(\alpha), \tag{3.183}$$

$$\begin{aligned} N^1_{n\pm}(\alpha) = (1+\delta_{1n}^{-1})^{1/2} \exp\Bigg\{ & -\frac{\delta_{1n}}{\pi} \int_{\pi/2}^{\arccos(\pm\alpha/k)} \frac{t\cos t}{\sin^2 t - \delta_{1n}^2} dt \\ & \pm \ln[\delta_{1n} + (\delta_{1n}^2 - 1)^{1/2}] \frac{i}{2\pi} \ln\left[\frac{ik(\delta_{1n}^2-1)^{1/2} + \alpha}{ik(\delta_{1n}^2-1)^{1/2} - \alpha}\right] \\ & + \frac{1}{4}\ln\left[1 + \frac{\alpha^2}{k^2(\delta_{1n}^2 - 1)}\right]\Bigg\}, \quad n = 1, 2, \end{aligned} \tag{3.184}$$

where

$$\delta_{11} = \frac{Z_0}{2R}, \quad \delta_{12} = 2Z_0Q. \tag{3.185}$$

Equations (3.172) and (3.173) are the Wiener-Hopf equations satisfied by unknown spectral functions.

Applying the asymptotic method established [40], we can derive a high-frequency representation of (3.178) for large ka with the result that

$$\begin{aligned} U^1_{(\pm)}(\alpha) \sim M^1_{\pm}(\alpha) \Bigg[& \mp \frac{A^1_{1,2}}{M^1_{\pm}(k\cos\theta_0)(\alpha - k\cos\theta_0)} + A^1_{2,1}\eta^1_{f1,f2}(\pm\alpha) \\ & + \frac{1}{2}\sum_{n=0}^{N} (f_n^{1us} \mp f_n^{1ud}) \xi^{1f}_{0n}(\pm\alpha) \Bigg] \end{aligned} \tag{3.186}$$

for $ka \to \infty$, where

$$f_n^{1us,1ud} = \frac{1}{n!} \frac{d^n \Phi_+^{s,d}(\alpha)}{d\alpha^n}\bigg|_{\alpha=k}, \tag{3.187}$$

$$\eta^1_{f1,f2}(\alpha)=\frac{\xi^{1f}_{00}(\alpha)-\xi^{1f}_{00}(\pm k\cos\theta_0)}{\alpha\mp k\cos\theta_0} \tag{3.188}$$

with

$$\Phi^{s,d}_{+}(\alpha)=\Phi_{+}(\alpha)\pm\Phi_{-}(-\alpha), \tag{3.189}$$

$$\xi^{1f}_{0n}(\alpha)=\frac{e^{2ika}}{\pi}\frac{i^{n-1/2}}{(2a)^{n+1/2}}\Gamma^{1f}_{1}[3/2+n,-2i(\alpha+k)a], \tag{3.190}$$

$$\Gamma^{1f}_{m}(u,w)=\int_0^\infty\frac{t^{u-1}e^{-t}}{(t+w)^m}F^1_{+}[k+it/(2a)]dt, \tag{3.191}$$

$$F^1_{+}(\beta)=\frac{2ikZ_0(\beta+k)^{1/2}M^1_{+}(\beta)}{4(\beta^2-k^2)R^2+k^2Z_0^2}. \tag{3.192}$$

Equation (3.186) provides complete, high-frequency asymptotic solutions to the Wiener-Hopf equations.

A similar procedure may also be applied to (3.179) for a high-frequency solution as follows:

$$V^1_{(+)}(\alpha)\sim K^1_{\pm}(\alpha)\left[\mp\frac{B^1_{1,2}}{K^1_{\pm}(k\cos\theta_0)(\alpha-k\cos\theta_0)}+B^1_{2,1}\eta^1_{t1,t2}(\pm\alpha)\right.$$
$$\left.+\frac{1}{2}\sum_{n=0}^{N}(f^{1vs}_n\mp f^{1vd}_n)\xi^{1t}_{0n}(\pm\alpha)\right] \tag{3.193}$$

for $ka\to\infty$, where

$$f^{1vs,1vd}_n=\frac{1}{n!}\frac{d^n\Phi'^{s,d}_{+}(\alpha)}{d\alpha^n}\bigg|_{\alpha=k}, \tag{3.194}$$

$$\eta^1_{t1,t2}(\alpha)=\frac{\xi^{1t}_{00}(\alpha)-\xi^{1t}_{00}(\pm k\cos\theta_0)}{\alpha\mp k\cos\theta_0} \tag{3.195}$$

with

$$\Phi'_{+}(\alpha)=\Phi'_{+}(\alpha)\pm\Phi'_{-}(-\alpha), \tag{3.196}$$

$$\xi^{1t}_{0n}(\alpha)=\frac{e^{2ika}}{\pi}\frac{i^{n-1/2}}{(2a)^{n+1/2}}\Gamma^{1t}_{1}[3/2+n,-2i(\alpha+k)a], \tag{3.197}$$

$$\Gamma_m^{1t}(u,w)=\int_0^\infty \frac{t^{u-1}e^{-t}}{(t+w)^m}T_+^1[k+it/(2a)]dt, \tag{3.198}$$

$$T_+^1(\beta)=\frac{(\beta+k)^{1/2}K_+^1(\beta)}{\beta^2-k^2+4k^2Z_0^2Q^2}. \tag{3.199}$$

Introducing the cylindrical coordinate $x=\rho\sin\theta,\quad z=\rho\cos\theta$ for $-\pi<\theta<\pi$ and applying the saddle point method, we derive a far field asymptotic expression with the result that

$$\phi(\rho,\theta)\sim\pm\hat{\Phi}^1(-k\cos\theta)k\sin\theta\frac{e^{i(k\rho-\pi/4)}}{(k\rho)^{1/2}},\quad x\gtrless 0 \tag{3.200}$$

as $k\rho\to\infty,$ where

$$\hat{\Phi}^1(\alpha)=-ikZ_0\frac{e^{-i\alpha a}U_-^1(\alpha)+e^{i\alpha a}U_{(+)}^1(\alpha)}{2\gamma M^1(\alpha)}\mp\frac{e^{-i\alpha a}V_-^1(\alpha)+e^{i\alpha a}V_{(+)}^1(\alpha)}{K^1(\alpha)},x\gtrless 0. \tag{3.201}$$

Equation (3.200) is uniformly valid for arbitrary incidence and observation angles.

3.9 Numerical Results and Discussion

In this section, we shall present numerical results on the RCS for E polarization, and discuss far field scattering characteristics of the strip in detail. The normalized RCS per unit length is defined by

$$\sigma/\lambda=\lim_{\rho\to\infty}\left(k\rho\left|\frac{\phi}{\phi^i}\right|^2\right) \tag{3.202}$$

with λ being the free-space wavelength. All the results are plotted in decibels [dB] by computing $10\log_{10}(\sigma/\lambda)$.

In computing (3.202), we have used the high-frequency asymptotic expressions as given by (3.152)-(3.155) for $U_{(\pm)}(\alpha)$ and $V_{(\pm)}(\alpha)$, where the truncation number N for the asymptotic series is contained. Let $\sigma^{(N)}$ and $\sigma^{(N+1)}$ be the RCS with the truncation numbers being N and $N+1,$ respectively. In numerical computation, we have employed the convergence criteria $\left|\sigma^{(N+1)}-\sigma^{(N)}\right|<10^{-3}$ in order to determine the desired truncation number N. By careful numerical investigation, we have verified that the choice of $N=3$ satisfies the aforementioned convergence criteria and hence provides sufficiently accurate solutions.

Figure 3.4 shows the normalized RCS as a function of observation angle $\theta,$ where the strip width is $2a=\lambda,5\lambda,10\lambda,$ the strip thickness is $b=0.01\lambda,\quad 0.04\lambda,\ 0.07\lambda,$ $0.10\lambda,$ and the incidence angle θ_0 is fixed as $60°$. As an example of existing lossy

materials, we have chosen the ferrite with $\varepsilon_r = 12.0 + i0$ and $\mu_r = 1.4 + i4.5$ in numerical computation [43]. It is seen from the figure that the RCS shows noticeable peaks along the reflected and incident shadow boundaries at $\theta = 120°$ and $\theta = -120°$, respectively. We observe by comparing the results for $2a = \lambda$, 5λ, and 10λ that the RCS shows sharp oscillation for larger strip width $2a$. We also notice that, for fixed $2a$, the RCS level becomes larger with an increase of the strip thickness b except in the neighborhood of the reflected shadow boundary at $\theta = 120°$. Scattering characteristics near $\theta = 120°$ need some considerations. We see that, for $b = 0.04\lambda$, 0.07λ, 0.10λ, the RCS level around $\theta = 120°$ becomes lower with an increase of the strip thickness. This is because, ferrite is an electromagnetic wave absorber and hence, the RCS reduction around the specular reflection direction becomes noticeable for larger strip thickness b.

Figure 3.5 shows the normalized RCS as a function of incidence angle θ_0, where the strip width is $2a = \lambda, 5\lambda, 10\lambda$, the strip thickness is $b = 0.01\lambda$, 0.04λ, 0.07λ, 0.10λ, and the same material parameters as in Fig. 2 have been chosen for computation. The truncation number is $N = 3$. It is obvious that the peaks at $\theta_0 = 90°$ in the figure correspond to the specular reflection from the strip. Comparing the RCS characteristics for $2a = \lambda$, 5λ, and 10λ, we observe that the RCS exhibits sharp oscillation for larger strip width $2a$. We also notice that, for fixed $2a$, the RCS level becomes larger with an increase of the strip thickness b except in the neighborhood of $\theta_0 = 90°$, whereas the RCS becomes lower with an increase of the strip thickness for $b = 0.04\lambda$, $0.07\lambda, 0.10\lambda$, around $\theta_0 = 90°$. This is due to the electromagnetic energy absorption for the ferrite material with larger strip thickness b, as has been investigated above for the normalized RCS as a function of observation angle.

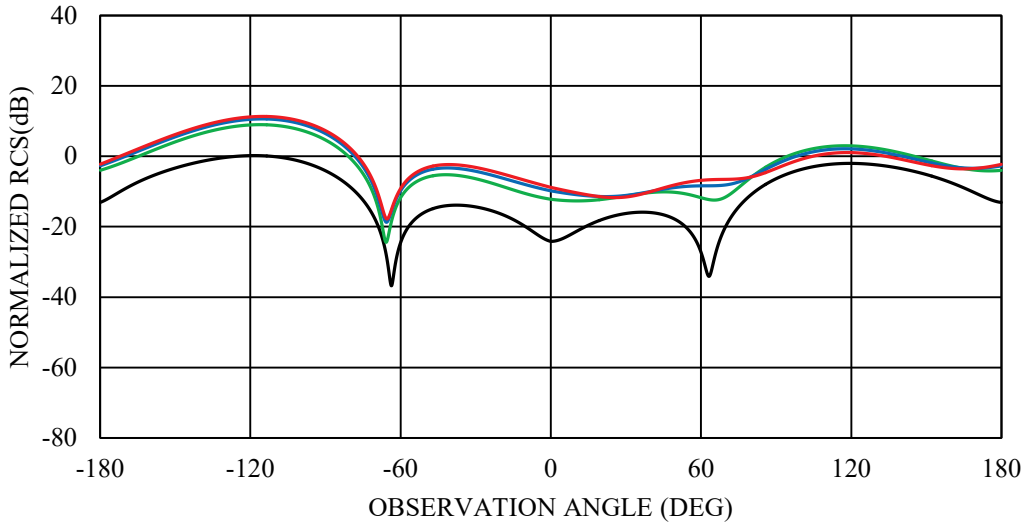

Fig. 3.4a Normalized RCS $\sigma^{(N)}/\lambda$ versus observation angle θ for E polarization, $\theta_0 = 60°$, $2a = 5\lambda$, $\varepsilon_r = 12.0 + i0$, $\mu_r = 1.4 + i4.5$, $N = 3$. ——: $b = 0.01\lambda$. ——: $b = 0.04\lambda$. ——: $b = 0.07\lambda$. ——: $b = 0.10\lambda$.

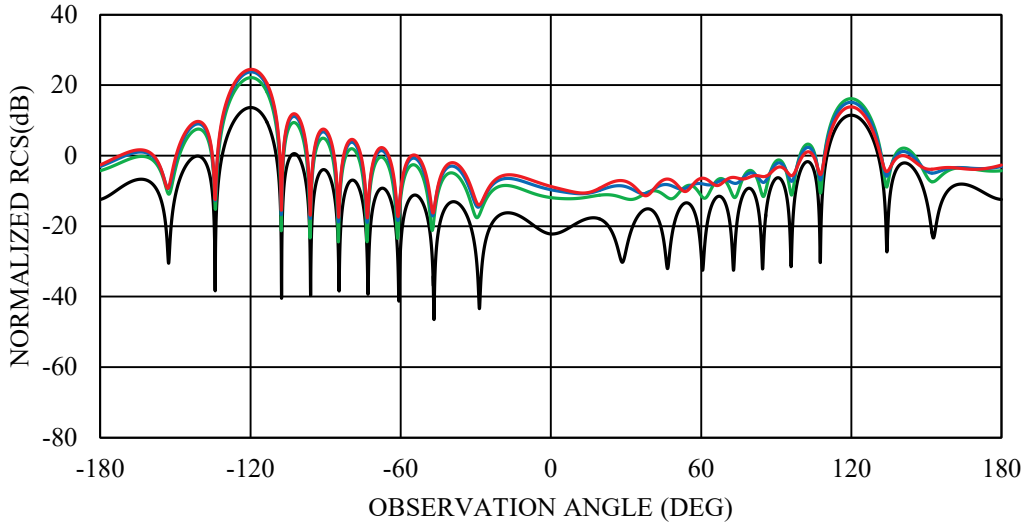

Fig. 3.4b Normalized RCS $\sigma^{(N)}/\lambda$ versus observation angle θ for E polarization, $\theta_0 = 60°$, $2a = 5\lambda$, $\varepsilon_r = 12.0 + i0$, $\mu_r = 1.4 + i4.5$, $N = 3$. ——: $b = 0.01\lambda$. ——: $b = 0.04\lambda$. ——: $b = 0.07\lambda$. ——: $b = 0.10\lambda$.

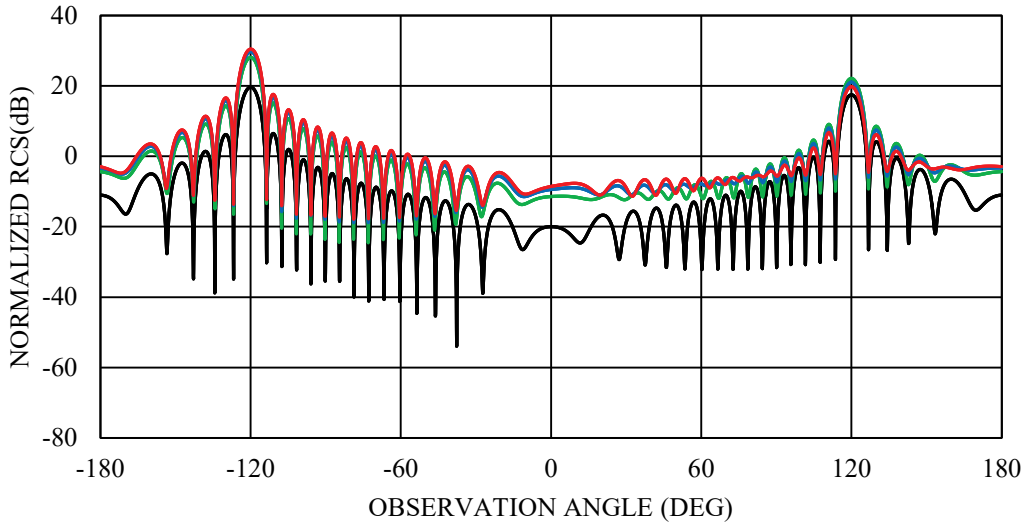

Fig. 3.4c Normalized RCS $\sigma^{(N)}/\lambda$ versus observation angle θ for E polarization, $\theta_0 = 60°$, $2a = 10\lambda$, $\varepsilon_r = 12.0 + i0$, $\mu_r = 1.4 + i4.5$, $N = 3$. ——: $b = 0.01\lambda$. ——: $b = 0.04\lambda$. ——: $b = 0.07\lambda$. ——: $b = 0.10\lambda$.

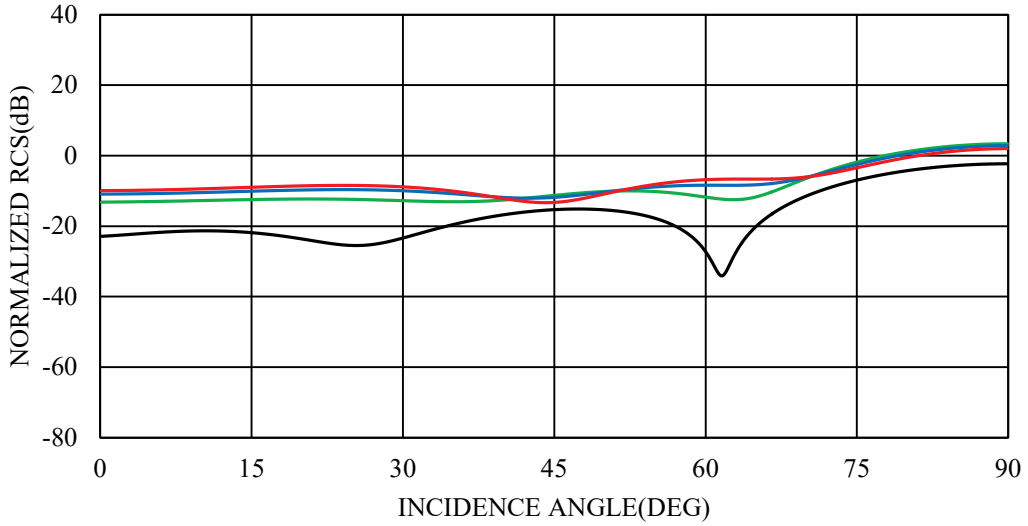

Fig. 3.5a Normalized RCS $\sigma^{(N)}/\lambda$ versus incidence angle θ_0 for E polarization $2a = \lambda$, $\varepsilon_r = 12.0 + i0$, $\mu_r = 1.4 + i4.5$, $N = 3$. ——: $b = 0.01\lambda$. ——: $b = 0.04\lambda$. ——: $b = 0.07\lambda$. ——: $b = 0.10\lambda$.

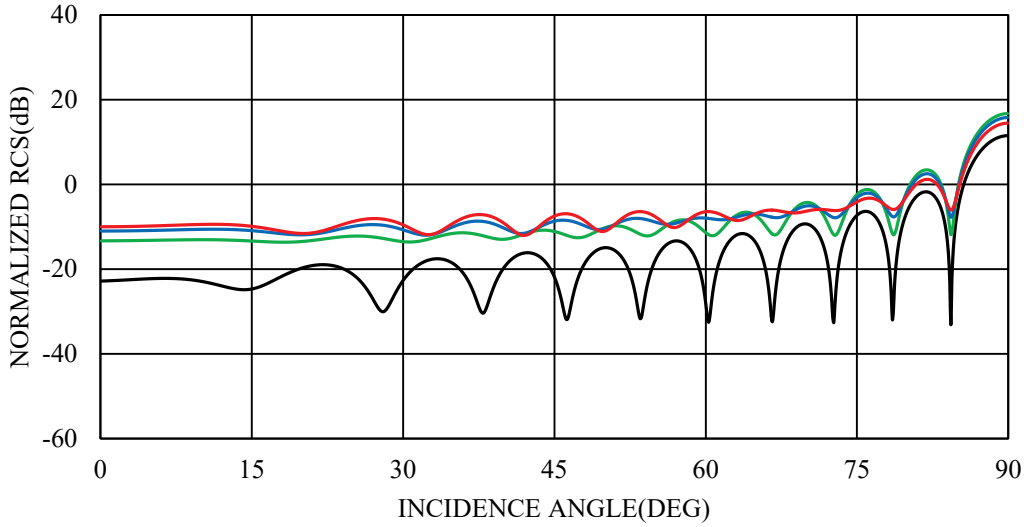

Fig. 3.5b Normalized RCS $\sigma^{(N)}/\lambda$ versus incidence angle θ_0 for E polarization $2a=5\lambda,\ \varepsilon_r=12.0+i0,\ \mu_r=1.4+i4.5,\ N=3.$ ——: $b=0.01\lambda.$ ——: $b=0.04\lambda.$ ——: $b=0.07\lambda.$ ——: $b=0.10\lambda.$

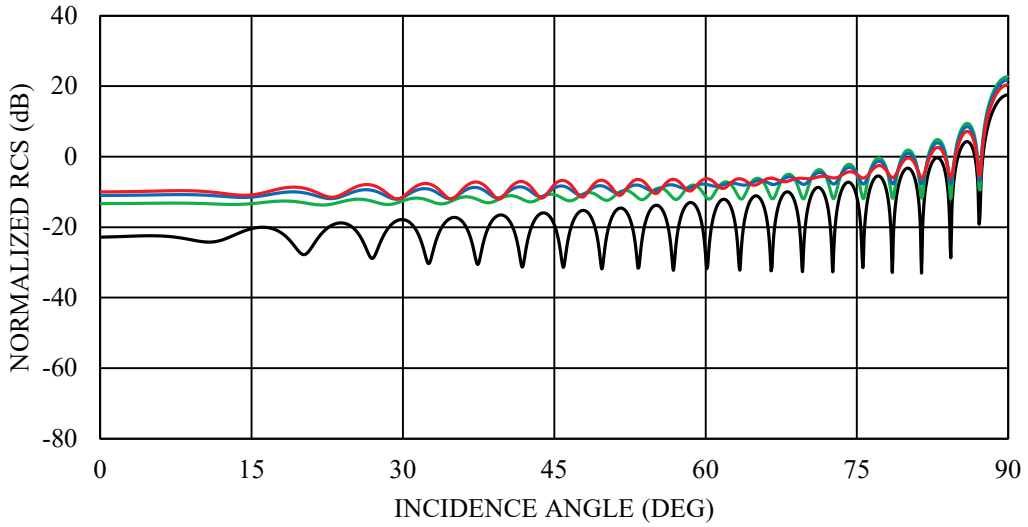

Fig. 3.5c Normalized RCS $\sigma^{(N)}/\lambda$ versus incidence angle θ_0 for E polarization. $2a=10\lambda,\ \varepsilon_r=12.0+i0,\ \mu_r=1.4+i4.5,\ N=3.$ ——: $b=0.01\lambda.$ ——: $b=0.04\lambda.$ ——: $b=0.07\lambda.$ ——: $b=0.10\lambda.$

We shall now make some comparison between two different polarizations. Figure 3.6 and 3.7 show the normalized RCS as a function of incidence angle θ_0 and as a function of observation angle θ, respectively, where the strip width is $2a = \lambda,\ 10\lambda,$ the strip thickness is $b = 0.01\lambda,$ and the same material parameters as in Fig. 3.4 have been chosen for computation. In Fig. 3.6, the incidence angle θ_0 has been $60°$. Comparing the RCS characteristics for E polarization with those for H polarization [39], we find that the RCS level for H polarization is lower than that for E polarization over the whole range of the incidence angle $\theta_0,$ in Figs. 3.6 and 3.7.

Let us now make comparison of the results obtained via a use of approximate boundary conditions by Senior and Volakis [29] ((3.5)-(3.7)) with those by Bleszynski *et al*. [35] ((3.169)-(3.171)). Figure 3.8 shows the normalized RCS as a function of incidence angle $\theta_0,$ where the strip dimension is $2a = 10\lambda, b = 0.01\lambda,$ and the other parameters are same as in Fig. 3.4. We see from the figure that the two results are in excellent agreement. By careful numerical experimentation for the case of $\varepsilon_r = 12.0 + i0,$ $\mu_r = 1.4 + i4.5,$ we have verified that the second order impedance boundary conditions [29] given by ((3.5)-(3.7)) can be employed for $|M| < 20$ with good accuracy.

Figures 3.9 and 3.10 show the normalized RCS versus incidence angle θ_0 and the frequency parameter $ka,$ respectively. In the figures, the results obtained by Shapoval [44] with the aid of the generalized boundary conditions and the Nystrom method [33], [34] are also plotted. It is observed from Figs. 3.9 and 3.10 that our results agree well with Shapoval's results.

We shall now make general remarks on the Wiener-Hopf solution and Shapoval's solution. In carrying out the Wiener-Hopf analysis, we have employed a high-frequency asymptotic method under the condition that the strip width is large compared with wavelength. Hence, our final solution becomes highly accurate with an increase of the strip width. On the other hand, Shapoval's results are obtained by using a numerical method based on the generalized boundary conditions and the singular integral equation. For this reason, the solution obtained by Shapoval is of better accuracy when the strip width becomes small compared with wavelength. Taking into account the essential differences between numerical methods and asymptotic methods, our method and Shapoval's method provide a better solution at higher and lower frequencies, respectively.

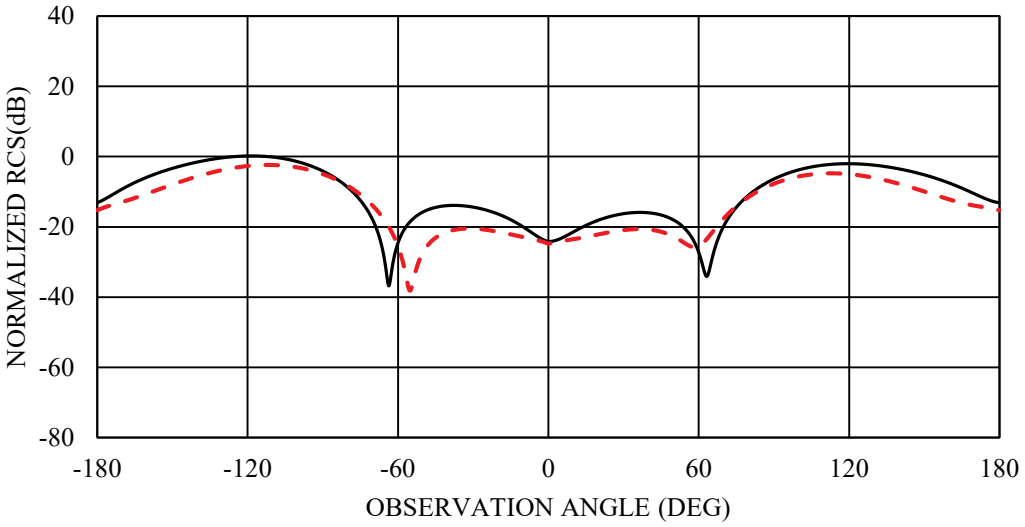

Fig. 3.6a Normalized RCS $\sigma^{(N)}/\lambda$ versus observation angle θ for E polarization, $2a=\lambda$, $b=0.01\lambda$, $\varepsilon_r=12.0+i0$, $\mu_r=1.4+i4.5$, $N=3$, and its comparison with H polarization [39]. ——: E polarization. - - - -: H polarization.

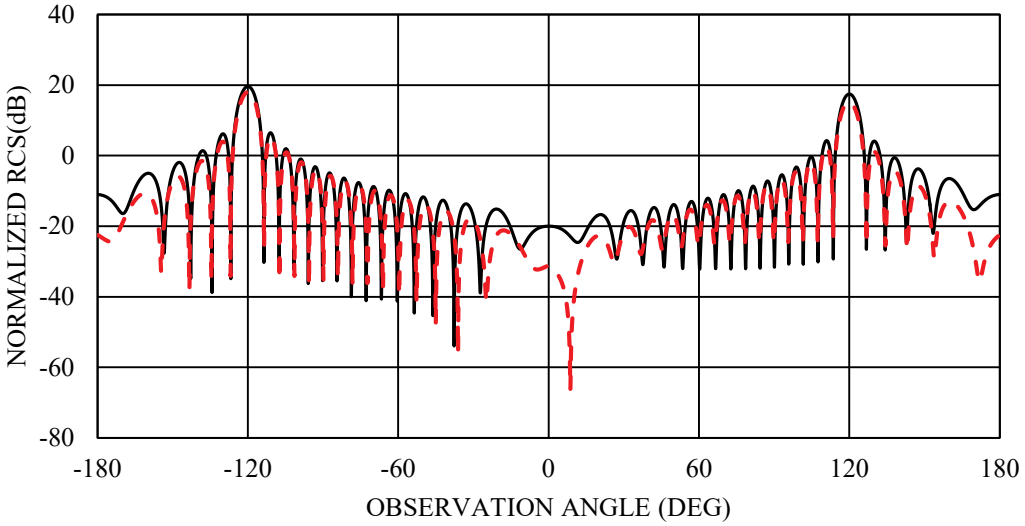

Fig. 3.6b Normalized RCS $\sigma^{(N)}/\lambda$ versus observation angle θ for E polarization, $2a=10\lambda$, $b=0.01\lambda$, $\varepsilon_r=12.0+i0$, $\mu_r=1.4+i4.5$, $N=3$, and its comparison with H polarization [39]. ——: E polarization. - - - -: H polarization.

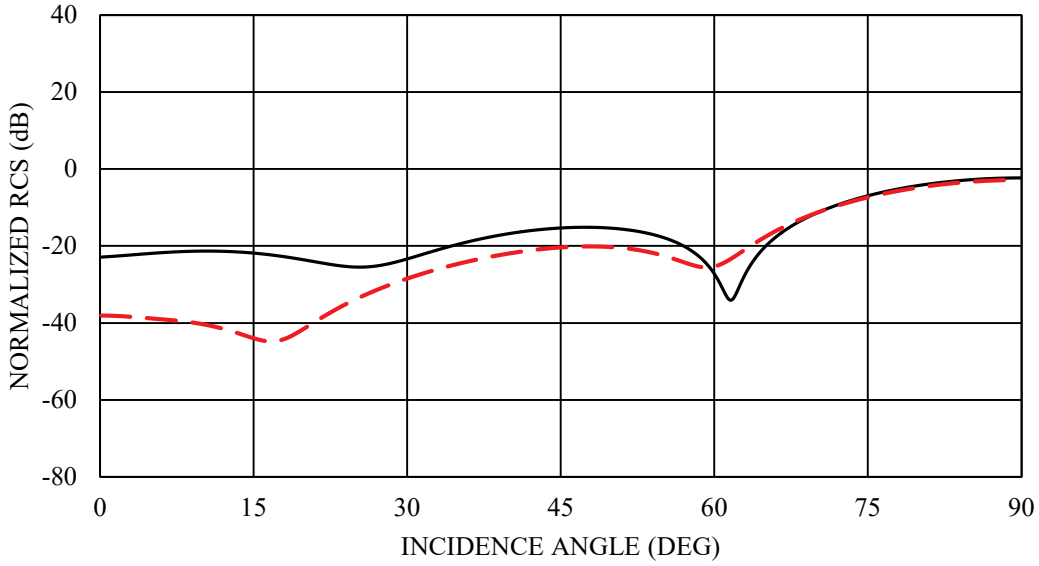

Fig. 3.7a Normalized RCS $\sigma^{(N)}/\lambda$ versus incidence angle θ_0 for E polarization, $2a=\lambda$, $b=0.01\lambda$, $\varepsilon_r=12.0+i0$, $\mu_r=1.4+i4.5$, $N=3$, and its comparison with H polarization [39]. ——— : E polarization. - - - - : H polarization.

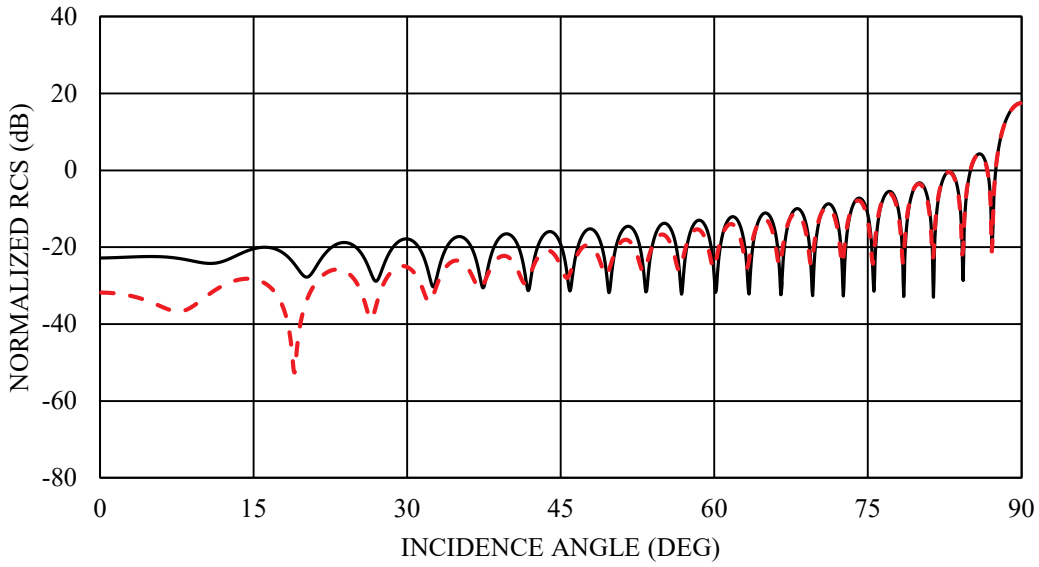

Fig. 3.7b Normalized RCS $\sigma^{(N)}/\lambda$ versus incidence angle θ_0 for E polarization, $2a=10\lambda$, $b=0.01\lambda$, $\varepsilon_r=12.0+i0$, $\mu_r=1.4+i4.5$, $N=3$, and its comparison with H polarization [39]. ——— : E polarization. - - - - : H polarization.

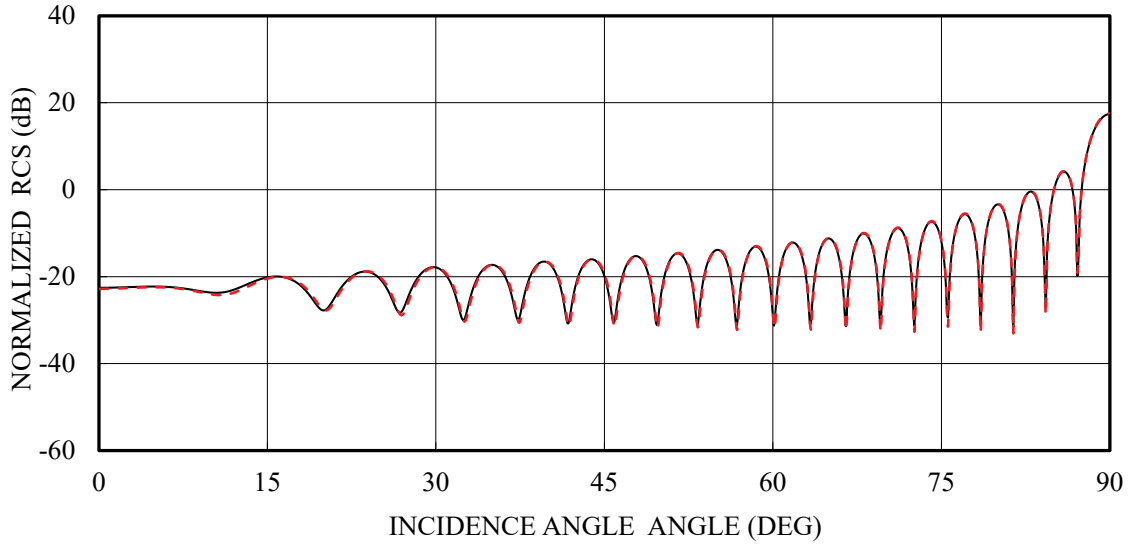

Fig. 3.8 Comparison of the normalized RCS $\sigma^{(N)}/\lambda$ versus incidence angle θ_0 between two different approximate boundary conditions for E polarization, $2a=10\lambda$, $b=0.01\lambda$, $\varepsilon_r=12.0+i0$, $\mu_r=1.4+i4.5$, $N=3$. ——— : approximate boundary conditions [32]. - - - - : approximate boundary conditions [35].

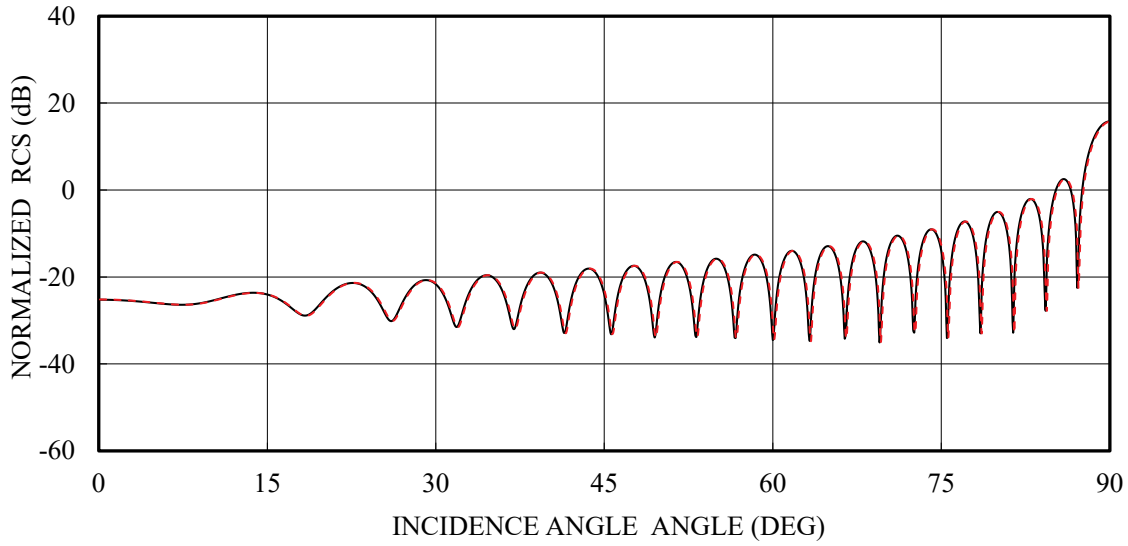

Fig. 3.9 Normalized RCS $\sigma^{(N)}/\lambda$ versus incidence angle θ_0 for E polarization, $2a=10\lambda$, $b=0.01\lambda$, $\varepsilon_r=3.4+i10$, $\mu_r=1$, $N=3$, and its comparison with Shapoval [44]. ——— : this paper. - - - - : Shapoval [44].

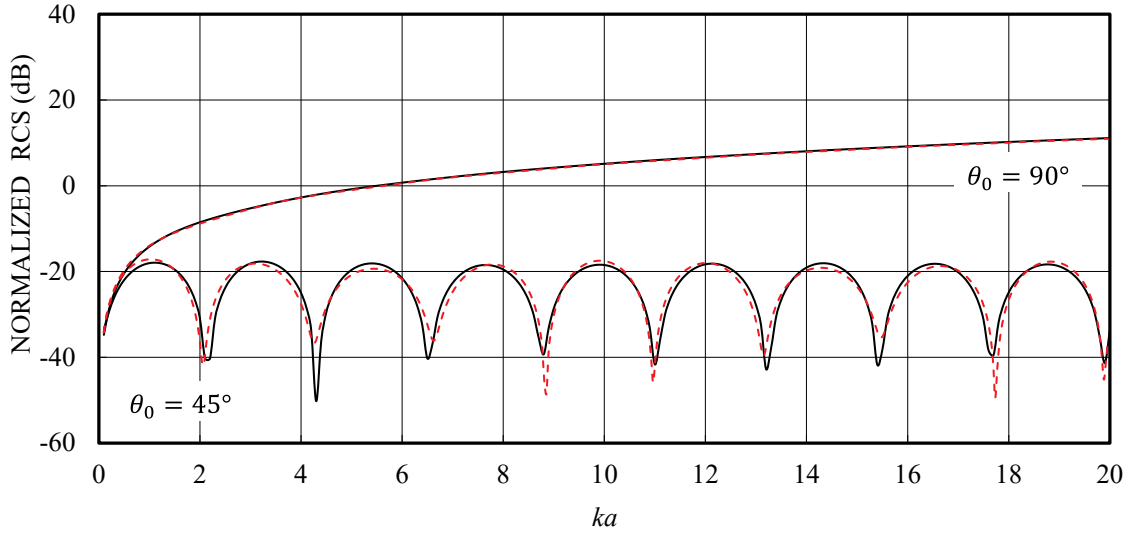

Fig. 3.10 Normalized RCS $\sigma^{(N)}/\lambda$ versus frequency parameter ka for E polarization, $\theta_0 = 45°, 90°$, $b = 0.025\lambda$, $\varepsilon_r = 4 + i0.4$, $\mu_r = 1$, $N = 3$, and its comparison with Shapoval[44]. ——— : this paper. - - - - : Shapoval [44].

3.10 The Difference of Resultant Solutions Compared with H polarized case

In this section, we shall consider the difference of resultant solutions obtained by above discussion between E and H polarizations. In discussions so far, we observe that our high frequency solutions $U_{(+)}(\alpha), U_{-}(\alpha), V_{(+)}(\alpha)$ and $V_{-}(\alpha)$ can be obtained under the transformation.

$$\left.\begin{array}{l} \varepsilon_0 \leftrightarrow \mu_0, \quad \varepsilon_r \leftrightarrow \mu_r, \quad Z_0 \leftrightarrow Y_0, \\ R_m \leftrightarrow R_e, \quad \tilde{R}_m \leftrightarrow \tilde{R}_e. \end{array}\right\} \tag{3.203}$$

Similarly, we also find that our high frequency solution $U^1_{(+)}(\alpha), U^1_{-}(\alpha), V^1_{(+)}(\alpha)$ and $V^1_{-}(\alpha)$ in section 2.8 and 3.8 can be obtained under the transformation.

$$\left.\begin{array}{l} \varepsilon_0 \leftrightarrow \mu_0, \quad \varepsilon_r \leftrightarrow \mu_r, \\ Z_0 \leftrightarrow Y_0, \quad R \leftrightarrow Q. \end{array}\right\} \tag{3.204}$$

It is verified that the transformations (3.203) and (3.204) are also valid for the other resultant equations except for the discussion in section 2.2 and 3.2. Taking into account the results obtained so far, our analytical results for chapter 2 and 3 may be treated via duality between E and H polarizations.

3.11 Summary

In this chapter, we have considered the same strip geometry as in chapter 2, and have analyzed the E-polarized plane wave diffraction by applying the Wiener-Hopf technique together with approximate boundary conditions. It is known that the approximate boundary conditions presented by Senior and Volakis [29] are valid under the condition that the absolute value of the complex refractive index of the medium is not too large. On the other hand, Bleszynski *et al.* [35] developed a different type of approximate boundary conditions, which is valid for the case where the absolute value of the complex refractive index is large. The main purpose of this paper is to use the two different approximate boundary conditions in [29] and [35] to extend the range of applicability of the Wiener-Hopf solution to the diffraction by a material strip, so that it becomes applicable to the strip having various material constants.

Introducing the Fourier transform of the scattered field and applying the approximate boundary conditions in the transform domain, the problem is formulated in terms of the simultaneous Wiener-Hopf equations satisfied by unknown spectral functions. The Wiener-Hopf equations are then solved via the factorization and decomposition procedure leading to the exact solution. However, the solution is formal in the sense that branch-cut integrals with unknown integrands are involved. Applying a rigorous asymptotic method similar to that used in [39], we shall derive a high-frequency solution to the Wiener-Hopf equations, which is valid for the strip width greater than about the incident wavelength. The scattered field in the real space is evaluated asymptotically by taking the Fourier inverse of the solution in the transform domain and applying the saddle point method of integration. Numerical examples of the RCS are presented for various physical parameters and far field scattering characteristics of the strip are discussed in detail. In particular, comparisons between E and H polarizations, between two different approximate boundary conditions, and with the other existing methods are given, and the validity of our approach is discussed.

4. CONCLUDING REMARKS

In this research, we have considered a thin material strip and analyzed the diffraction problem by using the Wiener-Hopf technique together with the two different approximate boundary conditions. This dissertation is composed of the following two parts:

(i) plane wave diffraction by a thin material strip: the case of H polarization.

(ii) plane wave diffraction by a thin material strip: the case of E polarization.

In chapter 2 we have analyzed the problem (i). by the method based on the Wiener-Hopf technique together with approximate boundary conditions. Assuming that the strip thickness is small compared with the wavelength, the problem has been reduced to the diffraction by a strip of zero thickness applying the approximate boundary conditions. Introducing the Fourier transform of the scattered field and applying approximate boundary conditions presented by Senior and Volakis [29] which is valid for the absolute value of the complex refractive index is not too large compared with unity, in transformed domain, the problem has been formulated in terms of the simultaneous Wiener-Hopf equations, which are solved exactly via the factorization and decomposition procedure. However, this solution has been formal since branch cut integrals with unknown integrands is involved. By using rigorous asymptotic method established in section 2.5 together with special function introduced by authors, we have derived a high-frequency solution of the Wiener-Hopf equations, which is expressed in terms of an infinite asymptotic series and account for all the higher order multiple diffracti0on effects rigorously. It has been shown that the higher-order multiple diffraction is expressed in term of the special function mentioned a bove. We have been obtained the solution valid for the strip width greater than about the incident wavelength. Taking the Fourier inverse of the solution in the transform domain and applying the saddle point method, we have been evacuated the scattered field in real space asymptotically. On the other hand, we have analyzed the different type of approximate boundary conditions developed by Bleszynski *et al.* [35], which is valid for the case where the absolute value of the complex refractive index is large compared with unity (see section 2.8). Numerical examples of the RCS has been presented for various physical parameters and far field scattering characteristics of the strip has been discussed in section 2.9.

In chapter 3, we have analyzed the problem (ii) by applying Wiener-Hopf technique together with approximate boundary conditions [29], [35]. Applying the similar procedure of the analysis in chapter 2, we have solved the diffraction problem (ii). In section 9 and 10, we have discussed the difference of resultant equations between E and H polarizations and the normalized RCS for various physical parameters and have also

provided some comparisons with other existing methods.

Taking into account the discussion in chapter 2 and 3, we have extended the range of applicability of the Wiener-Hopf solution to the diffraction by a material strip, so that it becomes applicable to the strip having various material constants using the two different approximate boundary conditions in [29] and [35].

All the results obtained in this dissertation are based on the Wiener-Hopf analysis, and can be used as reference solutions for validating other approximate methods such as numerical methods.

REFERENCES

[1] Jones, D. S., *The Theory of Electromagnetism*, Pergamon, Oxford, 1964.

[2] Felsen, L. B. and N. Marcuvitz, *Radiation and Scattering of Waves*, Prentice-Hall, Englewood Cliffs, 1973.

[3] Uslenghi, P. L. E., Ed., *Electromagnetic Scattering*, Academic, New York, 1978.

[4] Bowmann, J. J., T. B. A. Senior, and P. L. E. Uslenghi, Eds., *Electromagnetic and Acoustic Scattering by Simple Shapes*, Revised Printing, Hemispehere, New York, 1987.

[5] Jones, D. S., *Methods in Electromagnetic Wave Propagation*, Clarendon, Oxford, 1994.

[6] Sommerfeld, A., "Mathematische Theorie der Diffraction," *Math. Ann.*, Vol. 47, pp. 317-374, 1896.

[7] Baker, B. B., and E. T. Copson, *The Mathematical Theory of Huygens' Principle*, second edition, Oxford University Press, London, 124-152, 1950. See also, third edition, Chelsea Publishing, New York, 1987.

[8] Wiener, N. and E. Hopf, "Über eine Klasse singulärer Integralgleichungen," *Sitz. Ber. Preuss. Akad. Wiss., Phys.-Math. Kl.*, Verlag der Akademie der Wissenschaften, Berlin, pp. 696-706, 1931.

[9] Magnus, W., "Über die Beugung elektromagnetische Welln an einer Halbeben," *Z. Phys*., Vol. 117, 168-179, 1941.

[10] Copson, E. T., "On an integral equation arising in the theory of diffraction," *Quart. J. Math.*, Vol. 17, pp. 19-34, 1946.

[11] Schwinger, J., *Seminar on the Theory of Guided Waves,* MIT Radiation Laboratory, Boston, 1944.

[12] Noble, B., *Methods Based on the Wiener-Hopf Technique for the Solution of Partial Differential Equations*, Pergamon, London, 1958. See also, second edition, Chelsea Publishing, New York, 1988.

[13] Weinstein, L. A., *The Theory of Diffraction and the Factorization Method*, The Golem Press, Boulder, 1969.

[14] Mittra, R. and S.-W. Lee, *Analytical Techniques in the Theory of Guided Waves*, Macmillan, New York, 1971.

[15] Kobayashi, K., "Wiener-Hopf and modified residue calculus techniques," *Analysis Methods for Electromagnetic Wave Problems*, Chap. 8, Yamashita, E., Ed., Artech House, Boston, 1990.

[16] Daniele, V. G. and R. S. Zich, *The Wiener-Hopf Method in Electromagnetics,* The

Institution of Engineering and Technology, SciTech Publishing, Edison, NJ, 2014.

[17] Kobayashi, K., "Some diffraction problems involving modified Wiener-Hopf geometries," Analytical and Numerical Methods in Electromagnetic Wave Theory, Chap. 4, Hashimoto, M., M. Idemen, and O. A. Tretyakov, Eds., Science House, Tokyo, 1993.

[18] Shang, E. H. and K. Kobayashi, "Plane wave diffraction by a finite parallel-plate waveguide with four-layer material loading: Part II - The case of H polarization," *Progress In Electromagnetics Research B*, Vol. 6, 267-294, 2008.

[19] Shang, E. H. and K. Kobayashi, "Diffraction by a Terminated, Semi-Infinite Parallel-Plate Waveguide with Four-Layer Material Loading," *Progress In Electromagnetics Research B*, Vol. 12, 1-33, 2009.

[20] Shang, E. H., and K. Kobayashi, "Diffraction by a Terminated, Semi-Infinite Parallel-Plate Waveguide with Four Layer Material Loading: The Case of H Polarization," *Progress In Electromagnetics Research B*, Vol. 12, 139-162, 2009.

[21] Zheng, J. P. and K. Kobayashi, "Plane wave diffraction by a finite parallel-plate waveguide with four-layer material loading: part I - the case of E polarization," Progress In Electromagnetics Research B, Vol. 6, pp. 1-36, 2008.

[22] Zheng, J. P. and K. Kobayashi, "Diffraction by a semi-infinite parallel-plate waveguide with sinusoidal wall corrugation: combined perturbation and Wiener-Hopf analysis," *Progress In Electromagnetics Research B*, Vol. 13, pp. 75-110, 2009.

[23] Zheng, J. P. and K. Kobayashi, "Combined Wiener-Hopf and perturbation analysis of the *H*-polarized plane wave diffraction by a semi-infinite parallel-plate waveguide with sinusoidal wall corrugation," *Progress In Electromagnetics Research B*, Vol. 13, pp. 203-236, 2009.

[24] Eizawa, T. and K. Kobayashi, "Wiener-Hopf analysis of the *H*-polarized plane wave diffraction by a finite sinusoidal grating," *Progress In Electromagnetics Research*, Vol. 149, pp. 1-13, 2014.

[25] Eizawa, T. and K. Kobayashi, "Plane wave diffraction by a finite parallel-plate waveguide with sinusoidal wall corrugation," *Progress In Electromagnetics Research B*, Vol. 73, pp. 61-78, 2017.

[26] Serbest, A. H., and A Büyükaksoy, "Some approximate methods related to the diffraction by strips and slits," *Analytical and Numerical Methods in Electromagnetic Wave Theory*, Chap. 5, Hashimoto, M., M. Idemen, and O. A. Tretyakov, Eds., Science House, Tokyo, 1993.

[27] Büyükaksoy, A., and A. H. Serbest, "Matrix Wiener-Hopf factorization methods and

applications to some diffraction problem," *Analytical and Numerical Methods in Electromagnetic Wave Theory*, Chap. 5, Hashimoto, M., M. Idemen, and O. A. Tretyakov, Eds., Science House, Tokyo, 1993.

[28] Lüneburg, E., "Diffraction by an infinite set of parallel half-planes and by an infinite strip grating: comparison of different methods," *Analytical and Numerical Methods in Electromagnetic Wave Theory*, M. Hashimoto, M. Idemen, and O. A. Tretyakov (eds.), Chapter 7, Science House, Tokyo, 1993.

[29] Volakis, J. L., "High-frequency scattering by a thin material half plane and strip," *Radio Science*, Vol.23, No.3, pp.450-462, 1988.

[30] Clemmow, P. C., "A method for the exact solution of a class of two-dimensional diffraction problems," *Proc. R. Soc. London, Series A*, Vol.205, No.1081, pp.286-308, 1951.

[31] Herman, M. I. and J. L. Volakis, "High-frequency scattering by a resistive strip and extensions to conductive and impedance strips," *Radio Science*, Vol.22, No.3, pp.335-349, 1987.

[32] Senior, T. B. A. and J. L. Volakis, *Approximate Boundary Conditions in Electromagnetics*, IEE, London, 1995.

[33] Shapoval, O. V., R. Sauleau, and A. I. Nosich, "Scattering and absorption of waves by flat material strips analyzed using generalized boundary conditions and Nystrom-type algorithm," *IEEE Trans. Antennas Propag.*, Vol.59, No.9, pp.3339–3346, September 2011.

[34] Sukharevsky, I. O., O. V. Shapoval, A. Altintas, and A. I. Nosich, "Validity and limitations of the median-line integral equation technique in the scattering by material strips of sub-wavelength thickness," *IEEE Trans. Antennas Propag.*, Vol.62, No.7, pp.3623-3631, July 2014.

[35] Bleszynski, E., M. Bleszynski, and T. Jaroszewicz, "Surface-integral equations for electromagnetic scattering from impenetrable and penetrable sheets," *IEEE Antennas Propag. Mag.*, Vol.35, No.6, pp.14-25, December 1993.

[36] Koshikawa, S., K. Kobayashi, and T. Eizawa, "Wiener-Hopf analysis of the high-frequency diffraction by a strip: higher order asymptotics," *IEEJ Transactions on Fundamentals and Materials*, vol.113-A, No.3, pp.157-166, 1993.

[37] Kobayashi, K., "Solutions of wave scattering problems for a class of the modified Wiener-Hopf geometries," *IEEJ Transactions on Fundamentals and Materials*, Vol. 133, No. 5, pp. 233-241, 2013.

[38] Nagasaka, T. and K. Kobayashi, "Plane wave diffraction by a thin material strip:

higher order asymptotics," *Proc. Third International Conference on Telecommunications and Remote Sensing (ICTRS 2014)*, pp.94-99, June 2014.

[39] Nagasaka, T. and K. Kobayashi, "Wiener-Hopf analysis of the plane wave diffraction by a thin material strip," *IEICE Transactions on Electronics*, Vol. E100-C, No. 1, pp. 11-19, January 2017.

[40] Nagasaka, T. and K. Kobayashi, "Wiener-Hopf analysis of the plane wave diffraction by a thin material strip: the case of E polarization," *IEICE Transactions on Electronics*, Vol. E101-C, No. 1, pp. 12-19, January 2018.

[41] Senior, T. B. A. and J. L. Volakis, "Sheet simulation of a thin dielectric layer," *Radio Science*, Vol.22, No.7, pp.1261-1272, 1987.

[42] Meixner, J., "The behavior of electromagnetic fields at edges," *Res. Rep., Div. Electromagnetic Res., Inst. Math. Sci., New York Univ.,* No. EM-72,1954. See also, J. Meixner, *IEEE Trans. Antennas Propagat.,* Vol. AP-20, pp. 442-446, 1972.

[43] Komoni, T., F. Yasuda, and K. Saito, "Development of the demountable damped cavity," *Proc. 15th International Conference on RF Superconductivity (SRF 2011)*, pp.172-176, July 2011.

[44] Shapoval, O. V., private communication, September 2016.

APPENDICES

Appendix A. Approximate Boundary Conditions of a Thin Dielectric Layer

This appendix is concerned with the second order approximate boundary conditions [32] of a homogeneous dielectric layer, occupying the region $-b/2 < x < b/2$, $-\infty < y, z < \infty$, with free space surrounding the layer. It is assumed that the absolute complex refractive index $M(=|\varepsilon_r \mu_r|^{1/2})$ is not too large compared with unity. According to [32], if $\mu_r \neq 1$ and $\varepsilon_r \neq 1$ the second order approximate boundary condition can be written as

$$\left[\frac{1}{2R_m} + \frac{1}{2\tilde{R}_e}\left(1 + \frac{1}{k^2}\frac{\partial^2}{\partial x^2}\right)\right](E_x^+ + E_x^-) - \frac{iZ_0}{k}\left(\frac{\partial}{\partial x}E_x^+ - \frac{\partial}{\partial x}E_x^-\right) = 0 \tag{A.1}$$

$$\left(\frac{\partial}{\partial x}H_x^+ + \frac{\partial}{\partial x}H_x^-\right) + \frac{2ikR_m}{Y_0}(H_x^+ - H_x^-) = 0, \tag{A.2}$$

$$\left[\frac{1}{2R_e} + \frac{1}{2\tilde{R}_m}\left(1 + \frac{1}{k^2}\frac{\partial^2}{\partial x^2}\right)\right](H_x^+ + H_x^-) - \frac{iY_0}{k}\left(\frac{\partial}{\partial x}H_x^+ - \frac{\partial}{\partial x}H_x^-\right) = 0 \tag{A.3}$$

$$\left(\frac{\partial}{\partial x}E_x^+ + \frac{\partial}{\partial x}E_x^-\right) + \frac{2ikR_e}{Z_0}(E_x^+ - E_x^-) = 0, \tag{A.4}$$

where

$$R_e = \frac{iZ_0}{kb(\varepsilon_r - 1)}, \quad \tilde{R}_e = \frac{iY_0\varepsilon_r}{kb(\varepsilon_r - 1)}, \quad R_m = \frac{iY_0}{kb(\mu_r - 1)}, \quad \tilde{R}_m = \frac{iZ_0\mu_r}{kb(\mu_r - 1)}, \tag{A.5}$$

and the plus sign and minus sign superscripts refer to the upper and lower sides of the surface respectively, and they can define a combination sheet consisting of second order conductive and resistive sheets.

The corresponding refection coefficients for the incident plane wave are

$$R_{\parallel} = \left(1 + \frac{2R_e}{Z_0 \sin\theta_0}\right)^{-1} - \left(1 + \frac{2\tilde{R}_e}{Y_0}\frac{\sin\theta_0}{\cos^2\theta_0}\right)^{-1}, \tag{A.6}$$

$$R_{\perp} = \left(1 + \frac{2R_e}{Z_0 \sin\theta_0}\right)^{-1} - \left(1 + \frac{2\tilde{R}_e}{Y_0}\frac{\sin\theta_0}{\cos^2\theta_0}\right)^{-1}, \tag{A.7}$$

and (A.6) is the sum of the reflection coefficients for a first order resistive sheet and a second order conductive sheet in isolation because the two sheets scatter independently. The exact reflection of the dielectric layer can be derived using image theory and duality, and they are

$$R_{\parallel} = e^{-ikb\sin\theta_0}\left\{1+\frac{2}{(\varepsilon_r-1)(\varepsilon_r\sin^2\theta_0-\cos^2\theta_0)}\left[\varepsilon_r-\cos^2\theta_0\right.\right.$$
$$\left.\left.+i(\varepsilon_r-\cos^2\theta_0)^{1/2}\,\varepsilon_r\sin\theta_0\cot\left(kb(\varepsilon_r-\cos^2\theta_0)^{1/2}\right)\right]\right\}^{-1}, \tag{A.8}$$

$$R_{\perp} = -e^{-ikb\sin\theta_0}\left\{1+\frac{2\sin\theta_0}{\varepsilon_r-1}\left[\sin\theta_0\right.\right.$$
$$\left.\left.+i(\varepsilon_r-\cos^2\theta_0)^{1/2}\cot\left(kb(\varepsilon_r-\cos^2\theta_0)^{1/2}\right)\right]\right\}^{-1}, \tag{A.9}$$

where the phase factor has been introduced to account for the location of the upper surface at $x = b/2$.

Appendix B. Some First Order Approximate Boundary Conditions

The first order approximate boundary conditions can be written as following form:

$$\frac{1}{2}(E_T^+ + E_T^+) = R\vec{n}\times(H_T^+ - H_T^+) \tag{B.1}$$

$$\frac{1}{2}(H_T^+ + H_T^+) = -Q\vec{n}\times(E_T^+ - E_T^+), \tag{B.2}$$

where $\vec{n}$ is the unit normal vector, Z_0 is the free-space impedance, the indices $\pm$ correspond to the field limit values at the top and bottom sides of the dielectric layer, and the subscript of 'T' means the tangential components of the fields on the layer. The coefficients R and Q are called the electric and magnetic resistivities, which have several form depending material parameters ε_r and μ_r. If the absolute value of the complex refractive index is large case (e.g. section 2.8 and 3.8), then [35]

$$\left.\begin{aligned} R &= \frac{iZ_0}{2}\frac{\mu_r^{1/2}}{\varepsilon_r^{1/2}}\cot[kb(\varepsilon_r\mu_r)^{1/2}/2], \\ Q &= \frac{iY_0}{2}\frac{\varepsilon_r^{1/2}}{\mu_r^{1/2}}\cot[kb(\varepsilon_r\mu_r)^{1/2}/2]. \end{aligned}\right\} \tag{B.3}$$

If, alternatively, the absolute value of the complex refractive index is not too large case (e.g. section 2.1 and 3.8, Appendix A), then [29]

$$R = \frac{iZ_0}{\varepsilon_r^{1/2}kb(\varepsilon_r-1)}, \quad Q = \frac{iY_0\varepsilon_r^{1/2}}{kb(\varepsilon_r-1)}, \quad (\mu_r = 1), \tag{B.4}$$

and then [35]

$$R = \frac{iZ_0}{kb(\varepsilon_r - 1)}, \quad Q = \frac{iY_0}{kb(\mu_r - 1)}. \tag{B.5}$$

Equations (B.1) and (B.2) are approximate, however it is clearly a big step ahead from the PEC condition, to which it turns if $R = 0$ and $Q = \infty$ [34], [35].Note that (B.1) and (B.2) has the meaning of Ohm's law for the effective electric and magnetic currents, which correspond to the difference terms in their right-hand parts.

Appendix C. Saddle Point Method

There are a number of asymptotic methods for evaluation of branch-cut integrals. The saddle point method is known as a powerful tool for deriving asymptotic expansions of such integrals. In this appendix, we shall introduce typical infinite branch-cut integral occurring in the Wiener-Hopf technique, and discuss the derivation of its asymptotic expansion based on the saddle point method.

Let us introduce the function

$$\gamma = (\alpha^2 - k^2)^{1/2} \equiv (\alpha + k)^{1/2}(\alpha - k)^{1/2} \tag{C.1}$$

with $\alpha = \mathrm{Re}\,\alpha + i\,\mathrm{Im}\,\alpha (\equiv \sigma + i\tau)$, where

$$k = k_1 + ik_2, \quad k_1 > 0, \quad k_2 > 0. \tag{C.2}$$

It is seen that γ is a double-valued function of α and has branch points at $\alpha = \pm k$. We now choose branch cuts for γ as a portion of hyperbola defined by $\sigma\tau = k_1 k_2$, It can be verified that $\mathrm{Re}\,\gamma > 0$ for any α in the strip $-k_2 < \tau < k_2$.

Let $\Phi(\alpha)$ be regular in the strip $\tau_- < \tau < \tau_+$, where $\tau_\pm$ are some constants such that $-k_2 \le \tau_- < \tau < \tau_+ \le k_2$. We now introduce the integral

$$\phi(x,z) = (2\pi)^{-1/2} \int_{-\infty+ic}^{\infty+ic} \Phi(\alpha) e^{-\gamma|x| - i\alpha z} d\alpha \tag{C.3}$$

for real x and z, where c is an arbitrary constant satisfying $\tau_- < c < \tau_+$. Since the integrand possesses branch points at $\alpha = \pm k$ due to the presence of γ, it is generally difficult to evaluate (C.3) in a closed form. However, we can derive an asymptotic representation based on the saddle point method as $k(x^2 + z^2)^{1/2} \to \infty$ if the integrand has no singularities other than the branch points at $\alpha = \pm k$. Let (ρ, θ) be the cylindrical coordinate as defined by $x = \rho \sin\theta,\ z = \rho\cos\theta$ for $0 < |\theta| < \pi$. The fundamental theorem for the asymptotic expansion is now stated as follows:

Theorem C.1 *Let* $\Phi(\alpha)$ *be regular except for possible singularities at* $\alpha = \pm k$*, where these singularities are branch points due to the presence of* γ *in* $\Phi(\alpha)$*. Then the function* $\Phi(x,z)$ *defined by* (C.3) *has the asymptotic expansion*

$$\phi(\rho,\theta) \sim \frac{e^{ik\rho}}{(2k\rho)^{1/2}} \sum_{n=0}^{\infty} \frac{G^{(2n)}(0)}{n!2^{2n}} (k\rho)^{-n} \tag{C.4}$$

as $k\rho \to \infty$*, where*

$$G^{(2n)}(0) = \frac{d^{2n}}{dt^{2n}} G(t)\bigg|_{t=0} \tag{C.5}$$

with

$$G(t) = \frac{2^{1/2} e^{-i\pi/4}}{(1+it^2/2)^{1/2}} \Phi(-k\cos w) k \sin w \bigg|_{w=g(t)}, \tag{C.6}$$

$$g(t) = |\theta| + \cos^{-1}(1+it^2). \tag{C.7}$$

In (C.7)*, the arc cosine function is interpreted as the principal value.*

The above theorem gives a complete asymptotic expansion of $\phi(x,z)$ for $k(k^2+z^2)^{1/2} \to \infty$. Extracting out the dominant term from the asymptotic series, we have the following theorem:

Theorem C.2 *Let* $\Phi(\alpha)$ *satisfy the hypotheses stated in Theorem* C.1*. Then* $\phi(x,z)$ *defined by* (C.3) *has the asymptotic expansion*

$$\phi(\rho,\theta) \sim \Phi(-k\cos\theta) k \sin|\theta| \frac{e^{i(k\rho-\pi/4)}}{(k\rho)^{1/2}} \tag{C.8}$$

as $k\rho \to \infty$.

We have so far treated the case of complex k, but Theorems C.1 and C.2 hold as well for real k by taking the limit $k_2 \to +0$.

LIST OF PUBLICATIONS

1. Publications in Professional Journals

[1] Nagasaka, T. and K. Kobayashi, "Wiener-Hopf analysis of the plane wave diffraction by a thin material strip," *IEICE Transactions on Electronics*, Vol. E100-C, No. 1, pp. 11-19, January 2017.

[2] Nagasaka, T. and K. Kobayashi, "Wiener-Hopf analysis of the plane wave diffraction by a thin material strip: the case of E polarization," *IEICE Transactions on Electronics*, Vol. E101-C, No. 1, pp. 12-19, January 2018.

2. Refereed Papers Presented at International Conferences

[1] Nagasaka, T. and K. Kobayashi, "Wiener-Hopf analysis of the diffraction by a thin material strip," *Proc. 2013 Progress In Electromagnetics Research Symposium (PIERS 2013)*, Stockholm, Sweden, p. 804, August 2013.

[2] Nagasaka, T. and K. Kobayashi, "Plane wave diffraction by a thin material strip: higher order asymptotics," *Proc. Third International Conference on Telecommunications and Remote Sensing (ICTRS 2014)*, pp. 94-99, Luxembourg, Grand Duchy of Luxembourg, June 2014.

[3] Nagasaka, T., "Wiener-Hopf analysis of the plane wave diffraction by a thin material strip," *Proc. 2015 URSI-Japan Radio Science Meeting (URSI-JRSM 2015)*, p. 43, Tokyo, Japan, September 2015.

[4] Nagasaka, T. and K. Kobayashi, "Wiener-Hopf analysis of the plane wave diffraction by a thin material strip: the case of E polarization," *Proc. 17th International Conference on Electromagnetics in Advanced Applications (ICEAA 2015)*, pp. 622-625, Torino, Italy, September 2015.

[5] Nagasaka, T. and K. Kobayashi, "Wiener-Hopf analysis of the plane wave diffraction by a thin material strip: the case of H polarization," *Proc. 17th International Conference on Electromagnetics in Advanced Applications (ICEAA 2015)*, pp. 626-629, Torino, Italy, September 2015.

[6] Nagasaka, T. and K. Kobayashi, "Radar cross section of a thin material strip," *Proc. 2nd URSI Regional Conference on Radio Science (URSI-RCRS-2015)*, pp. 41-42, New Delhi, India, November 2015 (invited).

[7] Nagasaka, T. and K. Kobayashi, "Wiener-Hopf analysis of the radar cross section of a thin material strip," *Proc. 2016 International Conference on Mathematical Methods*

*in Electromagnetic Theory (MMET*2016)*, pp. 268-271, Lviv, Ukraine, July 2016.

[8] Nagasaka, T. and K. Kobayashi, "Wiener-Hopf analysis of the diffraction by a thin material strip," *Proc. 2016 URSI International Symposium on Electromagnetic Theory (URSI EMTS 2016)*, pp. 559-562, Espoo, Finland, August 2016 (invited).

[9] Nagasaka, T. and K. Kobayashi, "Radar cross section analysis of a thin material strip," *Proc. 2016 Asia-Pacific Radio Science Conference (URSI AP-RASC 2016)*, pp. 15-16, Seoul, Korea, August 2016 (invited).

[10] Nagasaka, T. and K. Kobayashi, "Plane wave diffraction by a thin material strip: the case of E polarization," *Proc. XXXIInd URSI General Assembly and Scientific Symposium (URSI GASS 2017)*, No. B23P-3 (1857), Montreal, Canada, August 2017.

[11] Nagasaka, T. and K. Kobayashi, "H-polarized plane wave diffraction by a thin material strip," *Proc. 19th International Conference on Electromagnetics in Advanced Applications (ICEAA 2017)*, pp. 804-807, Verona, Italy, September 2017.

[12] Nagasaka, T. and K. Kobayashi, "E-polarized plane wave diffraction by a thin material strip," *Proc. 19th International Conference on Electromagnetics in Advanced Applications (ICEAA 2017)*, pp. 796-799, Verona, Italy, September 2017.

3. Non-Refereed Conference Papers

[1] Nagasaka, T. and K. Kobayashi, "Wiener-Hopf analysis of the plane wave diffraction by a thin material strip: higher order asymptotics," *The Papers of Technical Meeting on Electromagnetic Theory, The Institute of Electrical Engineers of Japan (IEE Japan)*, No. EMT-15-123, October 2015.

4. Awards

[1] Honorary Mention: Next to the Best, MMET*2016 and URSI Young Scientist Paper Contest, 16th IEEE International Conference on Mathematical Methods in Electromagnetic Theory (MMET*2016), Lviv, Ukraine, July 2016.

[2] 2017 URSI Young Scientists Award, XXXIInd URSI General Assembly and Scientific Symposium (URSI GASS 2017), Montreal, Canada, August 2017.

[3] Third Prize, Fourth International URSI Student Prize Paper Competition, XXXIInd URSI General Assembly and Scientific Symposium (URSI GASS 2017), Montreal, Canada, August 2017.